## 1 Introduction

The aim of this project is the design, development and construction of equipment and instrumentation to enable users to observe recalescence and re-crystallisation during the cooling of molten alumina oxide from high temperatures into the super cooled region.

Re-crystallisation below the melting point is accompanied by a sudden release of the heat of fusion. This temporarily reheats the material to white heat, a phenomenon called recalescence.
The equipment, which comprised a laser heated aerodynamic levitation furnace, was developed at Aberystwyth University, Material Science Group, prior to installation and subsequent measurement of X-ray diffraction and small angle scattering at the Synchrotron Radiation Source on the 6.2 beamline at the Daresbury Laboratory.

The Thesis describes the initial design, development and construction of aerodynamic furnace, which enables a 2mm sphere of alumina to be levitated on a chemically inert stream of gas. The alumina sphere was heated to melting point by a 125 watt continuous wave Carbon Dioxide Laser. By gradually reducing the laser power, the temperature of the molten drop was lowered into the super cooled region.
Temperatures were measured by a Luxtron Optical Pyrometer, extending from 3000º down to 800º Kelvin.
Furnace operations were controlled by LabVIEW software designed to control laser power and read the optical pyrometer. The comprehensive control of instrumentation, which also included a high-speed camera allowed the experimental conditions to be tested in Aberystwyth, prior to installation into the synchrotron beamline at Daresbury Laboratory.

This dissertation describes the design, development and operation of the laser furnace on beamline 6.2.

Following a short overview of the instrumentation in Chapter 1, all of the components are separately described in Chapters 2 -7. X-ray beam alignment on beamline 6.2 is covered in Chapter 8. Computer control and interfacing in Chapter 9.

The laser shutter and the comprehensive safety protocol is included in Chapters 10 – 11.

Experimental x–ray results using the laser furnace are produced in Chapter 12.

Figure A outlines schematically the operation of the laser furnace, in conjunction with the equipment on beamline 6.2 at Daresbury Laboratory.

Figure B shows the laser furnace in operation in the x–ray hutch.

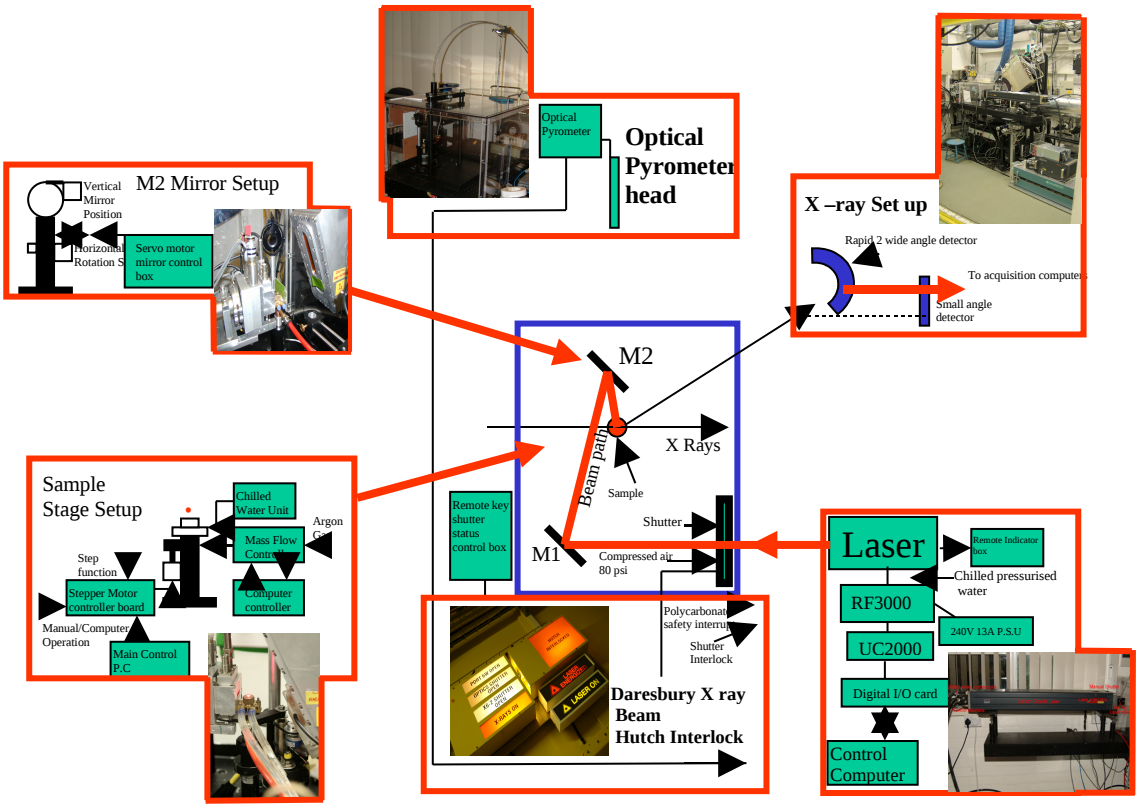


**Figure A: Schematic operation of the laser furnace in conjunction with the equipment on the 6.2 beamline at the Daresbury Synchrotron Radiation Source.**

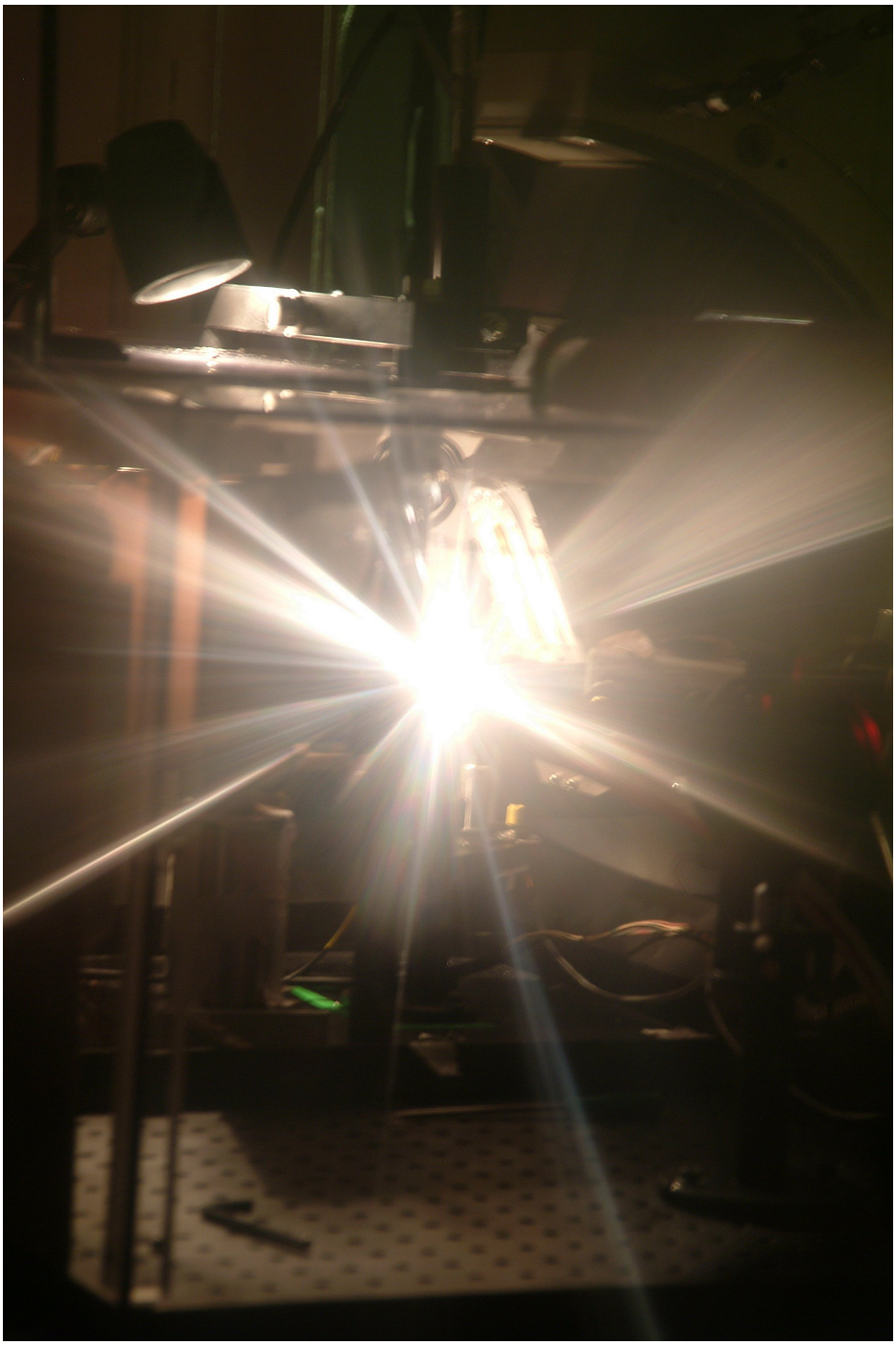

**Figure B: Molten sample levitating at 2000°K in the x-ray beam, picture taken through Pb window of 6.2 beamline hutch.**

# Chapter 1

## Overall Design

This Chapter provides a brief overview of the aerodynamic levitator furnace and its implementation on beamline 6.2 at the Synchrotron Radiation Source at Daresbury Laboratory.

The aim was to design and construct an experiment capable of heating and melting a 2mm sample of alumina at 2323ºK.

Once in the liquid state, the alumina could be heated further above the melting point or super cooled below 2323ºK. By employing container-less conditions, re-crystallization could be avoided and the liquid under cooled many hundreds of degrees.

Original ideas and concepts for developing high temperature measurements on aerodynamic levitation techniques for use in x-ray [1], [2] and neutron [3] experiments were investigated for the most appropriate designs.

Initially the design and construction was undertaken at Aberystwyth University using the Material Physics Group facilities. This involved designing a geometry that was compatible with the instrumentation on 6.2 Multipole wiggler beamline at the synchrotron radiation facilities at Daresbury Laboratory.

The design layout of the 6.2 beamline is shown in Figure1.1. That identifies the sample stage. This needed to be aligned with the incoming x –rays, the focus of the wide angle x–ray scattering (WAXS) detector, and the axis of the small angle x –ray scattering (SAXS) camera.
The sample stage was mounted on a table with horizontal and vertical adjustment – EXAFS table.

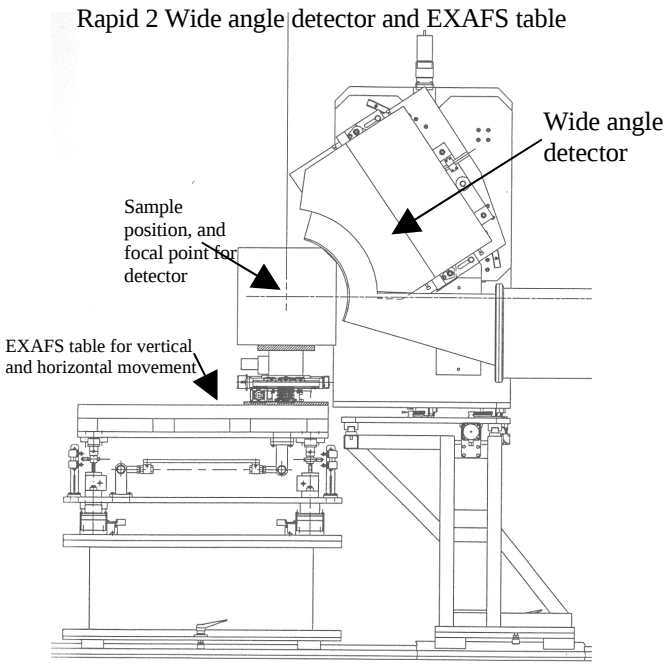


**Figure 1.1 Side elevation schematic, illustrating optimal sample position with respect to x –ray beam position and wide (WAXS) and small (SAXS) angle detectors.**

In the design of the aerodynamic levitator furnace of experiment, several factors needed to be considered prior to construction and installation on the 6.2 beamline.

- Overall construction and layout of furnace.
- Method of heating the sample.
- Method of measuring sample temperature and its environment.
- Computer control of the individual instruments and the experiments planned.
- Experimental environment and safety requirements on beamline 6.2.

### 1.1 Bench

An aluminum bench was designed in an “L” shaped configuration, as shown in Figure 1.2. This type of layout was designed so that the optics table could be clamped directly onto the EXAFS table at the 6.2 beamline Figure 1.1 and capable of adjustments in the vertical and horizontal directions. The bench construction was designed so that the sample could be positioned as close to the WAXS detector as possible, thereby reducing the amount of air scatter (Figure 1.6).

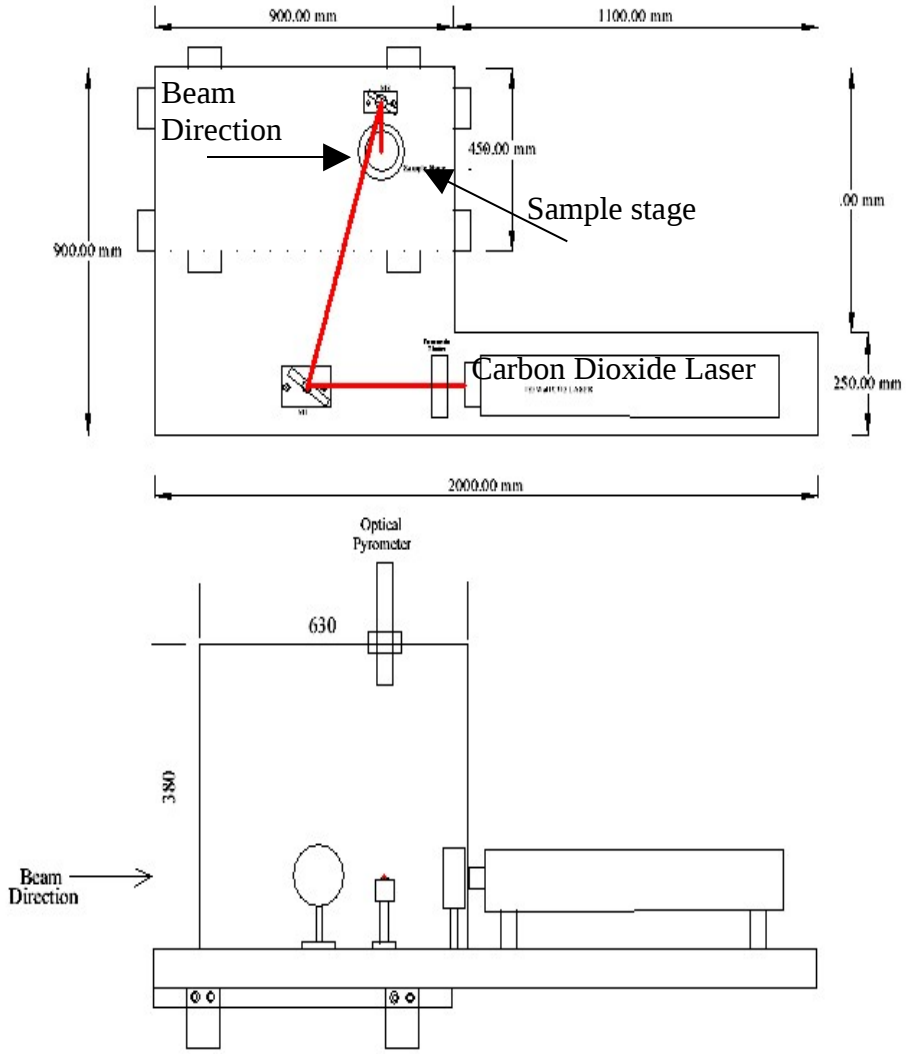


**Figure 1.2 Schematic plan and side view, illustrating initial component layout with respective dimensions.**

## 1.2 Optics table

The laser optics table was designed to support the entire set of optical components associated with the furnace, so that misalignments could be minimalised during furnace setup and x-ray alignment. The dedicated optics bench weighed in excess of 100kg, and had reinforced gussets to prevent any flexing of the cantilever arm that supports the laser, (Figure 1.2) in this way the bench and optics table could be raised or lowered accurately into the x- ray beam on 6.2.

Figure 1.3 and Figure 1.4 show the optics table and the arrangements of optical components for the aerodynamic levitator furnace.

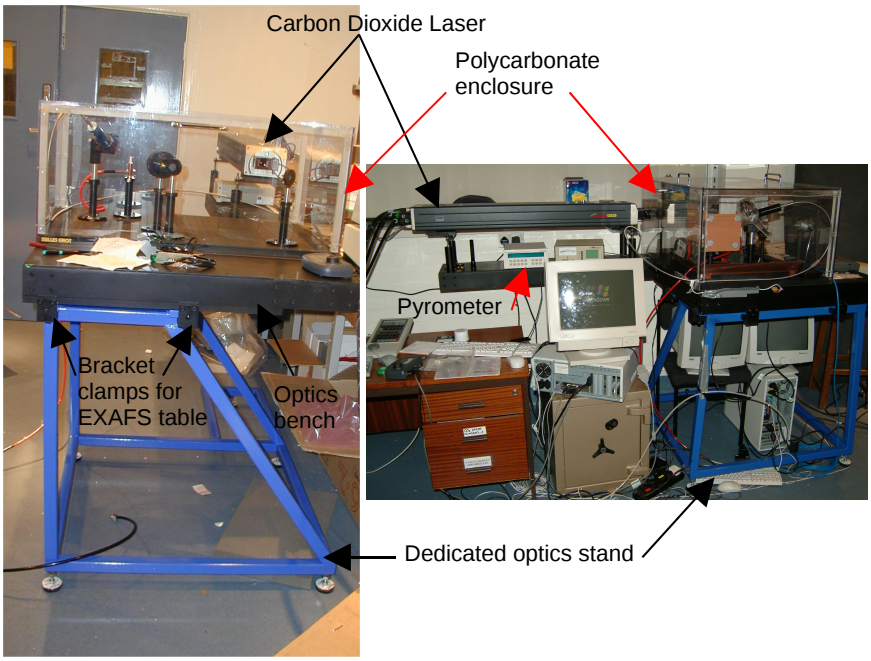


**Figure 1.3. Side and front view of all experimental components in position assembled on the optics bench on the dedicated laser stand at the Aberystwyth Material Physics Laboratory.**

## 1.3 Breadboard

The optics for the furnace were assembled on a 600 x 900mm optical breadboard with a matrix of 6mm holes pitched at 25mm spacing. This was used for securing all the optical mirrors, sample stages and pyrometer mounts. An additional component was a catch tray. This was added as a safety precaution for fire prevention, as some levitated molten samples would sometimes blow off the levitating stage, and fall into the foam packed hole in the matrix board.

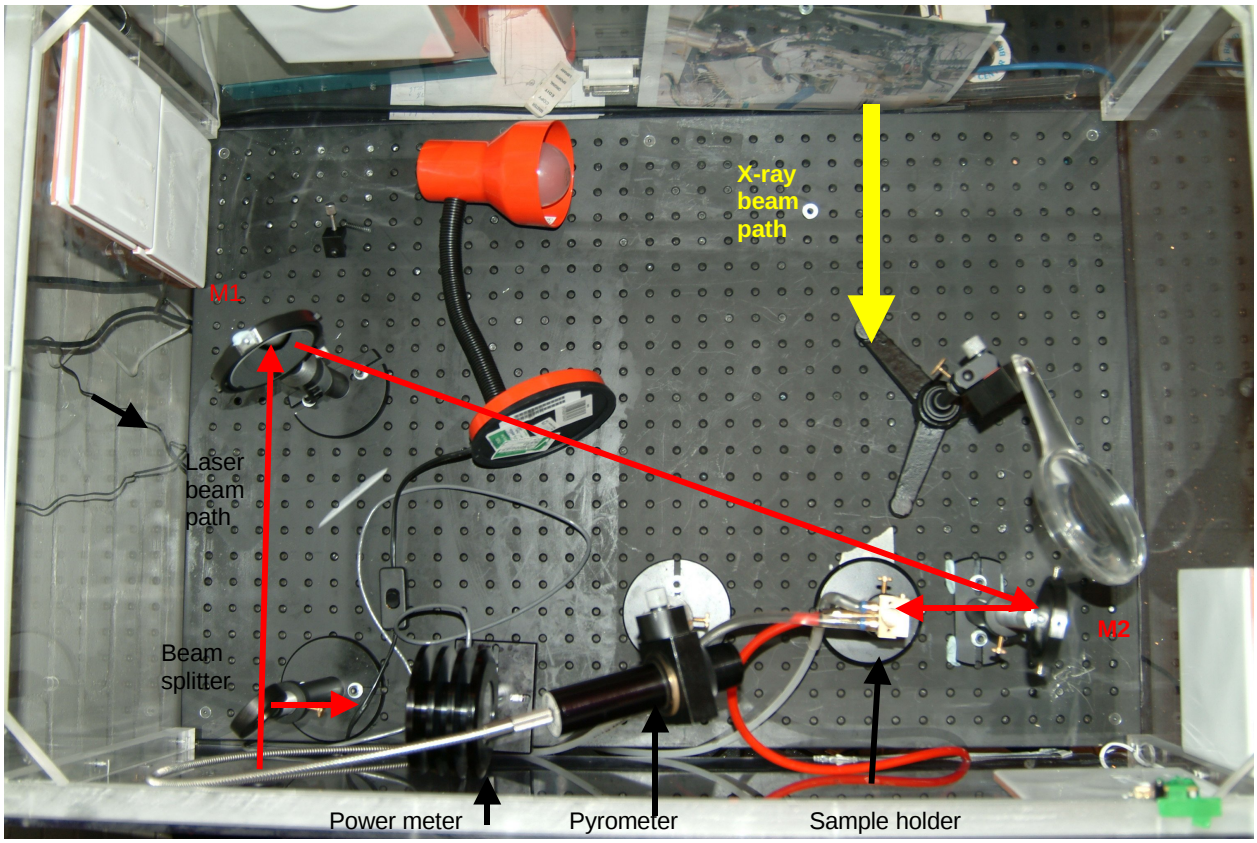


**Figure 1.4 Plan view looking into the Polycarbonate enclosure during furnace development.**

## 1.4 Polycarbonate box

The C02 laser is a class 4 laser, capable of producing 125 watts at 10.6µm, (see Chapter 12) To protect the local environment and users, a dedicated polycarbonate box was constructed to completely enclose the laser beam and optics, (Figure 1.3 and Figure 1.4).

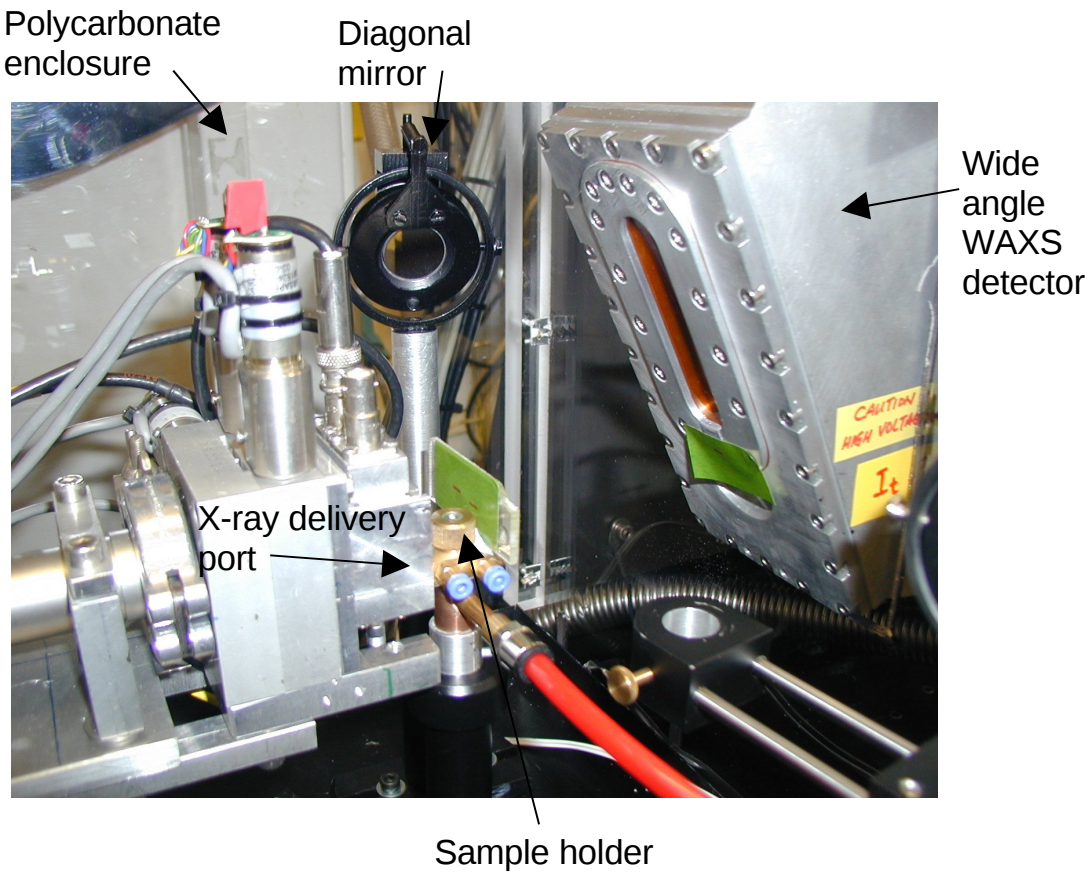


**Figure 1.5 Internal view of the Polycarbonate box during initial setup on the 6.2 beamline.**

The polycarbonate box was also adapted to incorporate the x-ray delivery tube and wide angle detector at the beamline (Figure 1.5). As part of the fabrication and to comply with safety protocol, all the access ports to the polycarbonate box were fitted with micro switches, which were subsequently wired into the station's interlock system.

### 1.5 Pyrometer mounts

Due to space limitations of the x-ray delivery port, and space restrictions between the sample holder and WAXS detector, the mounting of the optical pyrometer had to be fabricated in a way that enables the sample to be fixed at the focal point. This was achieved by support brackets straddling the delivery tube, enabling additional support and stability for the pyrometer during operation, as seen in Figure 3.8.

### 1.6 Sample Holder

The sample holder design and construction has had many alterations from the first initial trials. The details are given in Chapter 7. The final design is shown in Figure 1.5B and has reliably performed levitation under extreme conditions for many hours at a time.

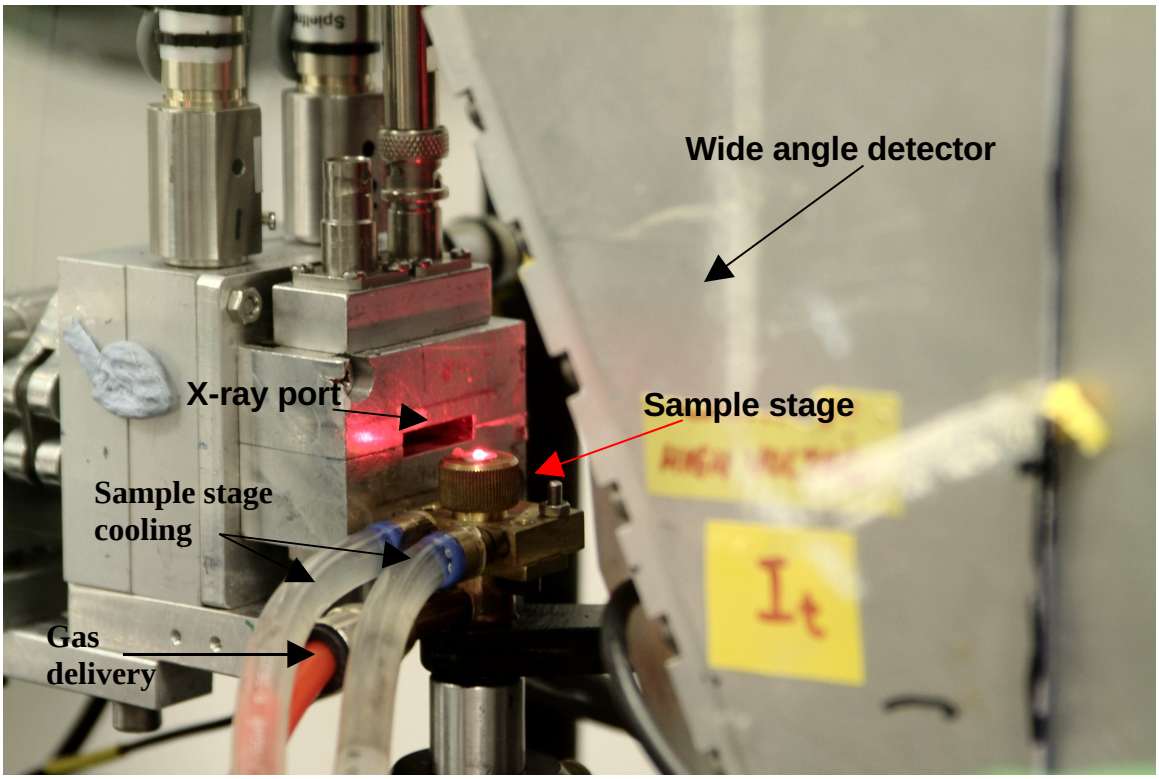


**Figure 1.6 Beamline view of the levitating furnace during setup, with the guide laser illuminating the levitating sample; also in view are the sample stage cooling pipes and the gas delivery pipes.**

### 1.7 Mirrors

The mirrors shown in Figure 1.5 also had radical design changes from the initial prototypes (see Chapter 6). Improvements were made in focusing and positioning, leading to customized focusing mirrors made of copper. The latest version incorporated remote control facilities for beam positioning on the levitating sample in the x-ray hutch on beamline 6.2 (Figure 6.7).

## 1.8 External interfacing

All other components of the furnace were located externally from the optics table, and were integrated with the SAXS/WAXS experiment which was designed to operate by computer remote control.

The other control devices, although they were not designed for this experiment, required substantial rewiring to enable them to be interfaced with the experimental x-ray hutch interlock system. More information can be found on the safety protocol in Chapter 12.

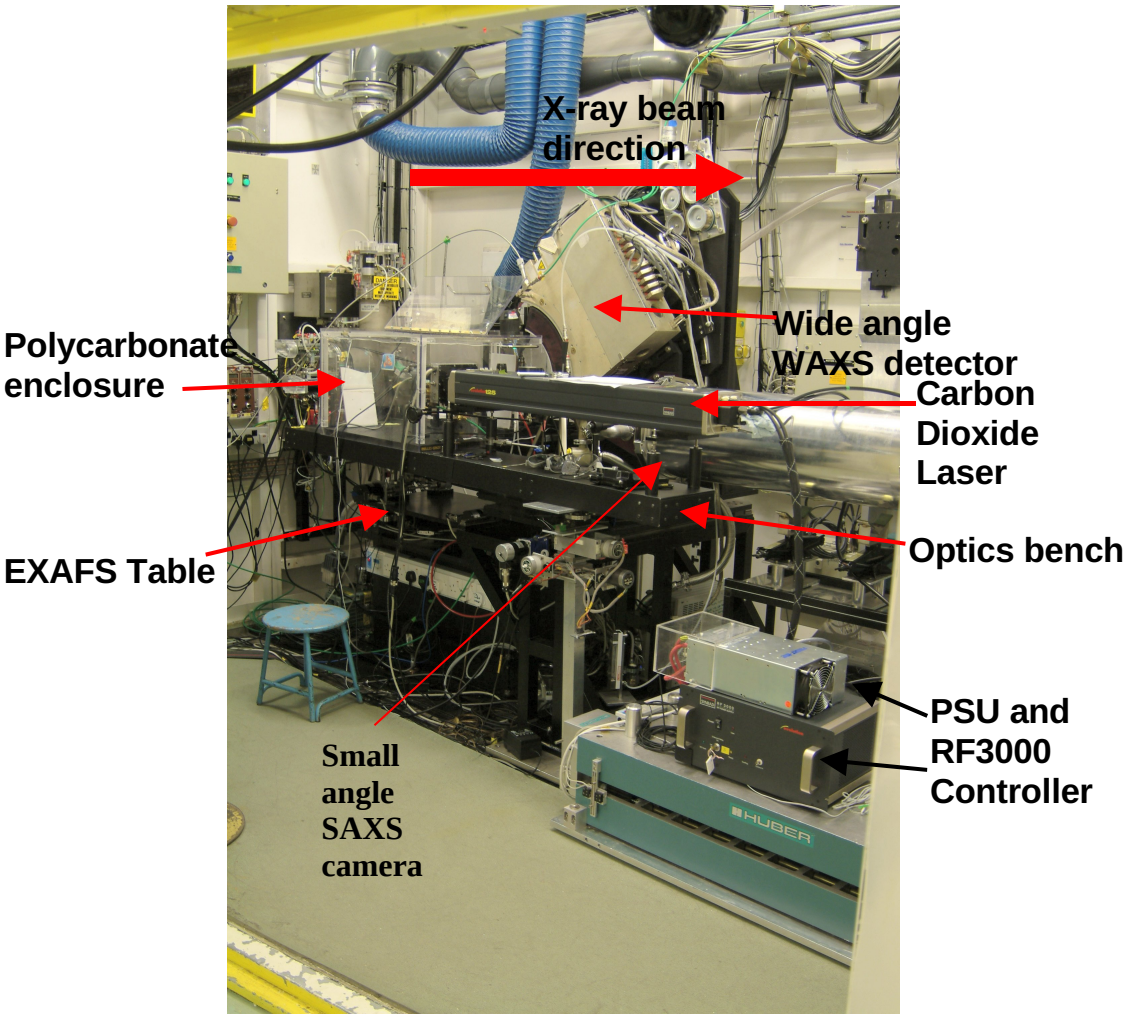


**Figure 1.7 Levitation furnace installed into the 6.2 beamline at Daresbury Laboratory**

The furnace and polycarbonate box are shown in Figure 1.6 assembled on the 6.2 SAXS/WAXS beamline at Daresbury Laboratory. The furnace was initially optically aligned in the experimental hutch. The control instrumentation was then removed and operated via its umbilical control cables.

These were routed via the station's labyrinth system to interface with the computers in the control room of beamline 6.2.

The following Chapters describe in detail the design and construction of the individual items associated with the high temperature experiments on molten alumina. They also include the advantages and problems encountered in the development, both before and following the installation onto the x-ray beamline on Daresbury Laboratory.

.

## 1.9 References

[1]. Structure of Liquid Aluminium Oxide, S. Ansell, S. Krishnan, J. K. R. Weber, J.J.Felton, P.C.Nordine, M.A.Beno, D.L.Price, M.L.Saboung Phys. Rev. Lett. **78,** 464 – 466(1997)

[2]. Development of a levitation cell for synchrotron radiation experiments at very high temperature, C.Landron, X.Launaya, J.C.Riffleta, P.Echeguta, Y.Augera, D.Ruffiera, J.P.Couturesa, M.Lemonierb, M.Gailhanoub, M.Bessiereb, D Bazinb and H.Dexpertb, Phys Res B.**124**, 627-632 (1997)

[3]. Aerodynamic laser heated contactless furnace for neutron scattering experiments at elevated temperatures, C.Landron, L.Hennet, J.P.Coutures, T.Jenkins, C.Aletru, G.N.Greaves, A.Soper and G.E.Derbyshire, Rev. Sci. Instrum. **71**, 1745-1751 (1999).

# Chapter 2

## Carbon Dioxide Laser

In this section, the experimental procedure required to heat up a range of samples, suitable for sample preparation, levitation and investigation, is discussed.

Several factors need to be considered

- Maximum temperatures that can be generated.
- Speed at which the temperature can be achieved.
- Controllability of the apparatus to give accurate sample temperatures during cooling process.
- Repeatability of the experiment.
- Portability.
- Size (the nozzle has space limitations) within the experimental area between the x-ray port and the detector head.
- Type of sample to be investigated.

To enable a 2mm sample of ceramic to be levitated in a container-less nozzle and rapidly heated to temperatures up to 3000K, followed by controllable cooling that will allow the (super cooled state) to be explored as well as crystallisation, requires demanding equipment design, construction and operation. Whilst the technique chosen for this experiment was a laser – heated aerodynamic levitator, consideration was also given to electromagnetic heating and levitation.

### 2.1 Inductive heating

Electromagnetic levitation was patented in 1923 by O.Muck [1]. The heating process is produced when an alternating current flows through two conically shaped coils powered by a high frequency power supply, as shown in Figure 2.1. The alternating electromagnetic field induces eddy currents within an

electrically conducting sample, producing a repulsive force against the primary electromagnetic field, simultaneously inducing a heating effect.

Previous experimentation by the Orléans group, who specialize in aerodynamic levitation, and the Cologne group, who specialize in liquid metal studies, have demonstrated that the system has limitations with the amount of heat that can be applied without sacrificing stability of the position of the sample within the magnetic field. This application also produces sample distortion, as the field heating effect deforms the spherical sample into an ellipsoid. This is due to high magnetic field amplitudes, low magnetic field gradients, high frequencies of 200 - 500 kHz, currents in the order of 100amps, and low electrical resistivity, for samples up to 5mm in diameter. Electromagnetic levitation is not suitable for our application, because of x-ray absorption limitations for WAXS and SAXS experiments, much smaller samples are needed as well as spherical shape and stability.

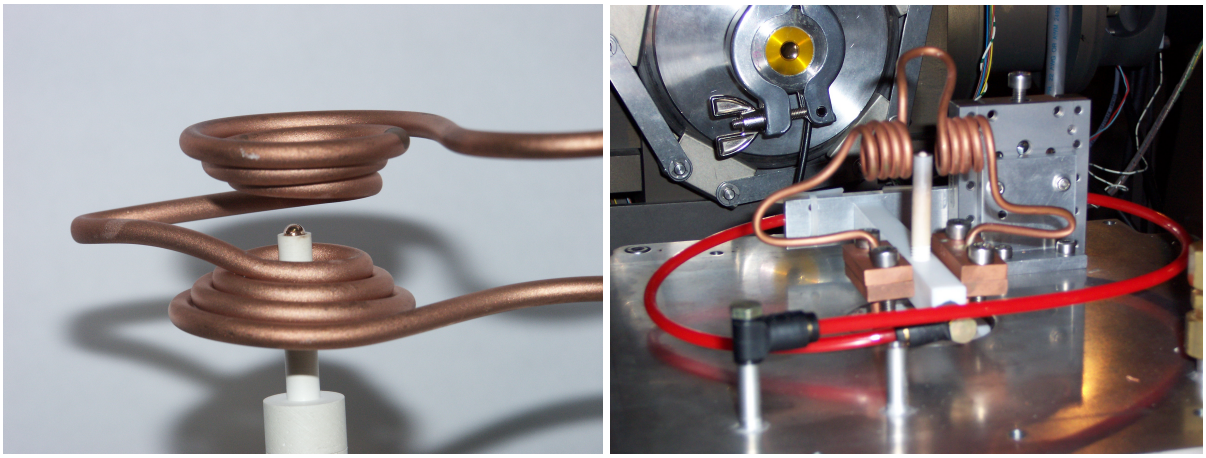

**Fig 2.1 Inductive heating and levitating techniques. Images courtesy of L.Hennet, CNRS, Orléans, France.**

## 2.2 Laser Operation

The next obvious heating application is by the use of lasers. The first ever laser was built in 1958; whilst they all work according to the same principle, they are differentiated on the bases of the medium they employ to create the laser action. In solid-state lasers, an electrical current pumps electrons into the laser medium – normally a semiconductor - exciting the electrons that are doped in the medium. Driven to a higher energy state, the condition known as population inversion occurs, the excited electrons quickly decay back into a lower energy state, releasing excess energy as photons. Carefully positioned mirrors reflect the photons hitting at normal incidence back and forth, in turn simulating other excited electrons to emit photons with identical wavelengths.

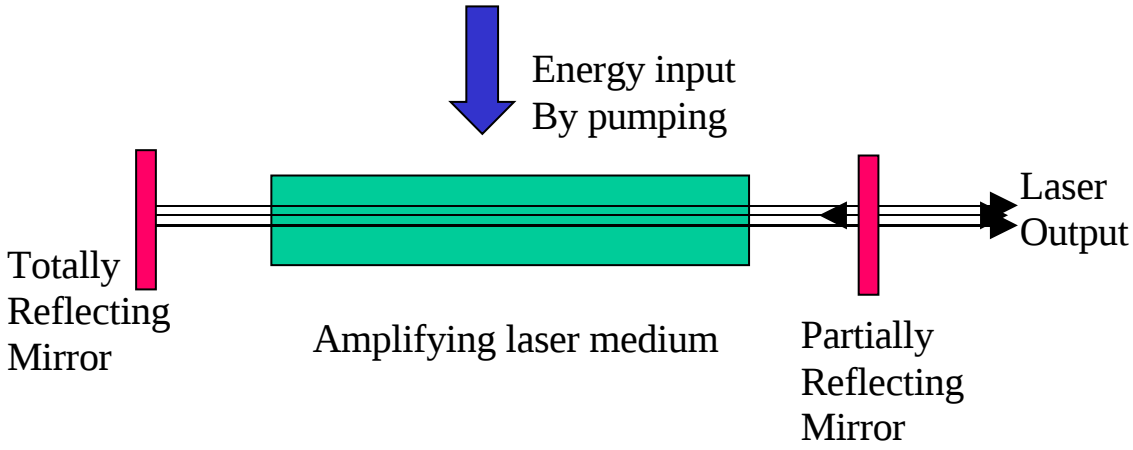


**Fig 2.2 Schematical laser operation**

Because the mirrors are of unequal reflectivity, the photons are eventually able to escape producing the laser beam. Gas lasers first appeared in the 1960's. They initially used a medium of helium and neon,

with carbon dioxide developed later. High voltages and high frequency electrical current creates an electrical discharge in a tube containing the gas medium. Gas lasers are generally the most powerful lasers and are used in a variety of military and industrial applications

Carbon Dioxide laser was the better option for melting ceramics, as the beam is focusable and more controllable over a range of temperatures, and beam delivery is continuous

**2.3 Synrad Evolution Laser**

A commercially available CO2 laser was specified for the aerodynamic levitation of alumina. This followed the development of a similar experimental method for use in an NMR experiment at Aberystwyth. This type of laser was capable of producing the infra-red intensities required, and could control the heating and melting of ceramics.

The operational specification of the laser gives an insight into how this laser interacts with the rest of the x –ray experiment.

Specifications of the Synrad Evolution 125 Watt CO2 Class 4 Laser.

- Wavelength 10.590nm (Infra Red)
- Power Output 400 Watts
- Power Stability -/+ 5%
- Beam Waist Size 4.4mm
- Polarization Vertical Linear
- Safety requirements Class 4 laser

Laser Interface



Laser Diode Indicator

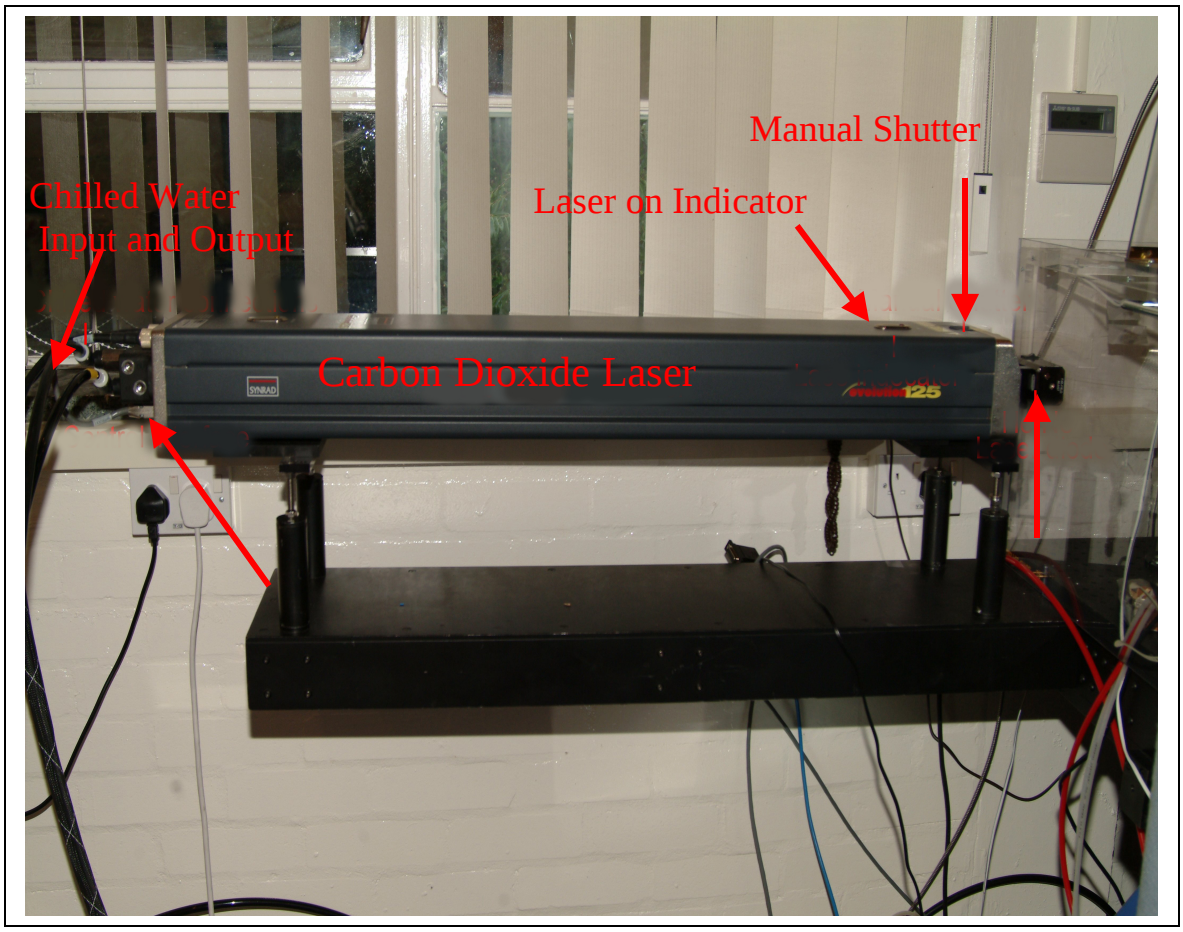


**Figure 2.3 Synrad Evolution laser attached via adjustable legs to optics bench.**

Laser Power rises from 0% duty cycle (tickle only) to a maximum at 95% duty cycle. Although the ratio of a laser's output to its power input is non linear, generally the laser output is approximately proportional to the Pulse Width Modulation duty cycle, and is adjustable across the range in 0.5% increments. This can be controlled manually with the UC2000 controller (Fig 2.6), or computer controlled via the LabVIEW software, as described later in Chapter 9.

## 2.4 RF3000 Laser Power Supply

Carbon Dioxide gas in the laser tube is excited by a 40.68 MHz radio frequency signal, which is applied to its electrodes by the RF3000 power supply.


**Figure 2.4 RF3000 controller and dedicated power supply**

The RF3000 converts the 30v input from the high current D.C. power supply into an R.F. signal by a Crystal Controlled Oscillator, which is then amplified by two parallel 600 watt amplifiers. The R.F signal from these amplifiers are subsequently routed to the electrodes in the laser head through the high power R.F. cables.

## 2.5 Environmental Control Facilities

The RF3000 also plays an important part in the environmental monitoring and control of the laser. Main Indicators are

1. Monitors cooling water flow and pressure in the head.
2. Interlock control of the laser and external devices interfaced onto the RF3000 to enable safe working conditions when the laser is operating (see Chapter 11 on Daresbury Interlock system).
3. Key Control, supplies D.C. power to the R.F. driver circuit to enable the laser to operate. Once the interlock system has been breached, full system key reset is required.
4. Power Indicators; Green indicates that D.C .power is available for the R.F. driver, illuminated when the D.C. voltage is applied.
5. Laser Ready Indicator, Illuminates Yellow when the key switch is activated, after a 5 second delay, lasing will begin when the control signal is applied.
6. Lasing, Illuminates Red to indicate operation, after the command signal is applied, and becomes brighter as the laser power increases.
7. The red indicator on the front of the RF3000 monitor's water pressure and temperature, as it passes through the laser head.
8. Cooling of the laser head and power supply is achieved by a circulatory chilled water system with a capability of delivering 2 gallons per minute with a minimum pressure of 70 P.S.I, to maintain a coolant temperature of between 18 – 22 degrees Celcius for a maximum heat load of 3 KW.
9. The heat generated by excited CO2 molecules is transferred to the bore walls of the tube by diffusion; the coolant path is enclosed in a corrosion-resistant stainless steel tube, which regulates the laser head temperature for maximum stability. Any drop in water pressure within the chilled water system will disable lasing.

Due to the operational layout of the x-ray beam experimental area and the control cabin, it is not practical to have the RF3000 within the control area, so monitoring of vital services for the laser head is not possible during the experiment; this includes key enable and reset of the laser beam. All these facilities were duplicated so remote monitoring was possible from the control cabin as described later in this Chapter.

**Aberystwyth chilled water system**

This was designed as a re-circulatory system with a pressure of 120psi, with a total capacity of 100 gallons. The chilling system has the facility to run several experiments simultaneously.

**Daresbury system**

Similar in principle to Aberystwyth's plant, but working on a re-circulating demineralised pressure water system that had a much larger capacity. It also operated at 120psi, feeding into a heat exchanger, running off an independent pump and chiller unit. This additional capacity has been useful on the beam line when the laser is operational for hours at a time.

**Figure 2.5A Chilled water pump unit for regulating temperature through the heat exchanger.**

**Figure 2.5B Heat exchanger for dissipating heat from the laser head through the demineralised water system at Daresbury Laboratory**

## 2.6 UC2000 Laser Controller


technical reference

**General specifications**

Table 3-9 UC-2000 general specifications

| Parameter | | |
|---|---|---|
| **UC-2000 Specifications** | | |
| Power Input | 15–50 VDC, 35 mA max. | |
| PWM Output | 100 mA, 50 Ω CMOS driver | |
| Gate Input | TTL or CMOS compatible, logic low 0–+0.9 VDC (laser off), logic high +2.8–+5.0 VDC (laser on) | |
| Gate On Time, min. In closed loop mode | 1 PWM pulse period >10 ms | |
| Clock Frequency | ±10% accuracy | |
| **Environmental Specifications** | | |
| Operating Temperature | 0°C–40°C | |
| Humidity | 0–80%, non-condensing | |
| **Physical Specifications** | | |
| Length | 17.79 cm | (7.00 in.) |
| Width | 10.74 cm | (4.23 in.) |
| Height | 5.33 cm | (2.10 in.) |
| Weight | 0.52 kg | (1.14 lbs) |
| **UC-2000 Operating Modes** | | |
| Standby | Input: none | Output: 1 µs, 5 kHz Tickle signal |
| Manual | Input: *PWM Adj Knob* | Output: 1 µs, 5 kHz Tickle signal, 0–95% (or 99%) PWM duty cycle signal at 5, 10, or 20 kHz |
| ANC | Input: 4–20 mA current, ±5%, 100 mA max, Input resistance=220 Ω to ground | Output: 1 µs, 5 kHz Tickle signal @ 4 mA, to 99% PWM duty cycle signal at 5, 10, or 20 kHz @ 20 mA |
| ANV | Input: 0–10 VDC, ±5%, +15 VDC max, Input resistance=10 kΩ to ground | Output: 1 µs, 5 kHz Tickle signal @ 0 V (<100 mV), to 99% PWM duty cycle signal at 5, 10, or 20 kHz @10 VDC |
| Man. Closed | Input: *PWM Adj Knob* | Output: 1 µs, 5 kHz Tickle signal, 0–99% PWM duty cycle signal at 5, 10, or 20 kHz |
| ANV Closed | Input: 0–10 VDC, ±5%, +15 VDC max, Input resistance=10 kΩ to ground | Output: 1 µs, 5 kHz Tickle signal @ 0 V (<100 mV), to 99% PWM duty cycle signal at 5, 10, or 20 kHz @10 VDC |
| Remote | Input: software commands via RS232 serial port protocols | Output: Manual, ANC, ANV, Man. Closed or ANV Closed mode signal |



**Figure 2.6 UC-2000 laser controller incorporating manual and remote control of the laser.**

The main control system of the CO2 laser, with all laser and interlocks operational, the UC2000 allows accurate heating of the sample in manual or remote mode.

### Standby Mode

During standby operation, (power applied to the UC2000 controller with the laser indicator off), the UC2000 sends out a 5khz pulse to pre ionise the laser gas to just below the lasing threshold, which allows the laser to respond instantaneously to command signals over a whole range of laser powers as the beam is switched on or off during experimental operations.

### Remote Mode

In the remote mode, a computer is used to control the desired laser output; the operating mode is controlled via an RS232 serial Communication link.

Once in the remote mode, the PWM laser adjust knob and laser off/on pushbutton are disabled, but the LCD display continues to display the current value of laser power used,

Extreme Caution needs to be taken in this mode; if programming is incorrect, this mode can result in 95% laser power instantaneously!! This area is covered as part of the failsafe coverage in Chapter 9.

**Analogue Voltage control**

In the control environment, the laser power and accuracy is paramount to the successful heating and melting and controlled cooling of the experimental samples. In the remote mode using the LabVIEW programming via an RS232 link, certain anomalies were observed causing sporadic spikes during the controlled cooling. These spikes were enough to critically de-stabilize the sample structure whilst levitating in the liquid state or whilst cooling in the super-cooled state causing the sample to crystallise.

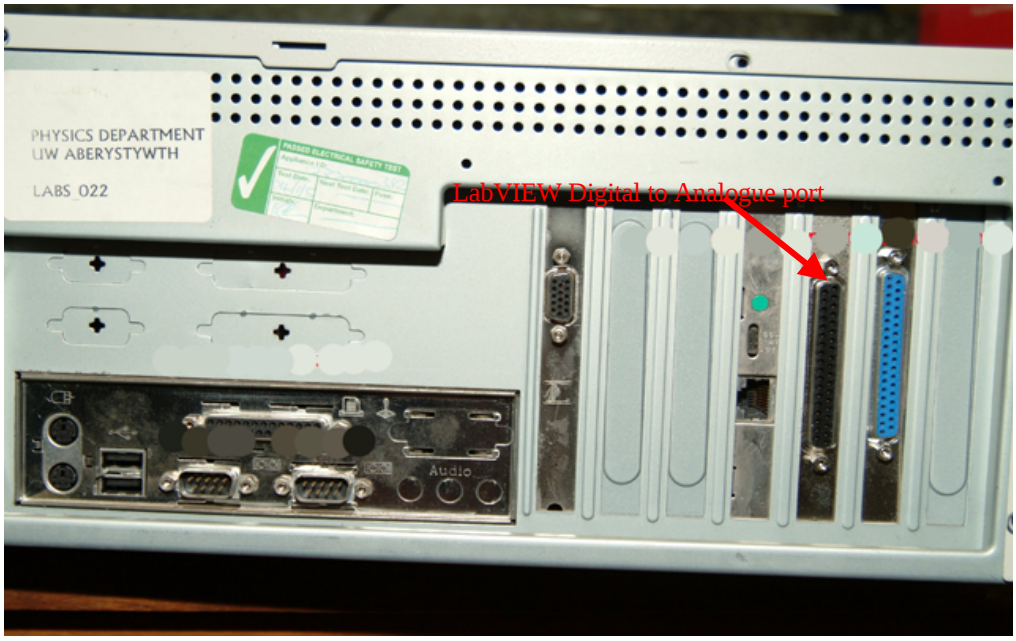


**Figure 2.7 Computer serial communication serial ports and LabVIEW digital to analogue communications port.**

With the installation of a National Instruments LabVIEW Digital to Analogue card into the computer, it is now capable of producing a linear 0 – 10volt D.C voltage (see Chapter 9). The software produced a voltage that was fed into the ANC input of the UC2000, allowing equally accurate control of the laser,

without the systematic problems, which arose from communications conflict between the two serial communications ports, due to the (IRQ) protocol used on the computer, (see Chapter 5).

LabVIEW software was then used to control the whole of the laser operations, including initial communications protocol, system operations and safety features. This is discussed in greater detail in Chapter 9.

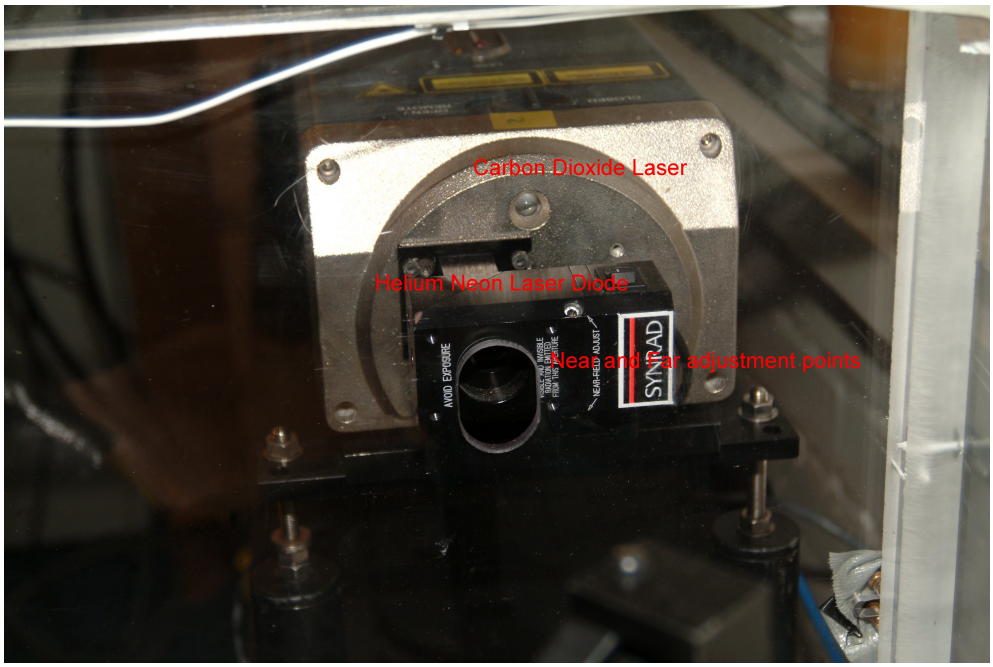


**Figure 2.8 Externally coupled laser diode used for optical alignment of the carbon dioxide laser.**

## 2.7 Laser Diode

Specification

Wavelength 650nm

Power output 5mw

Beam Diameter <3mm

Class 3A Laser product

Externally coupled onto the front of the CO2 laser.

The purpose of the laser diode is as follows

1. Enables all the optics to be aligned without the use of the CO2 laser.
2. Enables the optics to be aligned with the sample.
3. Illuminates the sample during set-up in the x-ray experimental area.

The laser diode pointer consists of a housing containing a Zinc Selenide beam combiner, which allows the simultaneous transmission of both laser beams along the same axis.
The angle of the combiner is adjustable for establishing near and far field coincidence between the CO2 laser and the laser diode beam.

For experimental alignment of the Carbon dioxide laser on the Beam line, see Chapter 8

**2.8 Auxiliary Signal Connector**

(9 way D-type) Provides output drive signals for several indicators from the RF3000:-

- Key switch.
- Laser ready.
- Lase.
- Over Temperature.
- D.C. Power In.

This connector has been essential as it has allowed the production of a remote monitoring box indicating the status level of the RF3000, which can be monitored remotely in the control cabin at the x-ray beam line.


**Figure 2.9 Remote monitoring indicator box for showing RF3000 and laser status; also included is solenoid activation indicator to confirm that the shutter is operational**.

Another useful feature of this connector is the accessibility of the interlock system.

Factory fitting allows normal use of the laser with interlocking (by the use of a 9 way D type connector). By adaptation of this socket, access to the control of the internal shutter of the CO2 laser and the separate laser pointer is allowed, by interfacing this into the control circuitry of the Daresbury synchrotron interlock system. This allows safe working procedures to be implemented (see wiring diagram and Daresbury interlock provision in Chapter11).

**Remote Terminals**

Located on the rear of the RF3000, are inputs from external interlocks. These have been coupled directly to the three safety micro switches situated on the access ports of the polycarbonate safety box, which in turn is also coupled to the interlock system of the 6.2 beam line hutch. Any breach of these switches will automatically close the internal shutters on the CO2 laser, requiring a full system reset on the laser to resume normal operation.

**Control In**

This receives pulse width modulation control commands from the UC2000, which controls the Laser output power.

**Laser Interlock Circuit**

This section deals with the circuitry in the RF3000 as it interrupts laser operation if any critical parameter is violated during operation and running of the CO2 Laser.

Switches and sensors in the RF3000 and in the laser head continuously monitor various conditions and parameters before and during operation. If violated, posing a risk of potential danger to the laser and possible subsequent physical injury to the operator, the laser is shut down.

In particular, laser operation is interrupted or because of operational response to the following conditions.

1. Laser aperture shutter closed. (Electromagnetic and manual shutter and indicator situated on top of the laser).
2. Coolant flow switch open (insufficient Flow).

   Temperature Switch open (excessive heat flow in the laser head or RF3000).
3. R.F. cables are not connected.
4. Remote interlock jumpers are open or not connected.
5. Door interlocks interrupted.
6. Polycarbonate experimental laser box and lid interrupted.
7. Daresbury Laser shutter box interrupted (more details in Chapter 10).
8. Experimental hutch interlock breached (more on this in Chapter 11).

With all these parameters in place, safe experimental operation of the laser can proceed. More information on the setup sequence is given in Chapter 11.

## 2.9 Conclusions

The carbon dioxide laser has proved very reliable and efficient in the delivery of laser power over the whole experimental research campaign (Chapter 12). Initially beam delivery and alignment with the sample was a problem as the laser beam needed to be split, focused then realigned onto the sample. This set up was problematic on the optics bench at Aberystwyth, so alignment would be critical on the beam line to get high enough intensities with limited space.

Initial interference spikes from the computer were also a major problem, as experiments needed to operate within the lower 5% range of the laser, making stable laser power critical. With some adaptation of the LabVIEW control computer and a laser power meter these instabilities were eliminated.

The LabVIEW software operation has been reliable over the whole experiment. One section of the laser control will need to be adapted to give higher laser intensities as laser power is “limited” to 30% laser power maximum, due to the “burn out” of the secondary mirrors. This can be rectified by the introduction of copper secondary mirrors that can dissipate heat, (this is discussed further in Chapter 6) which will allow temperatures in excess of 3000 degrees.

## 2.10 References

[1] O.Muck. German patent No **42204** (Oct 30, 1923)

# Chapter 3

## Optical Pyrometry

Many methods are available for measuring high temperatures, of which optical pyrometry enable this to be done effectively without contact with the specimen. The various samples of ceramic that are used in these experiments have spherical shape with optimum sizes of 1.5 > 2.0mm and are levitated contactlessly on a cushion of inert gas. The sample, although mechanically stable within its container-less nozzle, can reach temperatures as high as 3000 K within seconds. Stability is optimised particularly in the molten and super cooled states, so that an X-ray beam can be passed through the sample at high temperatures. The diffraction of X-rays in the liquid drop is measured by small SAXS, and wide angle WAXS detectors. Temperature measurement has to be compatible with aerodynamic levitation, laser heating and SAXS and WAXS detection.

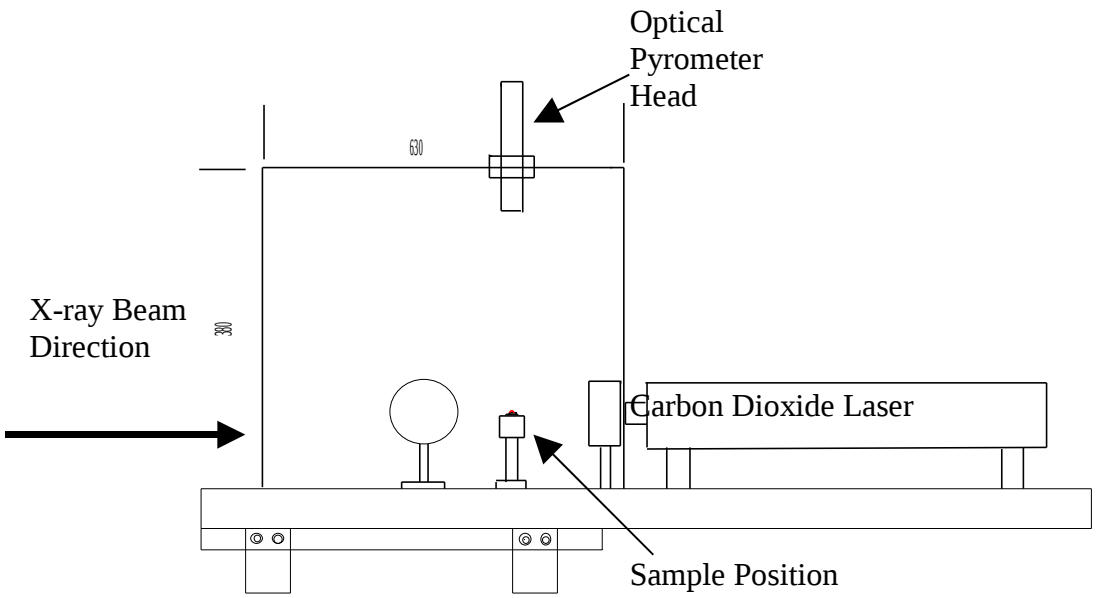


**Figure 3.1 Position of the optical pyrometer head with respect to the high temperature levitating sample**

## 3.1 Choice of optical pyrometry.

The factors that needed to be taken into consideration when attempting to measure the temperature of levitated liquids.

1. The method and measurement of temperatures up to 3000K.
2. Response of the sensor to temperature fluctuations.
3. The size of the sensor head for measurement.
4. The measuring environment for x-ray experiments.

The original idea was to use an industrial thermometer, normally used for temperature collection in steel furnaces. This was capable of handling the extreme temperatures associated with the levitation experiment, but was dismissed due to the large size of the detector head.

Infra red optical pyrometry initially looked the better option as the head reader was remote from the experimental setup, thereby saving on space. However, infra red thermometers were not capable of reading ultra high temperatures.

Optical pyrometry is a well established passive, non-contact thermometry technique in which thermal radiation emitted from a target is detected and the temperature is determined from the black body radiation spectrum.

## 3.2 Black Body Radiation

A “black body” is a theoretical perfect absorber, which absorbs radiation of all wavelengths falling on it. It reflects no light at normal temperatures and thus appears black.

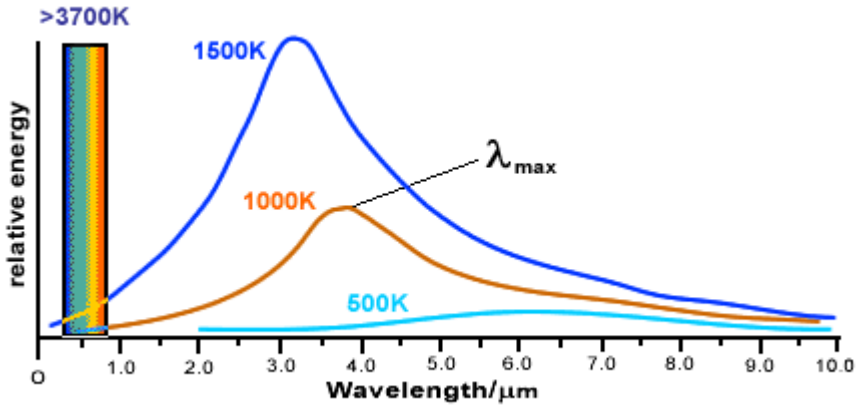


**Figure 3.2 Graph illustrating relationship between relative energy and wavelength [1].**

The higher the temperature of a black body, the more energy is emitted in each band of wavelengths. Radiation emitted at the highest intensity, represented by the peak of the spectrum, does not fall in the visible region unless the temperature is very high, typically over 3700$K$ [1].

### 3.3 Luxtron Optical Pyrometer.

Optical pyrometry therefore looked the best option. A range from Luxtron, a calibrated machine capable of auto ranging functions up to 3000 degrees, with a range of heat sensitive heads for different applications, was chosen.

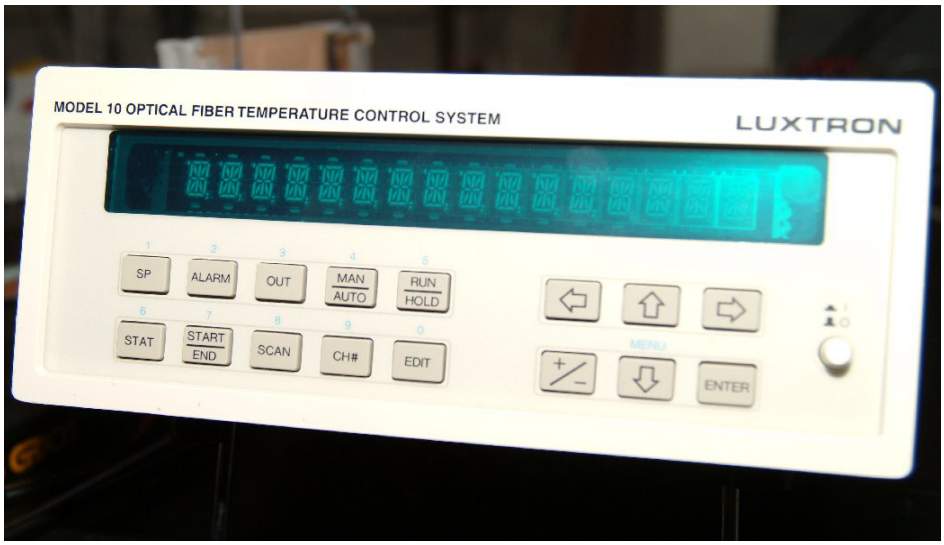


**Figure 3.3 Luxtron optical pyrometer**

## Specification

1. Temperature range 450 to 3000 Degrees Celsius.
2. Wavelength 950nm.
3. Resolution .01 C at 1000 Degrees Celsius.
4. Repeatability 0.01%.
5. Accuracy 0.2% of Readings.
6. Bandwidth 0.1Hz to 10Hz.
7. Sampling rate 30 measurements per second.

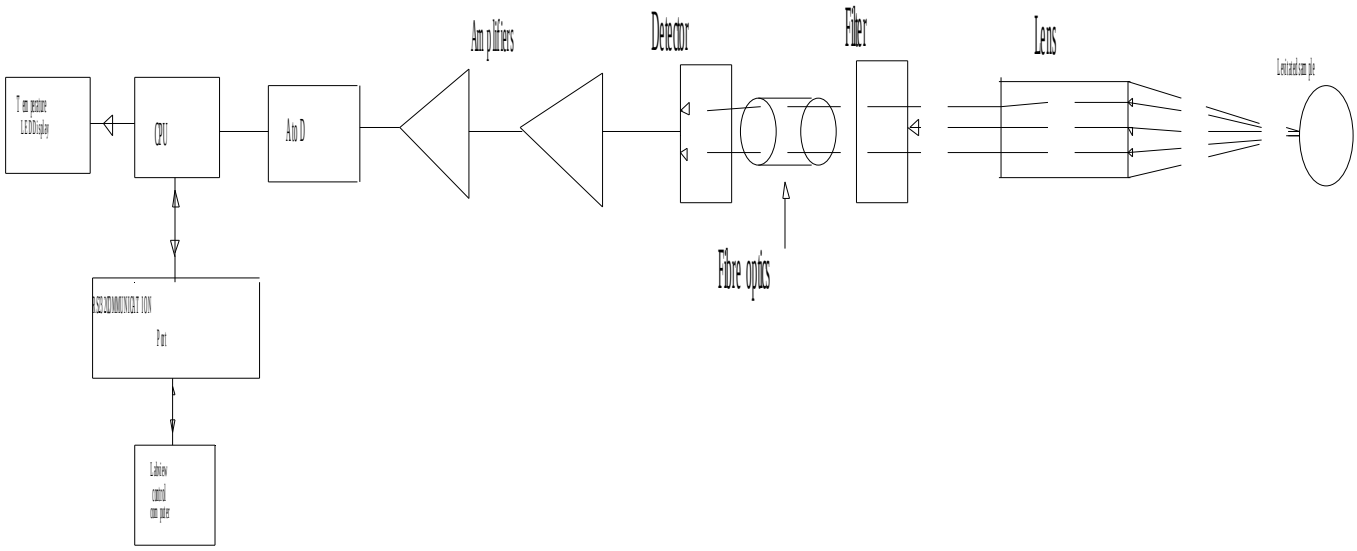


**Figure 3.4 Schematic block diagram of the operation of the Luxtron Optical Pyrometer.**

## 3.4 Basic pyrometer operation

All pyrometers have some form of light collection optics, to capture the thermal radiation emitted from the sample being heated. The infra red radiation is first passed through a filter tuned to the detector wavelength of 950nm. A high efficiency optical system maximises the number of photons reaching the detector, this is achieved

by the use of a fibre optics system, which allows flexibility of the apparatus orientation within the experiment. The detector converts the infra red energy into an electrical signal , which goes through various amplification stages, before being digitised. This signal is then processed via an algorithm to produce a digital output display temperature measurement.

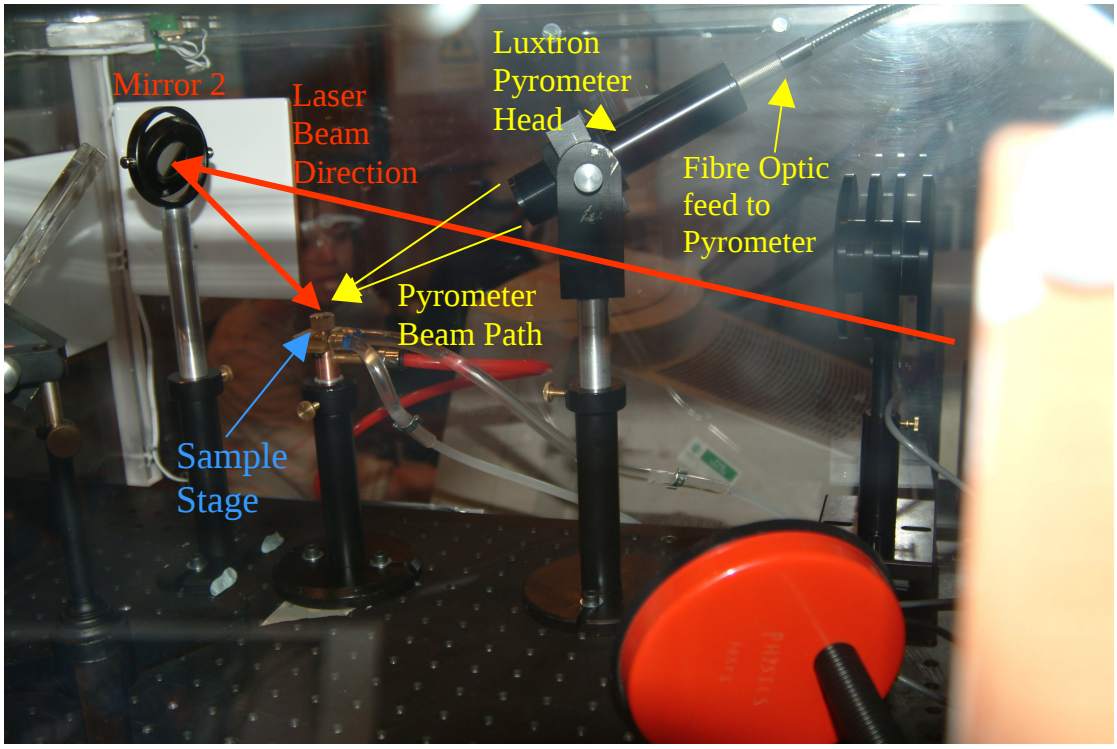


**Figure 3.5 Initial development layout of the pyrometer position prior to beamline installation.**

## 3.5 Pyrometer input options.

Optical Pyrometry

Thermocouple input

R.S.232 Communication

The pyrometer was positioned in the optical system so that the head was positioned at a focal length of 15.2 cm from the levitating sample. This was also optimised so that no damage could be done to the head due to overheating from the sample, and the detector head not too far away to pick up radiant heat from other sources which could be produced by the laser. Due to the sample size of 2mm, an optical system capable of focusing onto a levitated sample was the preferred option.

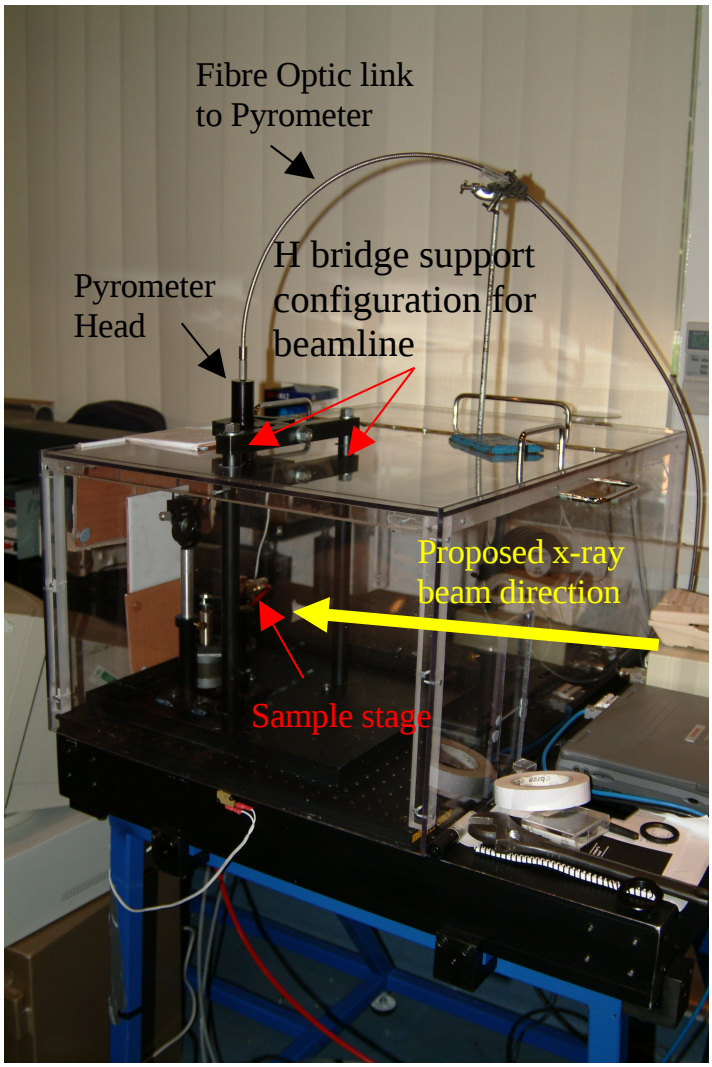


**Figure 3.6 Final position using a H bridge support enabling the pyrometer to straddle the x- ray delivery tube.**

Using a 3 metre dedicated fibre optic cable, allowed the control instrumentation of the pyrometer to be located externally to the polycarbonate safety enclosure.

### 3.6 Sample alignment.

This proved to be problematic initially, as focusing of the pyrometer onto the levitating sample was not accurate enough. Although stable sample levitation was obtainable, pyrometer positioning could result in temperature swings of several hundred degrees.

One method proposed for alignment was the use of a micrometer screw-gauge platform that could accurately focus the pyrometer head onto a portion of the curved sample. Without a sighting method, repeating this alignment for different samples, proved to be unworkable.

The optical pyrometer head is a complex series of filters and lenses, which focus the infra-red radiation onto the light tube, the optical fibre then carries that proportional intensity to the detector head located in the main body of the Luxtron pyrometer. If this information could be intercepted, and by some reverse engineering, i.e. shining a light down the fibre optic cable in the reverse direction, through the optical pyrometer and onto the sample, then a more accurate means of alignment and measurement was possible.

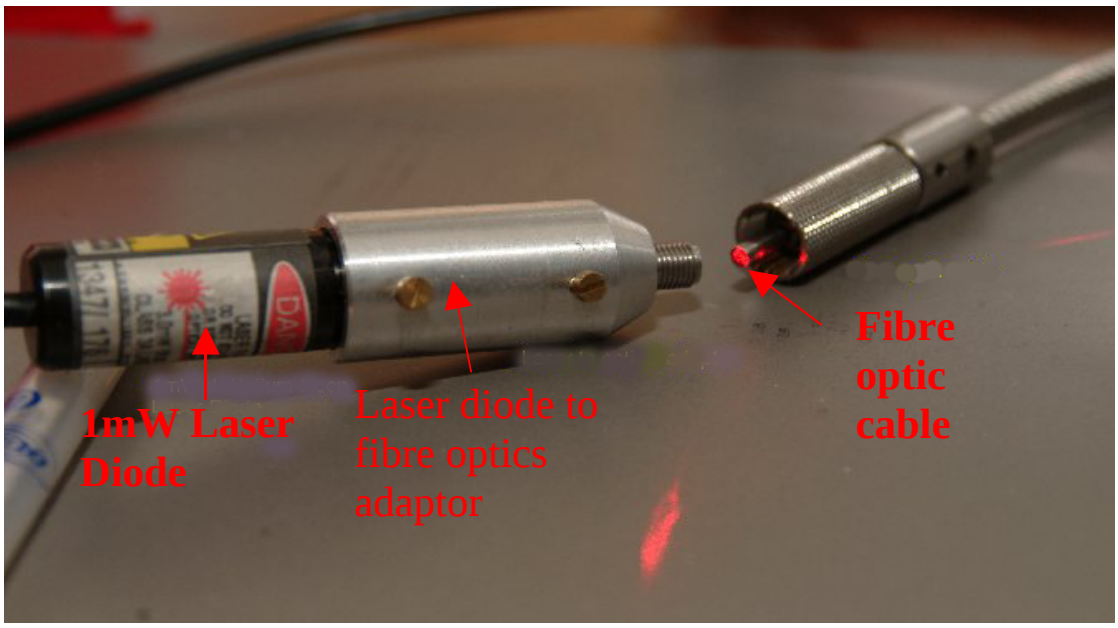


**Figure 3.7 Laser diode adaptor used for optical pyrometer alignment onto the levitating sample.**

By using a dedicated adaptor, a 1mW laser diode, a bright parallel beam can be passed down the fibre optic cable, as can be seen in Figure3.7. This facility has two advantages:-

1. The focusing element on the Luxtron head can also be used for focusing the infra-red radiation onto the fibre optic; it can also be employed in the reverse direction, to focus the laser diode beam onto the sample.
2. The laser diode beam can be accurately positioned by inspection onto the sample, as the beam width is only 1mm wide i.e. smaller than the levitating drops.

This practical solution now saves hours of setup time, with repeatable results for different experiments.

### 3.7 Daresbury synchrotron experimentation.

Initial installation inspections to incorporate the levitation furnace onto the 6.2 Beamline, physical dimensions would not allow freedom of movement of the optical pyrometer within the experimental polycarbonate box. This was due to the close proximity of the synchrotron beam delivery tube and the focal position of the wide angle WAXS detector.

A new configuration was adopted by positioning the pyrometer head in the vertical plane on a H Figure support stand. Incorporated into this were lateral adjustments for more accurate positioning of the pyrometer onto the sample, thereby providing greater stability for the head, and a clear access for the CO2 laser beam, and other instruments associated with the experiment, as can be seen in Figure3.7.

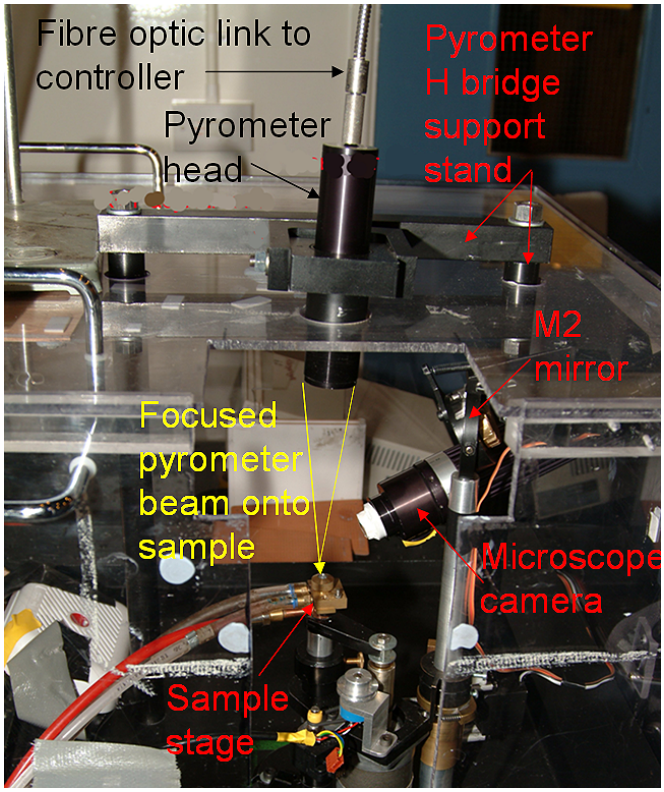


**Figure 3.8 H bridge pyrometer configuration suitable for straddling x-ray delivery tube.**

### 3.8 LabVIEW.

As with all experimental techniques, computational techniques are needed to control experiments, particularly where remote operation is required.

LabVIEW is now becoming recognised as the industry standard for external control of instrumentation, and to be read by RS232 communication protocol. Temperature measurements of the sample to be read via the optical pyrometer and to integrate the results as part of the computer control programme (see Chapter 9).

The RS232 serial link allows the Luxtron pyrometer to connect to a host computer, or “data terminal equipment” (DTE) and is therefore configured as a “data communication equipment” (DCE) device, allowing the transmission of all temperature data collected. The Luxtron pyrometer sends data to the computer every 100 mS. The other limits being set by the speed of the RS232 interface which is set at set at a 9600baud.

Regardless of the mode used, once power up and internal calibrations are set, the Luxtron pyrometer will send “ACCUFIBER M10” across the RS232 link (Figure 3.9), this enables the identification of communication protocols transmitted by the pyrometer.

Diagram of cable connections.

| Pin No. | Name | Notes/Description |
|---|---|---|
| 1 | DCD | Data Carrier Detect |
| 2 | RD | Receive Data (a.k.a RxD, Rx) |
| 3 | TD | Transmit Data (a.k.a TxD, Tx) |
| 4 | DTR | Data Terminal Ready |
| 5 | SGND | Ground |
| 6 | DSR | Data Set Ready |
| 7 | RTS | Request To Send |
| 8 | CTS | Clear To Send |
| 9 | RI | Ring Indicator |

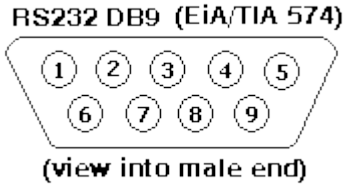


**Figure 3.9 RS232 pin identification and protocol**

Serial ports are a type of computer interface that complies with the RS232 standard. They are 9-pin connectors that relay information, incoming or outgoing, one byte at a time. Each byte is broken up into a series of eight bits, hence the term serial port.

Communication protocol for devices configured to use serial ports COM 1 and COM 3 could not be active at the same time, as they shared interrupt IRQ 4. The same was true of COM 2 and COM 4 port devices, this was another reason that the alternative LabVIEW board was installed.

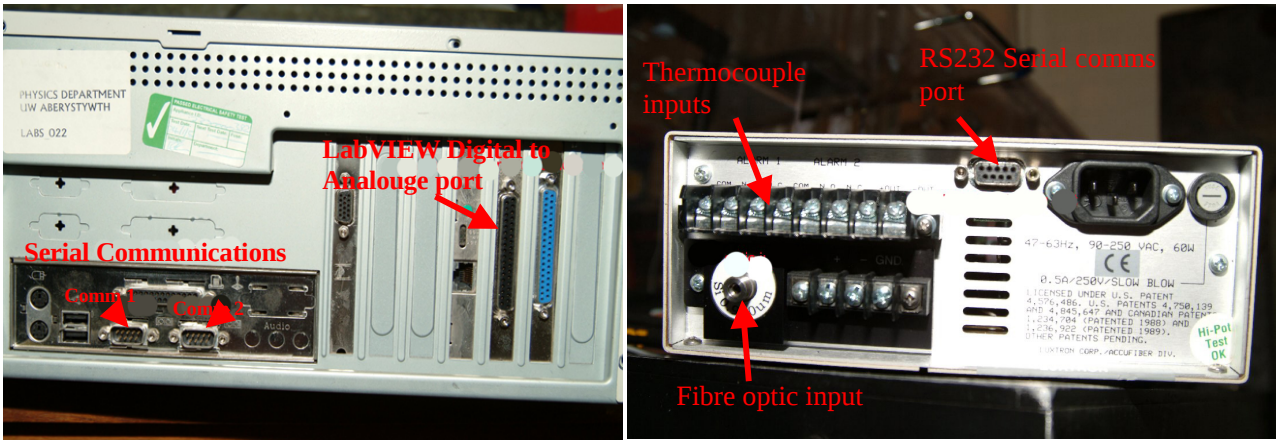


**Figure 4.0 Computer port communication and Luxtron communication facilities**

### 3.9 Conclusions

Alignment of the pyrometer is critical for accurate temperature readings of the sample. Inaccurate positioning can otherwise result in discrepancies of hundreds of degrees. This is especially critical when the sample is in the super cooled-region, where real changes in temperature on this scale, can cause the sample to re-crystallize from the liquid state.

The small spot size of the pyrometer will also give a reading on only one part of the levitated sample, reinforcing the need for sample mechanical stability and accurate pyrometer positioning. The installation of a second pyrometer operating at a different wavelength, and focused at a different point on the sample would help monitor sample temperatures more comprehensively during the melting, super cooling and crystallisation.

Future upgrades to the Aberystwyth aerodynamic levitator furnace include incorporating serial to USB adaptors for improved instrumentation communication.

As the Luxtron instrument is also capable of measuring temperatures from thermocouples, these could be incorporated into the sample stage for more effective monitoring of the experimental environment.

### 3.10 References.

[1] Black Body Radiation, Thinkquest. http://library.thinkquest.org.

**Insert calibration cert luxtron here**

# Chapter 4

## Mass Flow Controller

In this section, the supply of inert gas to the nozzle for sample levitation will be discussed.

The stable levitation of the sample is critical to the experimental process for two main reasons.

1. Homogeneous heating of the samples
2. Accurate positioning of the x-ray source through the sample

Different means of gas delivery have been investigated.

### 4.1 Volume reservoir

This system uses a volume of gas stored in a tank reservoir fed from a pressurized gas cylinder, a gas regulator that decreases the pressure from 3000 psi to a variable low volume. As the reservoir fills, this delivers a measured volume to the nozzle.

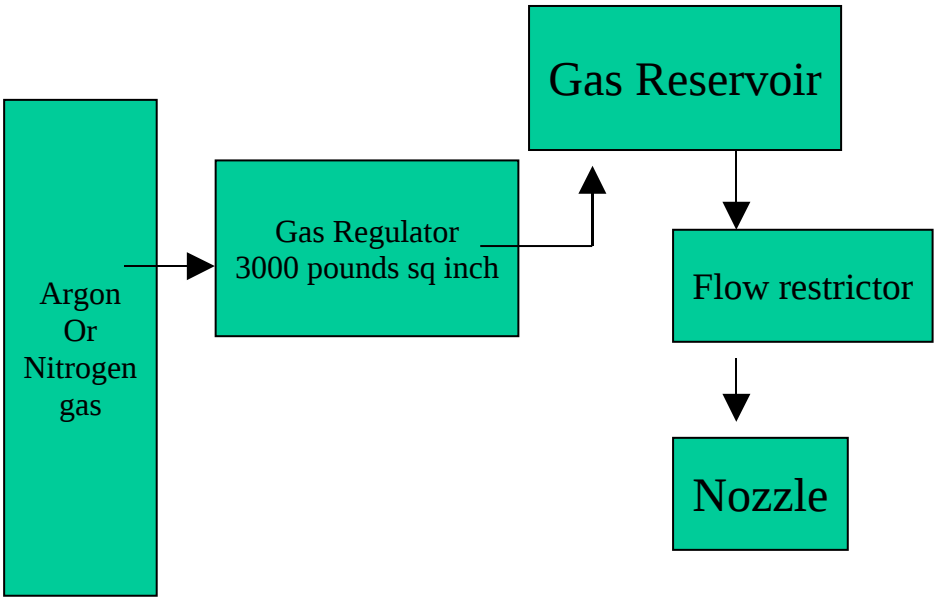


**Figure 4.1 Schematic layout requirements of controlled gas delivery for levitation.**

This system works well as a buffering tank and is controllable via the flow restrictor, but it has its limitations, as it does not have the ability to control the flow accurately, and is not responsive enough to cater with the erratic instabilities in the sample as it goes through the transition phase between solid and liquid.

### 4.2 Brooks Mass flow controller

The Brooks Smart mass flow controller is the preferred choice as it has the ability to provide accurate delivery and measurement of gas flows. The Smart DDE model is a powerful Dynamic Data Exchange software product allowing bi-directional communication between the mass flow controller and the computer.

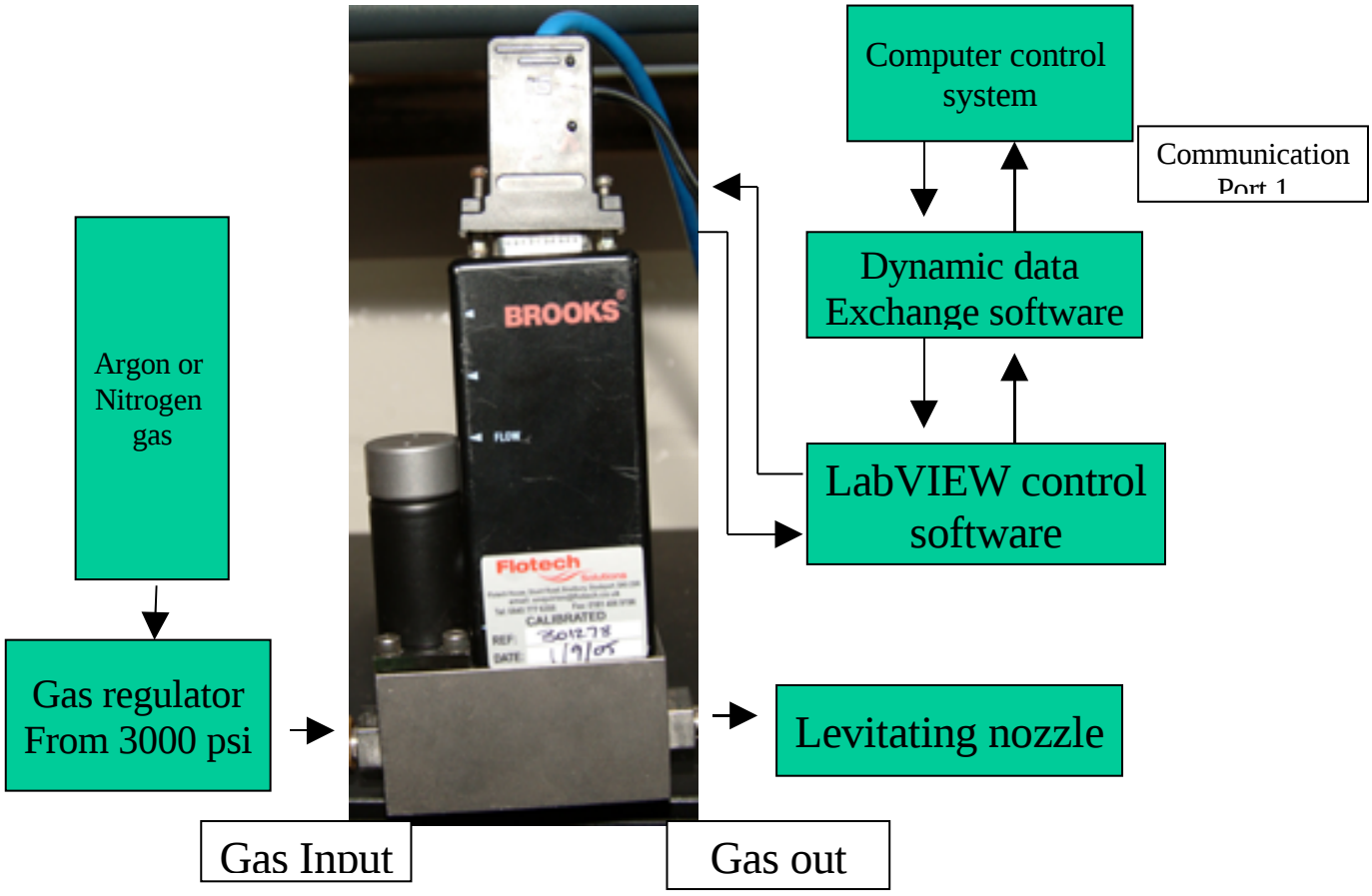


**Figure 4.2 Schematic operation of the Brooks Mass flow controller, enabling controlled delivery of gas to the sample head for levitation.**

### 4.3 Description of Mass Flow Controller

The heart of this system is the Thermal mass flow sensor, which produces an electrical output signal as a function of flow rate.

| **Mass Flow Controller** | **Flow ranges** | |
|---|---|---|
| **Model** | **min.** | **max.** |
| ***5850S*** | ***0.003 l/min*** | ***30 l/min*** |

The supplied inlet adaptor has a built-in, upstream inlet filter for flow straightening. Besides reducing the effects of changes in upstream piping, this also protects the measuring element from occasional debris in the flow stream, and also eliminates the need for additional inlet filtering.
Output dampening provides a constant scale reading under fluctuating flow rate conditions.
Output limiting prevents possible damage to the delicate acquisition devices by limiting the voltage signal output to 0 – 5.25v dc and 0-21 mA on the output current, thus preventing the system from being over driven.
An inert gas such as nitrogen or argon is used to levitate the sample in the aerodynamic furnace. This gas is delivered to the mass flow controller via a two-stage regulator which reduces the pressure from 3000 psi to 15 psi / 1 bar, but typically 3 l/min for levitation is used. The thermal mass flow sensor provides an electrical output signal as a function of flow rate. A microprocessor based on a stand-alone control valve module can deliver stable gas flow rates over a range of .003 to 30 litres of gas per minute. With a 200 mS response time in flow conditions, it enables solid and liquid samples to be levitated stably on a cushion of gas.

### 4.4 Computer use of DDE software

The principles of Dynamic Data Exchange are based on a conversation between two applications, a client and a server.

*Client* The application requesting information or initiating an action.

*Server* The application providing the information requested by the client or executable as an action that is Smart DDE.

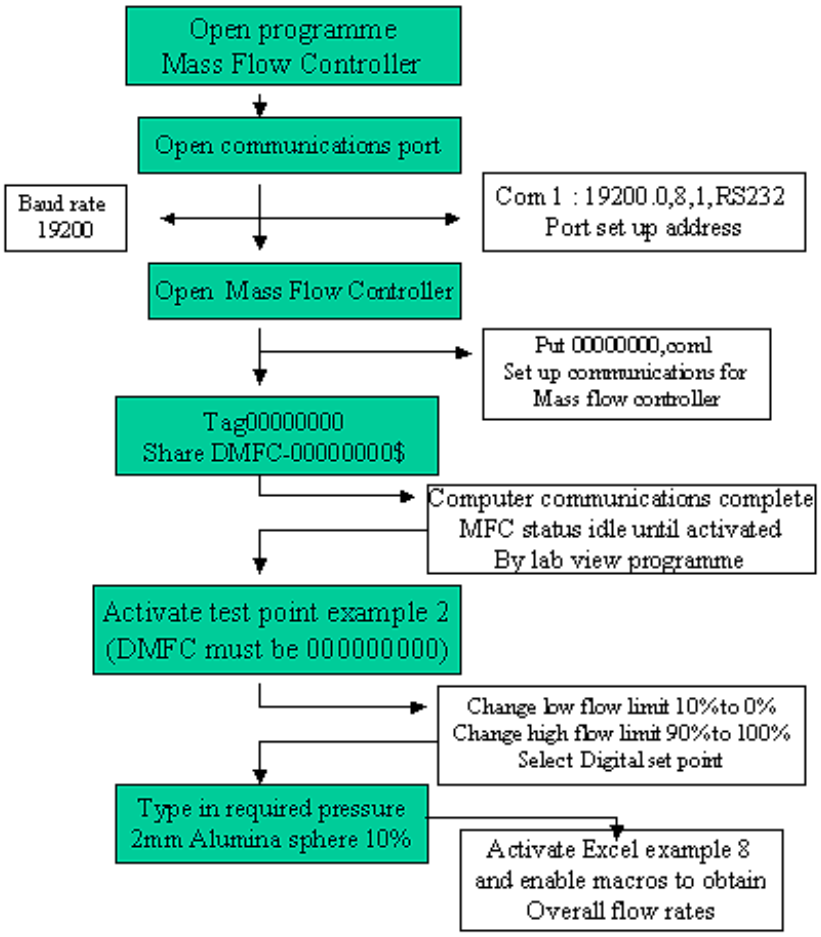


**Figure 4.3 Computer communications port and mass flow controller set-up**

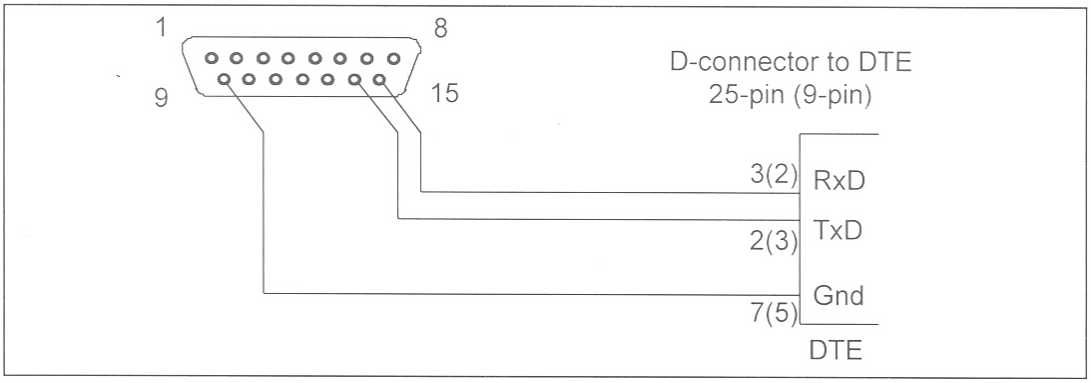


**Figure 4.4 RS232 Interconnections between Digital Mass Flow Controller and Computer.**

Once the mass flow controller has been set up to communicate with the computer, the desired gas flow can be set or varied dependant on the instabilities from the sample. This can be varied in 0·5% steps up to maximum.

Nominally for 2mm alumina samples, gas flows of 10% are enough to cover overall levitation. As the sample goes through the melting phase from solid into the liquid state, instabilities do occur. These can be overcome by increasing flow rate by 1 to 2%. Another common difficulty associated with levitation is the sample sticking to the side of the nozzle whilst in the molten state, caused by excessive turbulence of the sample within the air stream. This can be rectified by stopping the laser, then restarting levitation.

Oscillations of the sample can sometimes become so extreme that this can be blown out of the laminar airflow and off the sample stage.

One of the limiting factors associated with the DDE software is that the control of the gas can only be adjusted in one degree steps. By including the operational dongle associated with the DDE software into a LabVIEW programme, will enable a much higher resolution to be achieved.

The mass flow controller is operated from a separate computer from that of the laser system, in order that there should be no software conflict between both systems, and as a safety issue, the laser system cannot be corrupted or influenced by any other operations. Accordingly, the interfacing of the mass flow controller is operated via the communication port. With one system already operational on the communication port, and with interrupt protocols on the communications port already causing conflict, the second computer was the obvious choice, using RS232 protocols between the laptop and the mass flow controller.

The operational dongle associated with this software is connected to the parallel port of the computer. This software "key" allows exclusive use of the licensed DDE software.

**4.5 Conclusions and future experiments.**

Future improvements will include a system where a variety of gases are mixed together by a mass flow controller and fed into the levitating nozzle, for example an argon and oxygen mixture can prevent oxidization of specific oxide samples.

Sample viscosity is also an area of interesting investigation, where pulsed air pressure from the mass flow controller enables the sample to oscillate whilst in the liquid state. This may be achieved by passing the measured gas through a pair of piezo sounders, set at a specific frequency. The resulting pulsed gas induces oscillation in the sample, and the resonant frequency can be found.

As the sample levitates, a spin is also induced in it, which is discussed in greater detail in Chapter 7. Spin is also induced by the partial melt of the sphere. One future experiment is therefore to monitor sample spin and temperature characteristics by monitoring with infra-red and high-speed cameras.

**Appendix**

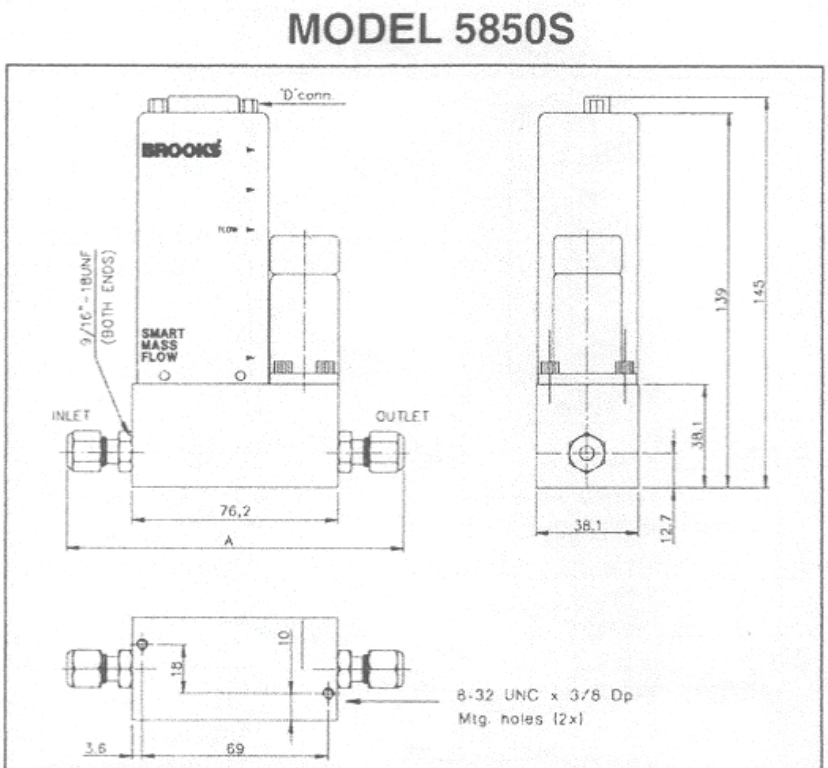


| 5850S CONNECTIONS | A (mm) | Inches |
|---|---|---|
| 9/16-18 UNF (no adapters) | 76 | 3,00 |
| 3/8" TUBE COMPR. | 131 | 5,14 |
| 1/4" TUBE COMPR. | 128 | 5,02 |
| 1/8" TUBE COMPR. | 123 | 4,84 |
| 1/4" VCR | 124 | 4,88 |
| 1/4" VCO | 116 | 4,56 |
| 1/4" NPT | 116 | 4,58 |
| 6mm TUBE COMPR. | 128 | 5,02 |
| 10mm TUBE COMPR. | 131 | 5,14 |
| 1/4" BSP | 116 | 4,58 |

**Figure 4.5 Manufacturer schematics of the Brooks Mass Flow Controller.**

**INSERT FLOW TECH CALIBRATION CERT HERE**

# Chapter 5.

## Laser Power Meter

This section describes a Laser Power Meter, Molectron Laser Power Meter MP5200 incorporating a PM30 Power Meter Probe, Calibration wavelength 514 nm. This was tested for possible application in the aerodynamic laser-heated furnace.

### 5.1 Introduction

The Power Max 5200 laser power meter is a microprocessor based power meter. When connected to one of the Power Max series of intelligent probes, it has an auto ranging power facility to automatically configure itself for that particular probe, with meter scale ranges from 3mw to 12kw.


**Figure 5.1 Molectron laser power meter**

## 5.2 Probe

The probe used in this study has a maximum rating of 40w, which was within the power range to be monitored. This is coupled via a 25way D type connector providing a “smart” interface to the Power Max series of probes. During factory calibration of the head, the memory chip inside the connector is programmed with information to specify the probe’s responsitivity, its maximum power rating and wavelength correction data for the absorber. In addition to the probe’s output voltage, there is an internal thermocouple probe measuring surface temperature of the probe head.

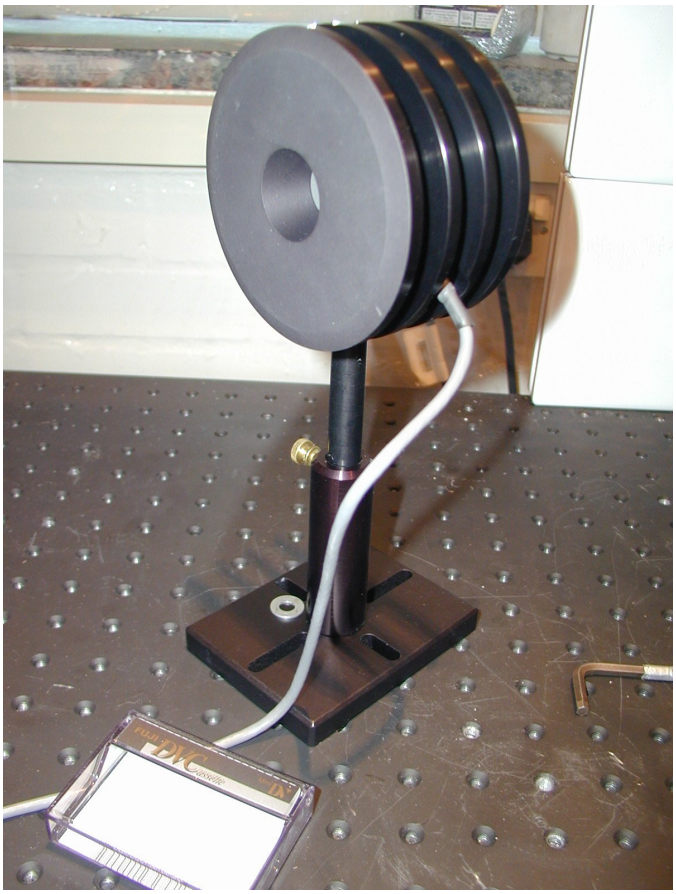

**Figure 5.2 Molectron Power Head.**

### 5.3 RS232 serial communication

A 9 pin D type connector for P.C. communication, to allow compatibility with RS232 controllers which use hardware handshaking, the controller is configureud to instruct the host that the PM5200 is continuously in the RX and TX mode, allowing instantaneous readout of the power head. This in turn is fed to the communication port of the P.C.

As the experimental design progressed, certain anomalies became apparent with the laser. With the introduction of LabVIEW software, simultaneous monitoring of laser beam power output and optical pyrometry of the sample became possible.

### 5.4 Experimental procedure

Although the system has auto ranging facilities, the laser head was rated only to 40 watts. With this in mind the power head was located behind a beam splitter, thereby only taking 50% of laser power as can be seen in Figure 5.3.

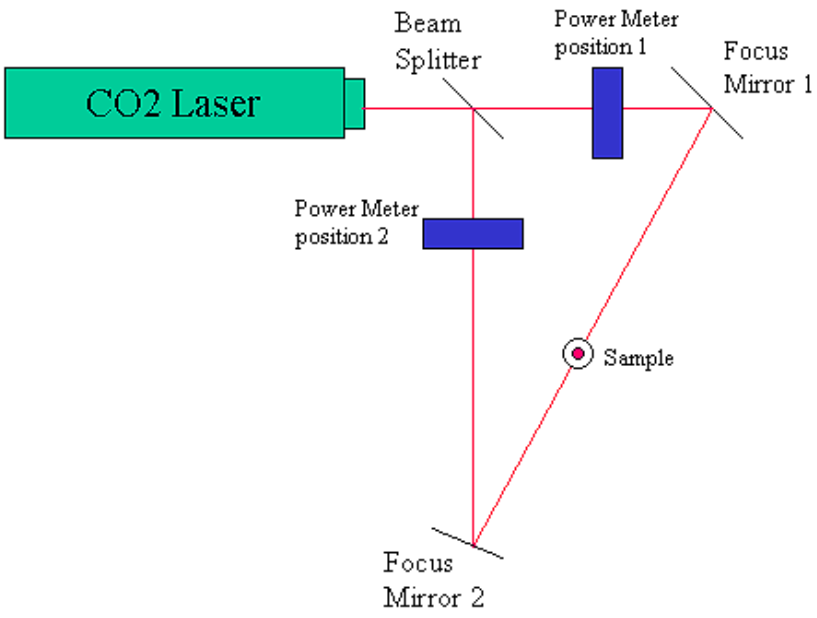


**Figure 5.3 Schematic experimental layout of power meter**

Instantaneous spikes during lasing caused the sample to become unstable during levitation, especially during the super cooled period when the sample was undergoing controlled cooling. These spikes caused the sample to quench instantly and recrystalize.

Possible causes for these spikes were:

1. Instabilities within the laser, especially as it was being used within the lower 5% region of the laser range.

2. Faults within the laser control system

3. External influences from mains borne interference, e.g. heavy plant switching in adjacent laboratories or workshops.

The computer controlling the laser via the UC200 controller was eventually determined to be the problem, with communication conflict between the communications ports. The digital control of the RS232 was abandoned in favour of a dedicated digital to analogue control card. The programme on LabVIEW was then redesigned to give a proportional analogue output, (more details on this design in Chapter 9). This, coupled into the ANV input on the UC2000, produced identical conditions for the laser control system, and the spikes in the output of the laser disappeared.

**5.5 Further Investigations**

With the optical path in its final configuration, another possible investigation is to measure the amount of power absorbed by the focusing mirrors, which can be achieved by placing the power meter in front and behind each of the focused mirrors. It would then be possible to calculate the amount of power incident on the sample.

**Figure 5.4 Calibration certificate**

CERTIFICATE OF POWERMETER PROBE HERE

# Chapter 6

## OPTICS.

This section details the set-up of the optics used in the laser-heated aerodynamic levitator furnace. These were briefly described in Chapter 1.

### 6.1 Objectives and initial configuration

The main objective of the mirrors was to transfer the Carbon Dioxide laser beam onto the sample to enable it to melt. The main limiting factor in the final optics configuration was the position of the sample relative to the X-ray port and the focus point of the wide angle detector. Any deviation of the intended laser path could lead to serious consequences of the laser beam breach into the Daresbury synchrotron equipment.

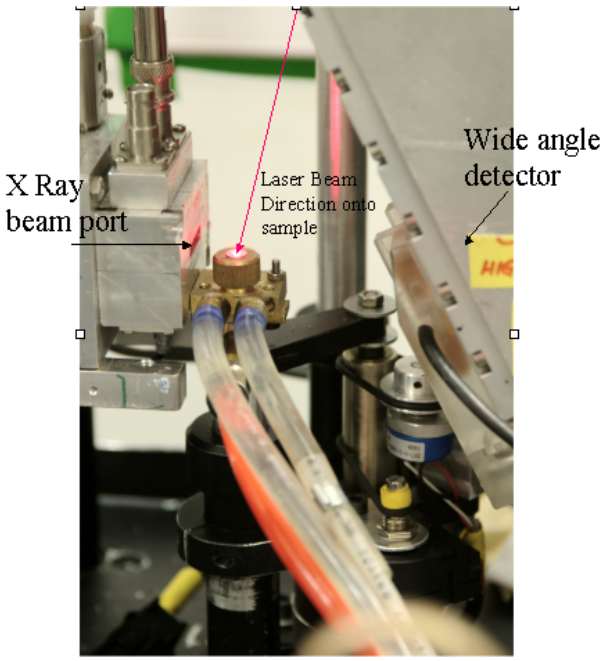


**Figure 6.1 Sample stage position on the 6.2 beamline with X-ray and laser beam paths**

## 6.2 Optics table.

As discussed earlier in Chapter 1, the optics table and laser bench (shown in Figure 6.2) were produced to take into account the physical size and dimensions of the experimental area at the Daresbury synchrotron. As all the optics needed to be aligned horizontally, an optics table capable of supporting all elements of the experiment was produced. Due to the layout and positioning of the laser, a cantilevered arm supported the laser, so that all the optical elements moved together on the one bench, thereby reducing alignment problems with individual components. The experimental area of the optics bench was fitted with a solid aluminum breadboard with a standard grid of 25mm M6 holes, which facilitated the mounting of all the optical components, thereby reducing vibration through individual components and reducing risk of beam breach due to mirror movement.

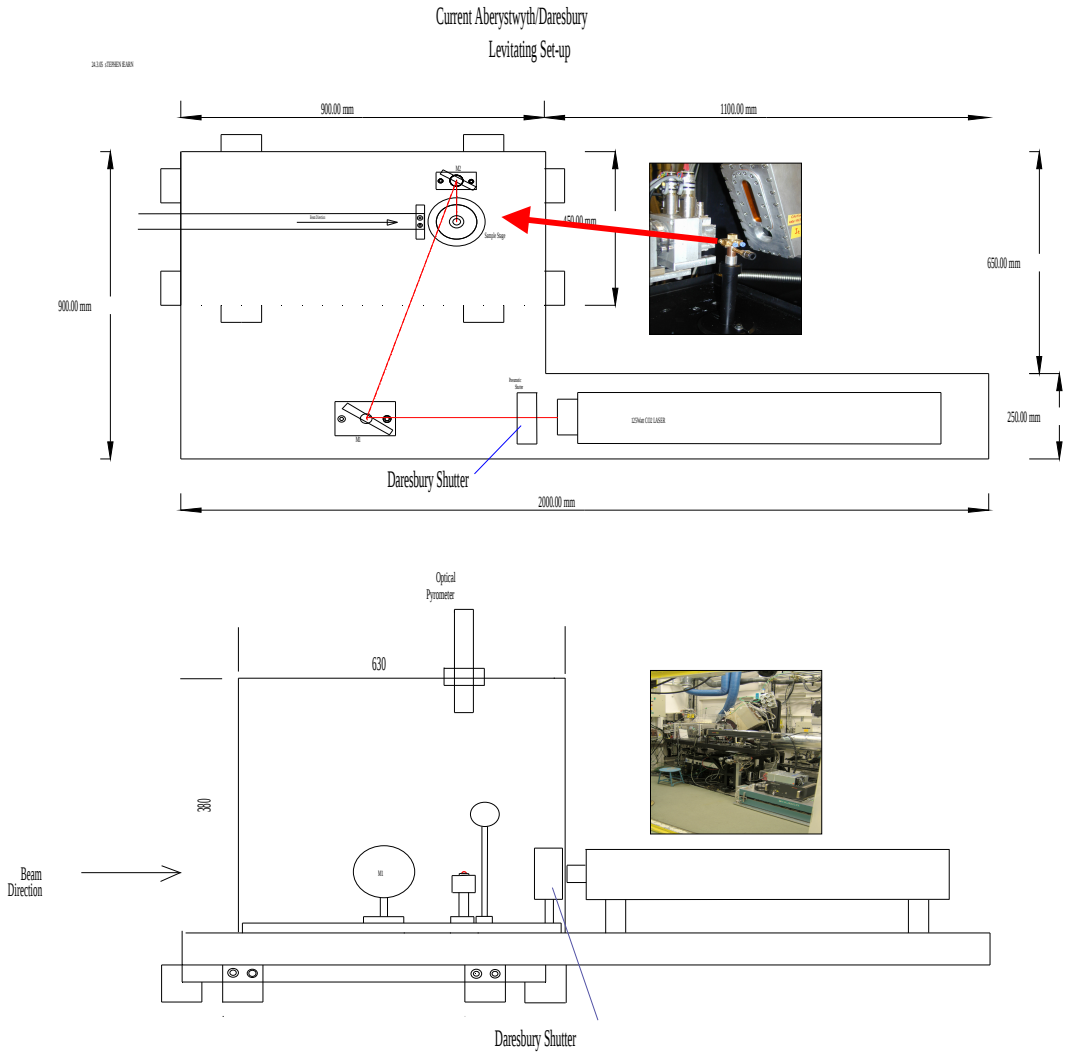


**Figure 6.2 Schematic component layout of aerodynamic laser-heated furnace.**

Mirror alignment was optimized for sample heating by the CO2 laser, by the use of a diode laser situated at the front of the laser head, as described in Chapter 2.

### 6.3 Beam Splitter

The initial optical setup was to use a two-mirror system via a zinc-selenide beam splitter, directing the two beams back onto the sample, as can be seen in Figure 6.3.

The use of the beam splitter allows proportional splitting of beam into two paths enabling it to evenly illuminate and heat the sample from two directions simultaneously, thus producing an even temperature across the surface of the sample.

### 6.4 Mirrors

The original set of 25mm plane mirrors enabled an accurate alignment of the beam onto the sample, using front-silvered glass mirrors with an average reflectance of 98.5% from 700 – 1064nm. In the initial experimentation, these produced acceptable results, with good alignment and stable sample levitation, but the high temperatures needed to melt various ceramics was not enough, even when the laser was running at 95% capacity.

### 6.5 Focusing lenses

As the experimental technique was not producing enough heat to melt the ceramic, an alternative optical arrangement was to use a pair of variable focal length lenses placed in the beam path; this focused the laser beam onto the sample.

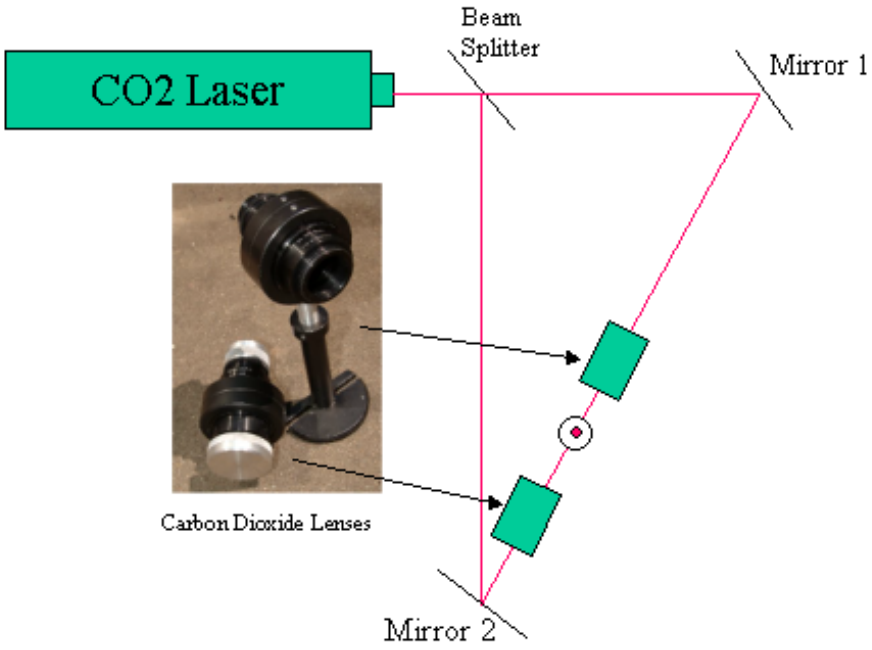


**Figure 6.3 Schematic experimental layout of plane mirrors and carbon dioxide focusing lenses.**

Beam alignment is critical as any stray emissions from the CO2 laser reflected within the lens caused excessive heat to build up between the optical elements also reducing the power delivered onto the sample. One way to overcome this problem was the use of pinhole covers at each end of the lens system enabling the beam to be accurately aligned.

Due to the physical size of the variable focal length lenses, plus limited space available for them on the experiment when attached to the beamline, there was no practical advantage in using this setup (especially as there was no significant increase in sample temperature). This avenue of experimentation was therefore not continued.

### 6.6 Fixed focal length mirrors

This configuration introduced the use of fixed focal length mirrors, which had the advantage that the mirrors system was significantly smaller than the lens system. However this had the disadvantage that the laser beam could not be variably de-focused onto the sample.

With mirrors in fixed positions, appropriate dimensions for fixed focal length were calculated.

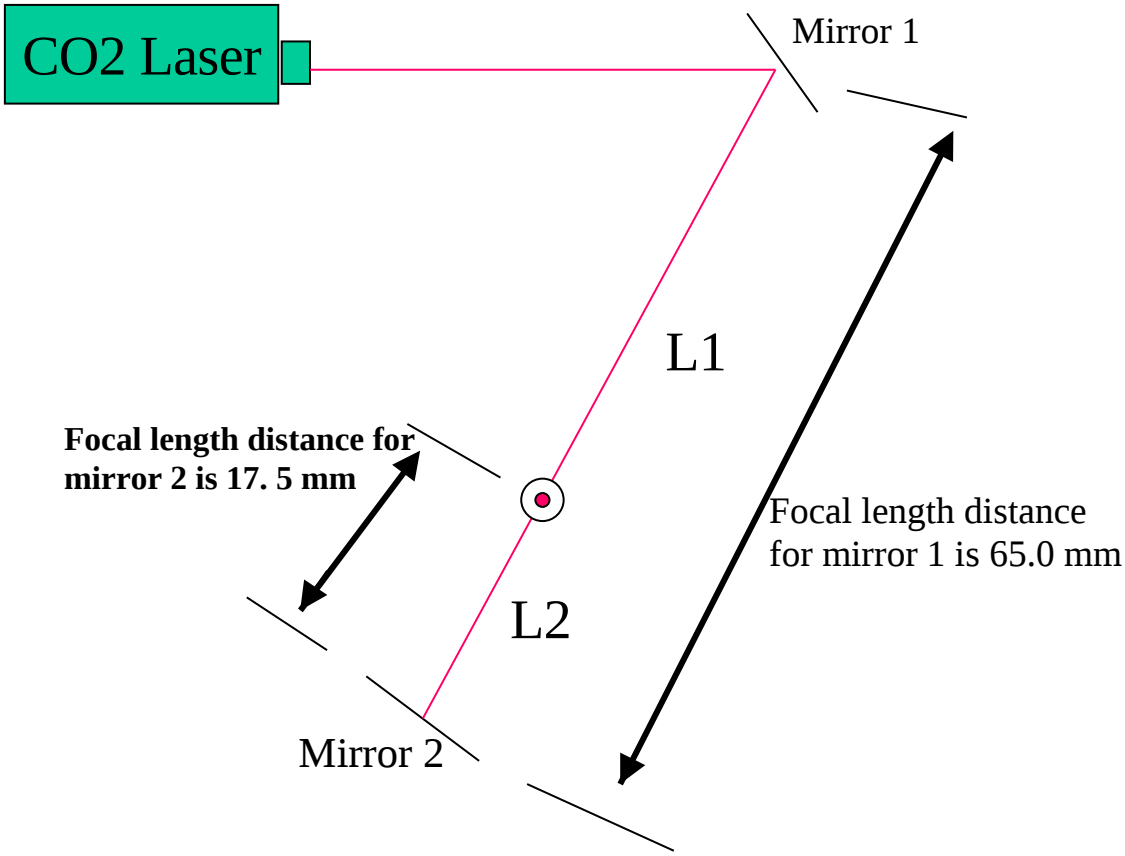


**Figure 6.4 Illustration of relative positions of focused mirrors and respective focal lengths.**

Two 25mm diameter focused mirrors direct the laser beam onto the sample, with L1 focused beam of 65mm focused onto the second mirror L2. This in turn is focused again from L2 and onto the sample with a focal length of 17.5 mm. Finally producing a focused beam of 0·5 mm. This type of layout using a single beam path was used due to the configuration of the synchrotron x-ray beam line as described later in this chapter.

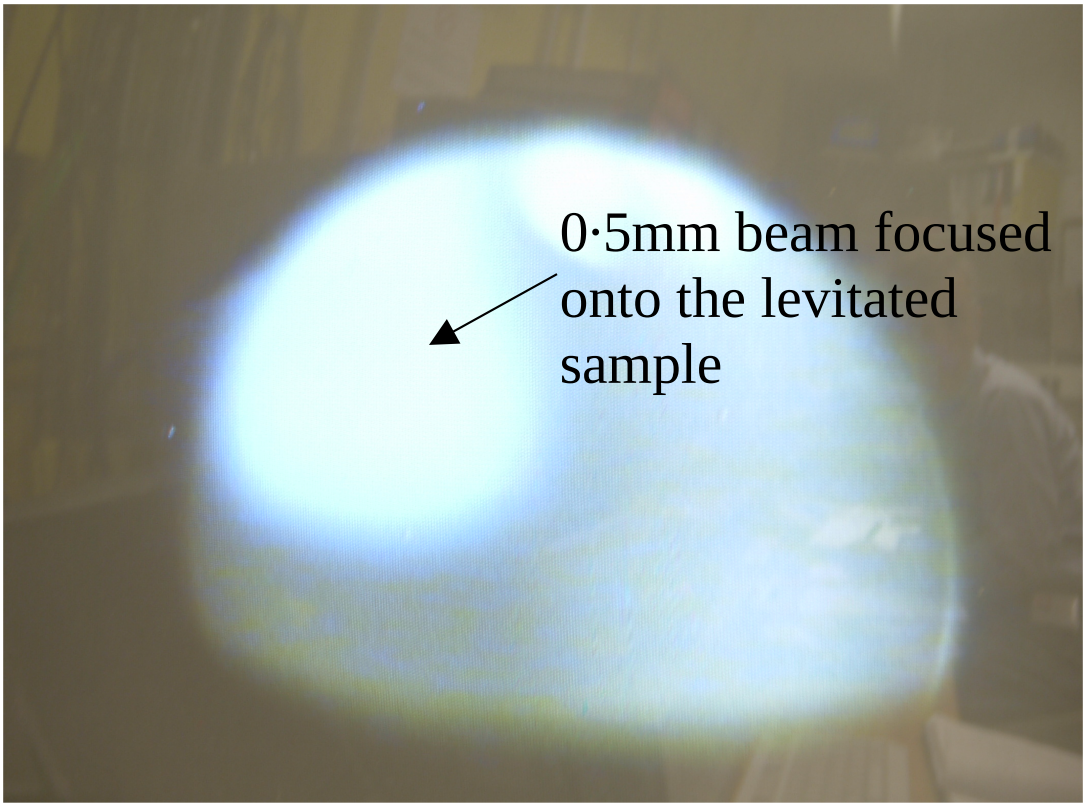


**Figure 6. 5 Video image taken from microscope camera, illustrating levitating molten sample with heated laser beam position.**

This configuration significantly improved the heating of the sample, and allowed a much larger range of laser power and temperatures up to 3000 degrees were reached. Therefore the beam splitter was not incorporated into the experiment, and only one leg of the optical path was used as there was enough even temperature spread across the surface of the sample to achieve melting.

### 6.7 Mirror Alignment

The laser beam had to be accurately aligned onto the sample, the first series of stands therefore included a screw adjustment, allowing fine-tuning of the mirrors in the vertical and horizontal plane, as can be seen in Figure 6.5.

**Figure 6.6 Mirror profiles illustrating vertical and horizontal adjustment, allowing accurate positioning of the laser beam onto the sample.**

### 6.8 Daresbury configuration.

The alignment of the optical beam path had to be altered due to the beamline configuration, involving directing the main laser beam over the top of the x-ray delivery port, (as can be seen in Figure 6.7), then diagonally down onto the levitating sample.

Extreme care had to be taken at this stage in the optical alignment, due to the close proximity of the wide angle detector, and the final shutter motor drives situated at the top of the x-ray beam port. Any stay beam in the initial alignment, or scatter from the sample stage, could burn the window on the front of the wide angle and small angle cameras, or in turn damage the x-ray delivery tube. This could cause a significant chain reaction within the experimental hutch and the operations of the synchrotron facility.

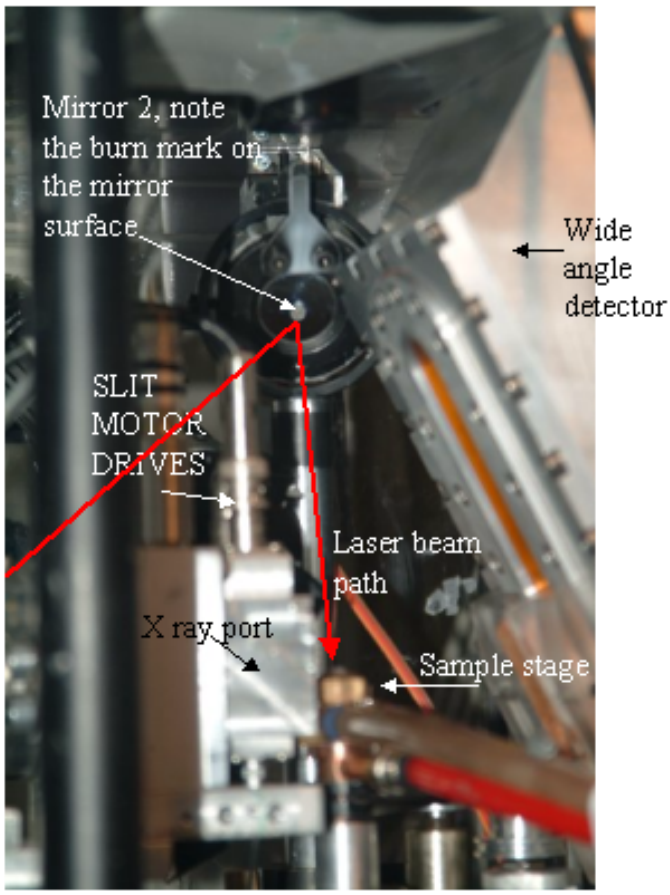


.

**Figure 6.7 Confined geometry of the levitator laser furnace installed onto the 6.2 beamline.**

### 6.9 Remote control mirrors.

As can be seen from Figure 6.7, there is a very narrow path for the laser beam to be delivered onto the sample. Another difficulty is that with restricted access to mirror 2 within the polycarbonate box, fine adjustments to this mirror due to sample or table variations was not possible without partial strip down of the system, which then had to be rebuilt and realigned. To overcome this, a flexible drive shaft coupled to the vertical and horizontal screw drives on the mirrors was added, however as the part for the drives were not aligned, this did not produce accurate enough positioning due to backlash.

The final design employed servo control motors as shown in Figure 6.8. By removal of the limiting pin in the gear box of the servo, it operated as a high torque motor with 360º revolution. This coupled onto

the screw drive of the mirror adjusters proved the ideal solution as they were reasonably discrete and had very high torque. When coupled to a drive system (as can be see in Figure 6.8) with its own integral power supply, it enabled control of the secondary mirror from outside the experimental hutch inside the control room. The circuit diagram to drive and control both servo motors is shown in Figure 6.11.

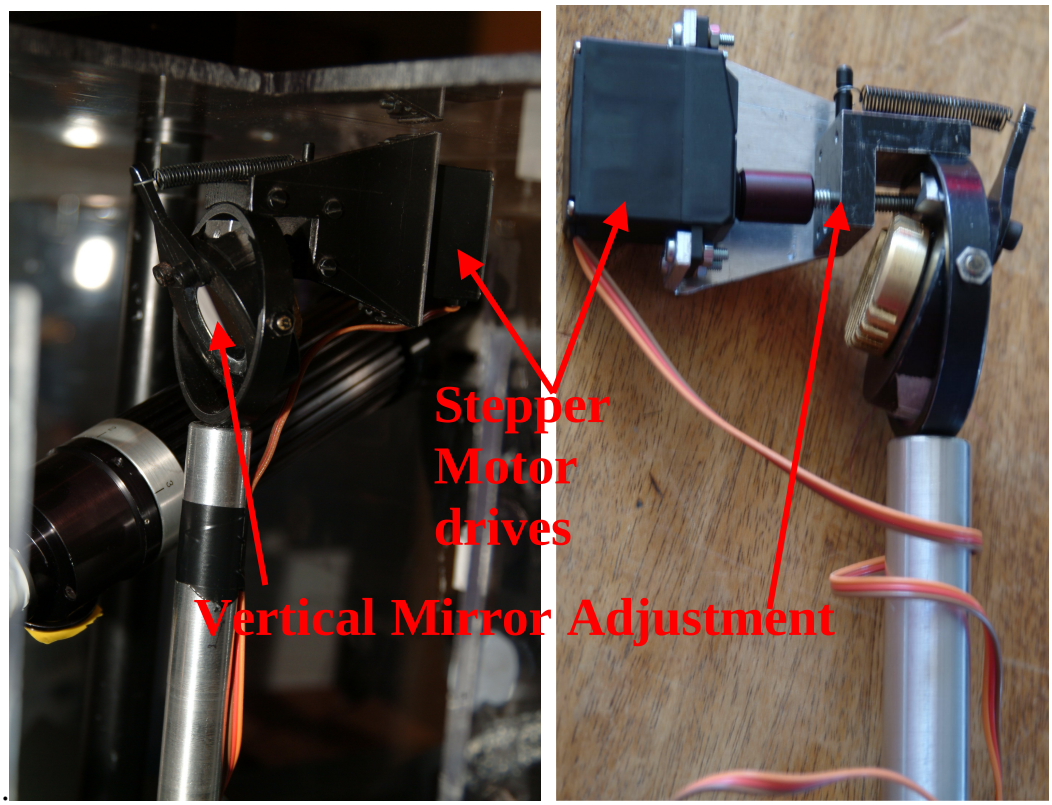


**Figure 6.8 Servo motors illustrating vertical mirror position adjustment.**

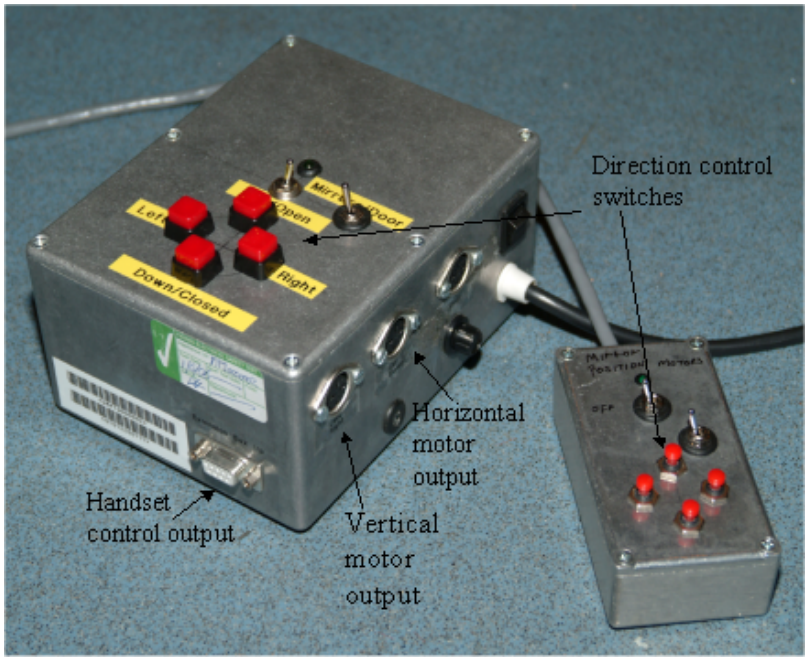


**Figure 6.9 Master and Slave control box used for remotely controlling the accurate positioning of mirrors**

## 6.10 Thermal Mirrors

Due to the high temperatures required to melt some ceramic samples, focussed mirror temperatures can rise causing permanent damage by vaporizing the mirror surface and eventually cracking the mirror. To enable the heat to be dissipated, thermal conductive paste and a customised heat sink attached to the rear plate of the mirror was used as can be seen in Figure 6.10. In this application, sample heating for periods of 3 hours was attainable without damage.

However the laser power had to be limited by the LabVIEW software, to 30%, this had the disadvantage in that ceramics such as zirconia only achieve a partial melt.

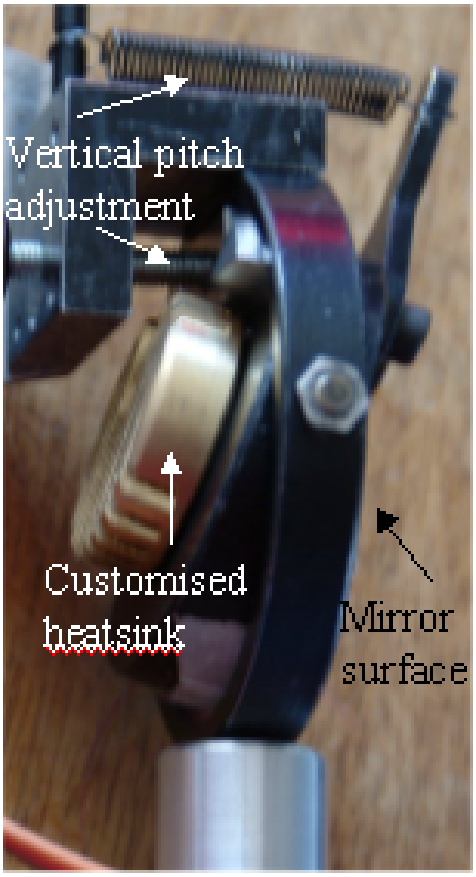


**Figure 6.10 Customized mirror heat sink for dissipating heat generated by laser power, including remote vertical pitch adjustment.**

### 6.11 Final Mirror Choice.

The installation of gold-coated copper fixed focus mirrors into the system facilitates sample temperatures of 3000 degrees, with 98 % laser power. This now enables a whole range of samples to be investigated without subsequent mirror damage.

## Appendix

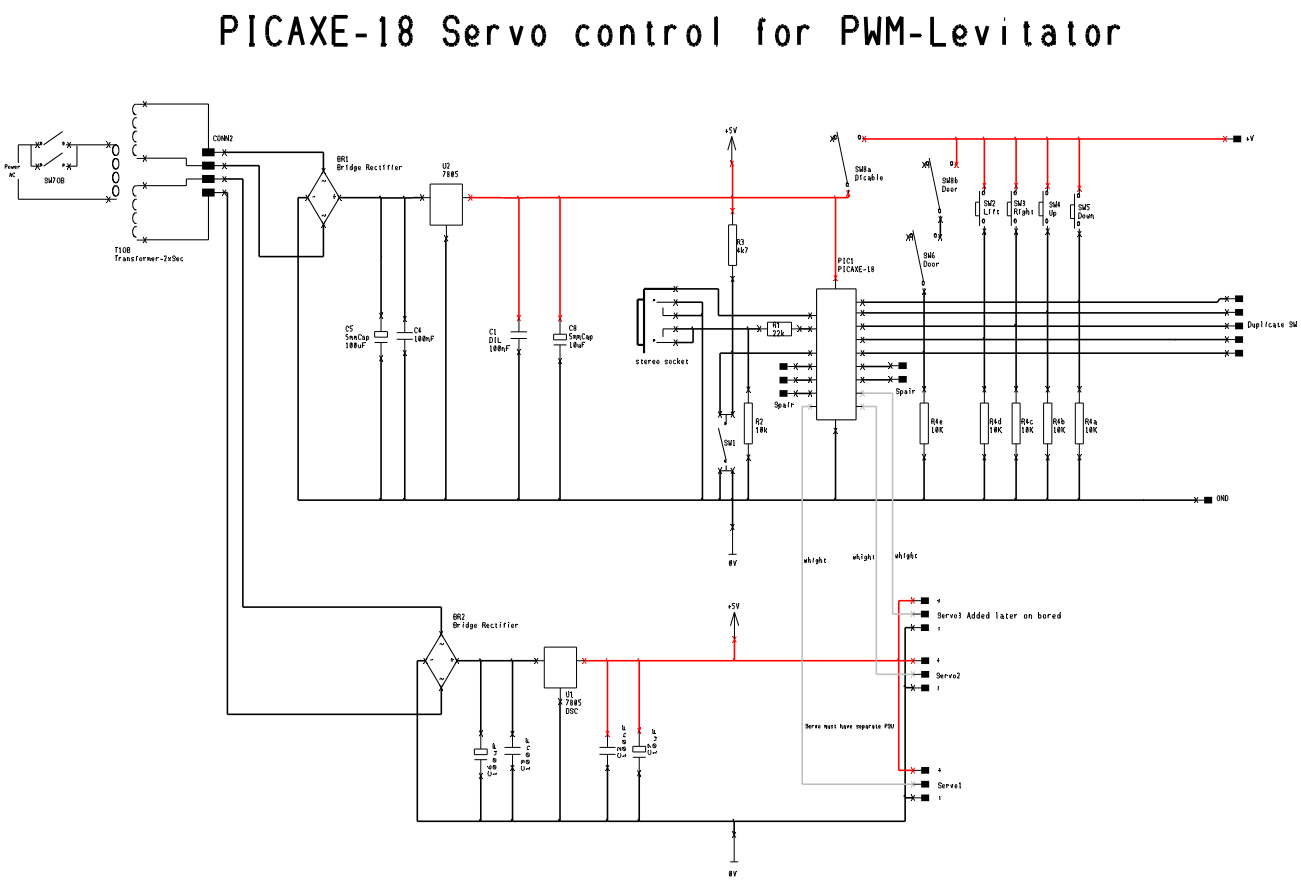


**Figure 6.11 Circuit design of servo controlled motors, adapted for mirror motor control.**

Acknowledgements

Circuit diagram courtesy of the Electronic Workshop, IMAPS, U.W.A

# Chapter 7

**Nozzle design and sample stage for liquid levitation.**

This Chapter discusses the principle of aerodynamic levitation of a liquid drop in a container-less furnace. Central to this is the design of a sample holder capable of maintaining stable levitation continuously over long periods of time at extreme temperatures with repeatable parameters.
Liquid levitation is possible by a variety of techniques, including acoustic positioning and electromagnetic levitation in a container-less environment. These techniques are not appropriate for the size of the sample and the area available between the x-ray port and the wide-angle and small angle detectors in synchrotron radiation experimentation.
Laser heated aerodynamic levitation, however, fulfils both of these requirements. An inert gas flow of nitrogen or argon, pass through a mass flow controller into a specially designed nozzle allowing vertical adjustment with respect to the x-ray beam path, enabling the sample to “float” and be heated by the carbon dioxide laser. Various materials were considered, and the final designs incorporated boron nitride and alumina.

## 7.1 Boron Nitride Nozzles

Boron nitride is a ceramic-based material capable of withstanding extreme temperatures with little expansion or contraction.
Key properties are:

1. Excellent solid-solid lubricating properties
2. Complex shapes can be produced from hot pressed billets, which can be machined using conventional techniques.
3. High dielectric breakdown strength in electrical applications.
4. Chemically inert.

Nozzles were initially produced and designed from boron nitride. Several geometry prototypes were explored and the final nozzle designed to be interchangeable, so that after several experiments the nozzle could be replaced without interference to the optical setup. To optimise the sample levitation, several designs were produced using boron nitride rods in the IMAPS Mechanical workshops. Examples are illustrated in Figure 7.1

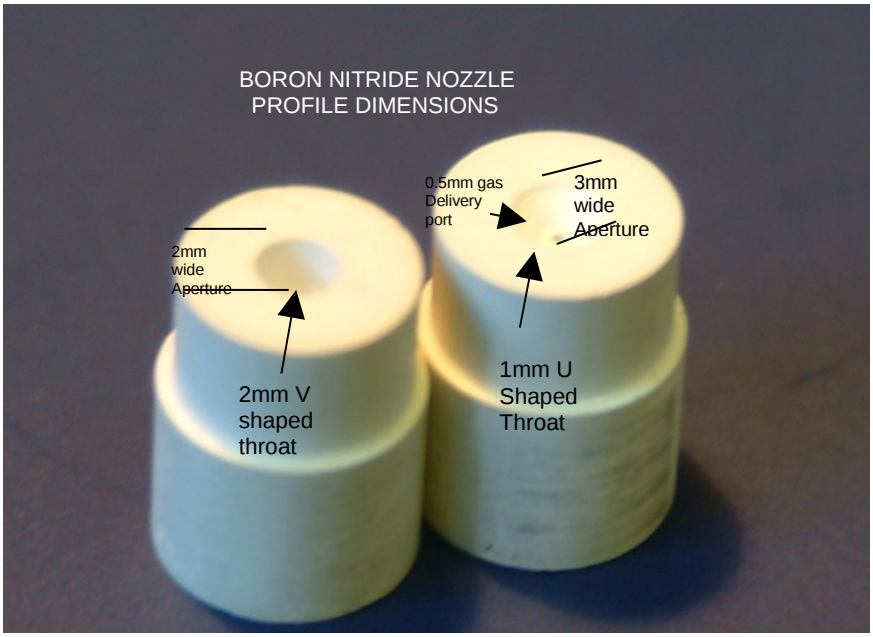


**Figure 7.1 Examples of boron nitride nozzles showing the dimensions of the sample throat and gas inlet.**

Despite polishing, the roughness of the nozzle surface caused the sample to stick whilst rotating in the liquid state, this caused the sample to re-crystallise at various stages during the experiment. Different throat diameters flow rates, and polishing techniques were employed to reduce the sticking problem, but this could not be eradicated. Examples of nozzle roughness are shown in Figures 7.2 and 7.3.

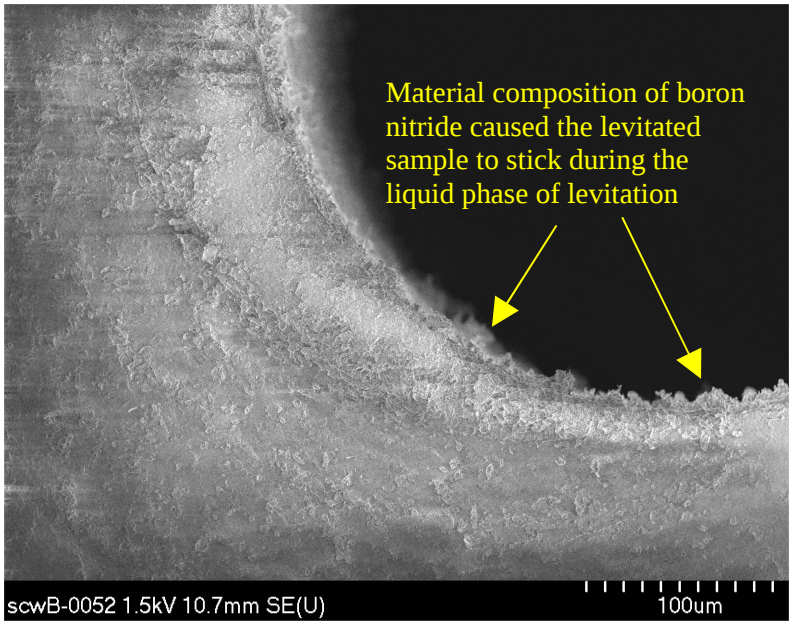


**Figure 7.2 Boron nitride nozzle viewed through electron microscope. Images courtesy of SEM Dept, Biological Sciences, Aberystwyth University.**

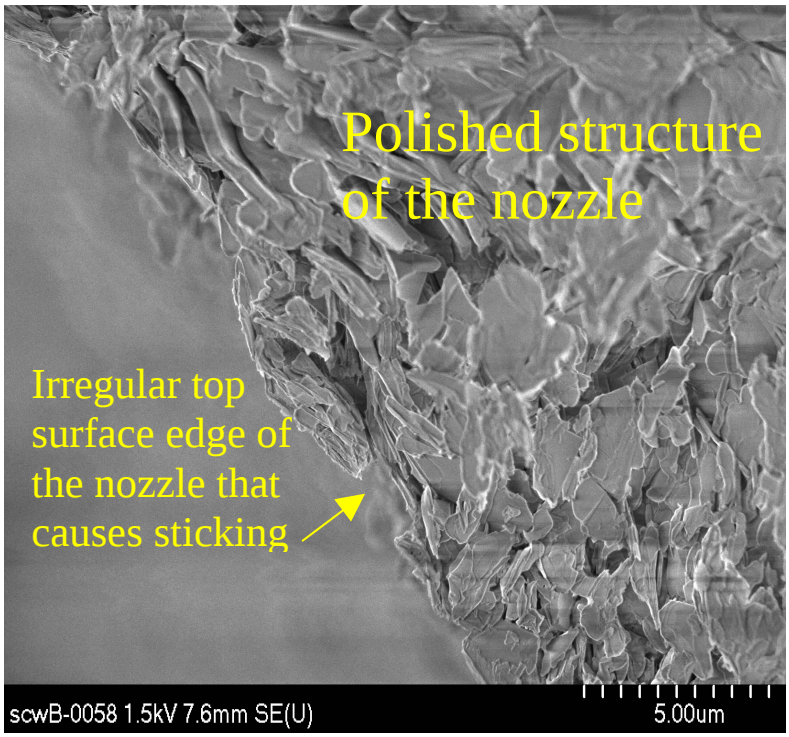


**Figure 7.3 Polished surface structure of boron nitride nozzle. Images courtesy of SEM Dept, Biological Sciences, Aberystwyth University.**

### 7.2 Sample sphere characteristics during levitation.

As the experiment design progressed, several anomalies needed to be addressed for stable levitation of high temperature liquid drops.

1. Stable gas flow is achieved by the use of a computer controlled mass flow controller, which delivers lamina air flow to the nozzle at sufficient velocity to allow the sample to levitate but insufficient to “blow off” the nozzle and out of the laser beam.
2. The sample levitates supported by viscous drag, but otherwise operates as a frictionless bearing. Coriolis forces can cause the sphere to rotate. The rotation speed is variable as the sample goes through the melt phase from solid to liquid.
3. During the initial heating by the laser, the sample is rotated freely in the gas flow. High and low density phases produced by the initial sample melting, however, causes additional rotations.
4. As the sample begins to melt, severe oscillations can cause the sample to bounce horizontally off the lamina air walls. If, part of, the molten sample, came into contact with the nozzle head this will stop the levitation and cause the sample to “stick” to the nozzle. Boron Nitride nozzles are particularly prone to this problem; one remedy is to polish the inner walls.

### 7.3 Nozzle dimensions.

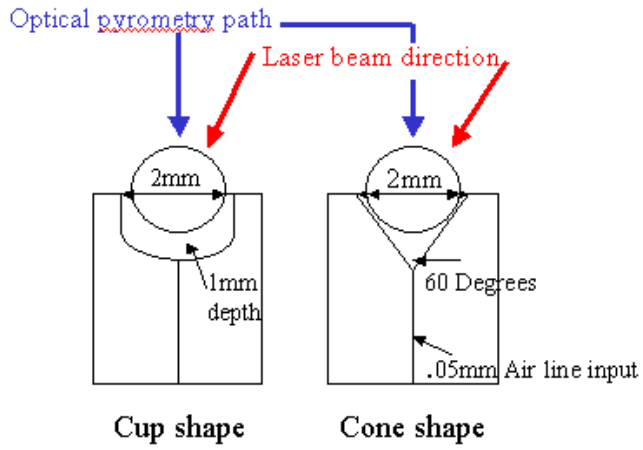


**Figure 7.4 Nozzle schematic for cup and cone shape designs**

To optimise levitation, several nozzle designs were produced which allowed investigation of sample stability as it passed from the solid into the liquid phase. This transition can produce violent oscillations during levitation. By the use of high speed cameras, it was possible to observe the severity of the oscillations, these were enough to cause the sample sphere to jump out of the air flow completely or attach itself to the side of the nozzle during the melt phase. From the camera footage these could be distinguished as shown in Figure 7.5

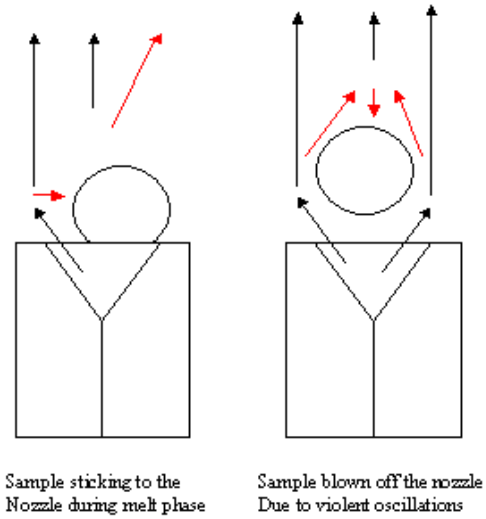


**Figure 7.5 Illustration of sample instability during levitation.**

### 7.4 Aluminium Nozzles

In consultation with the Orléans CNRS Group, aluminium nozzles proved to be a better option than boron nitride. The same design criteria (Figure 7.4) were used with interchangeable nozzles. Aluminium is a good conductor of heat, and although it has a melting temperature of 660ºC, with a cushion of gas between the hot sample, and the cooled nozzle surface, reliable levitation became possible.

Irregular samples and compositions can now be levitated to produce spheres.

Different funnel throat sizes can now produce different size spheres.

The completed nozzle geometry designed at Aberystwyth is shown in Figure 7.6

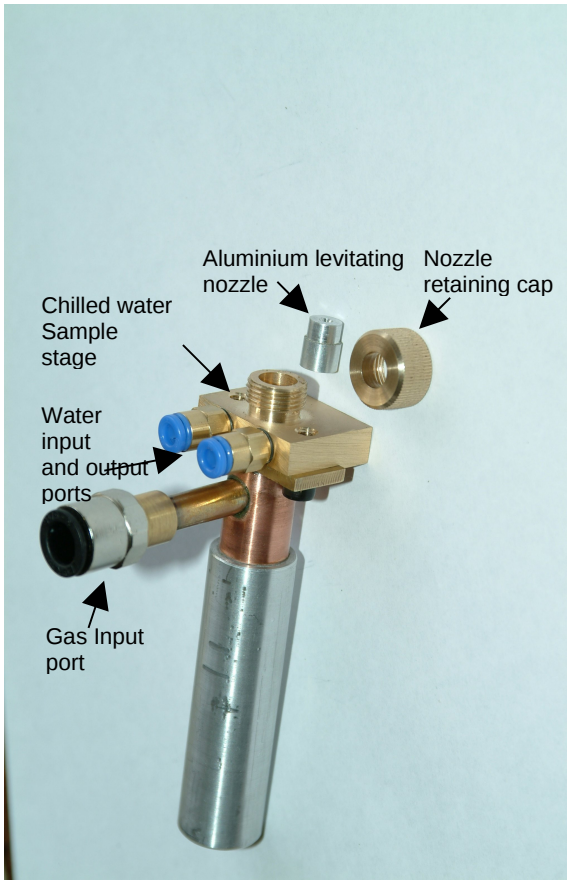


**Figure 7.6 Nozzle design and cooled sample stage**

**Water cooled sample stage.**

The ideal solution that minimised sample sticking was to cool the sample stage with a recirculating water system. One option was the use of high volume chilled water to cool the laser head. Adaption and regulation of pressurised water used to cool the laser head from 120 psi proved to be overkill for the sample stage, as the water channels used for cooling were unable to cater for this amount of pressure.

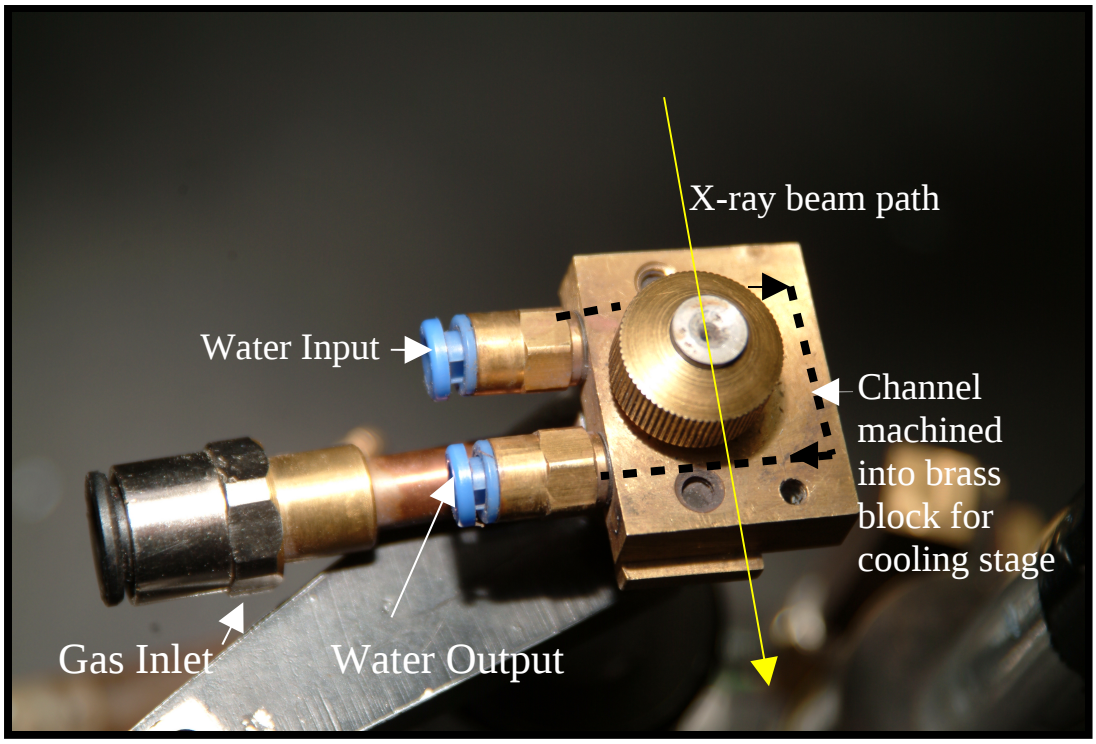


**Figure 7.7 Plan view of cooled sample stage, incorporating gas inlet and X-ray beam path**

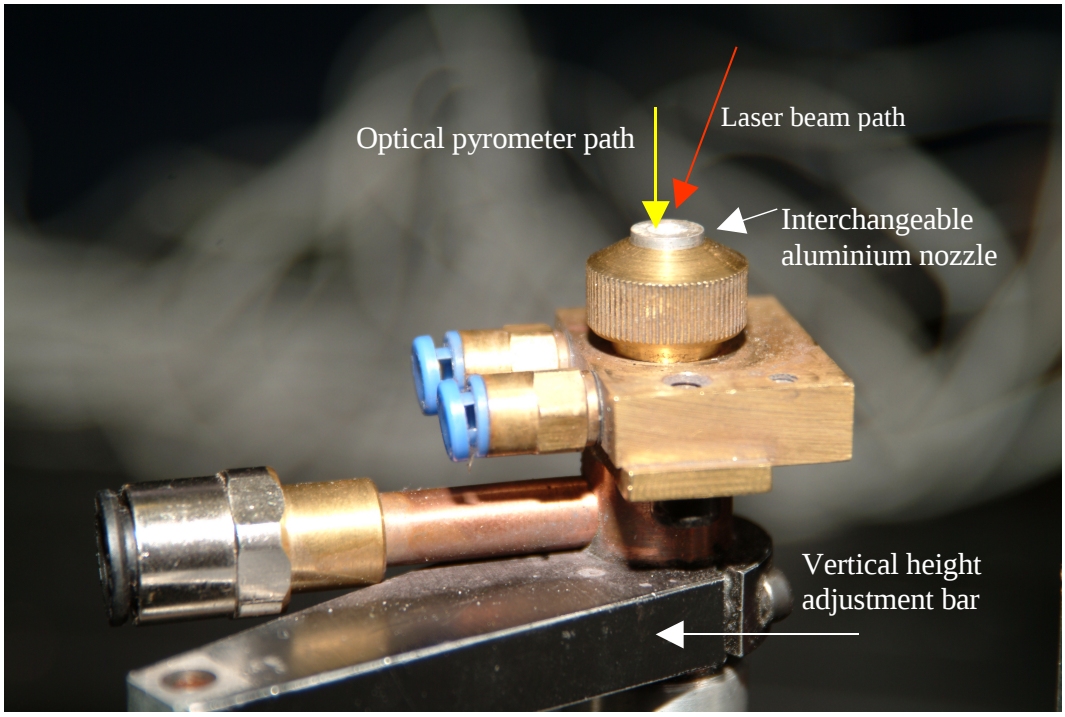


**Figure 7.8 Profile view of cooled sample stage illustrating optical pyrometer and laser beam path.**

The improvised use of a Bermuda recyclable water fountain with a flow range of 0·5ℓmin$^{-1}$. This contained its own cooled water system and was now sufficient to keep the sample stage at a constant temperature. This solution was so successful, stable levitated liquid drops in the super cooled region have been maintained for hours at a time, including samples like Zirconia that melt at over 2500º C

.

**7.6 Sample stage vertical adjustment**.

Vertical adjustment is required, as the height of the sample varies with temperature and for SAXS/WAXS experimentation needs to be adjusted to a fixed height in the x-ray beam. The sample position is first aligned with the x-ray beam by the use of Polaroid film and x-ray sensitive tape exposed behind the levitator. This position is then set as the datum line for the alignment of all the optics and laser position. In the initial set-up, it proved to be too coarse an adjustment, so a means of vertical drive was required to accommodate changes in the height of the drop in the nozzle. This was achieved by the use of a stepper motor with a vertical screw thread, and allowed the sample to be manipulated in the x-ray beam to whatever position required whilst the experiment progressed; this allowed a significant degree of accuracy of movement as the levitator height was changed.

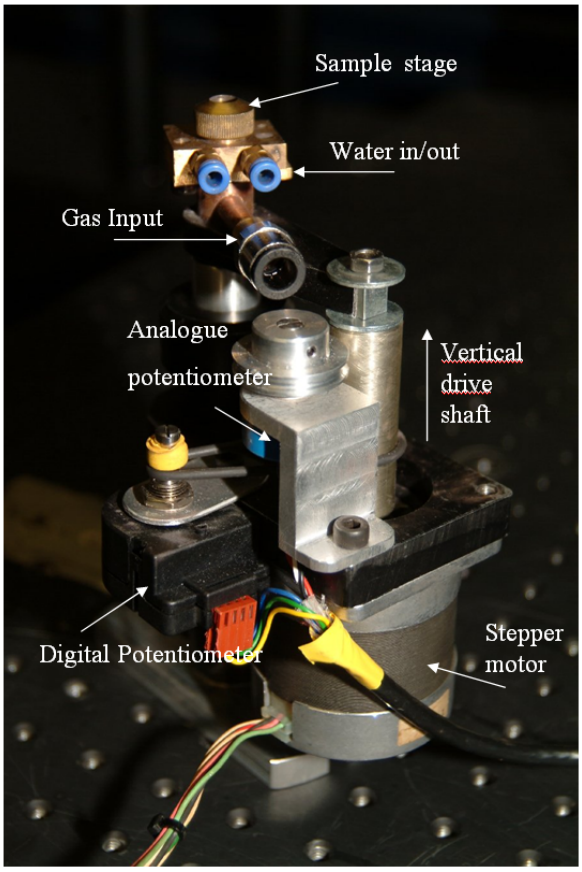


**Figure 7.9 Vertical sample stage movement incorporating analogue and digital feedback**.

The stepper motor has movement of 1/2500 inch per revolution = 1.016 x 10-3 mm/rev

The stepper motor drive moves in 1.8 ° steps, so 1 step 0.5 micrometers, 2 steps = 1 micrometer and 200,000 steps = 1mm.

To obtain repeatable sample position with the stepper motor, a feedback potentiometer was employed with non-stop rotational facilities. This was coupled to the LabVIEW interface system and allowed the vertical height to be adjusted accurately in situ.

A description of the operation of the sample stage vertical adjustment control is explained in Chapter 9.

The arrangement is illustrated in Figure 7.9

### 7.7 Future developments of the sample stage

Ideal conditions require the sample to be located as close as possible to the X-ray port, to minimise attenuation of the X-rays in air. Improvements to the instrumentation arrangements described in Chapter 1 may be achieved by customising the levitator with dedicated cooling facilities located within 1mm of the x-ray port. Such a design would also allow the sample to be levitated in a pure argon atmosphere, whilst still maintaining access for heating and pyrometry.

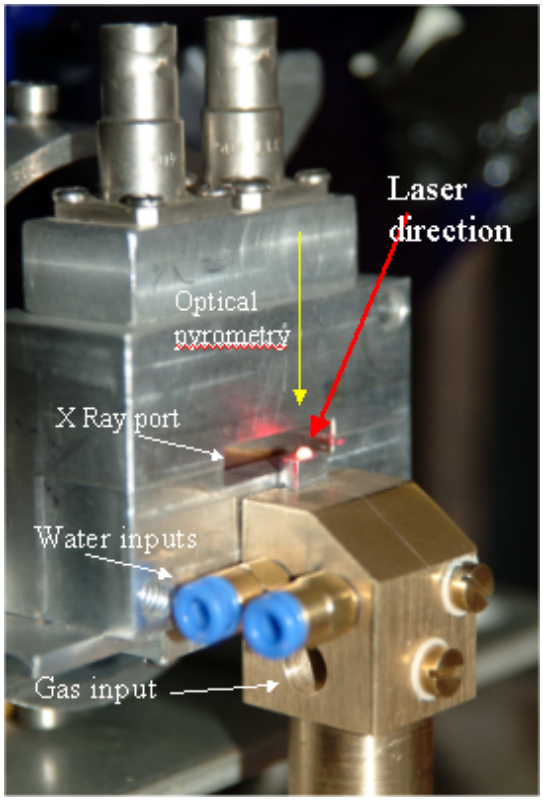


**Figure 7.10 Customised levitator head with sample stage cooling, designed to minimise air scatter**

Whilst this layout, appears ideal for minimising the cause of air scatter, it has other potential limitations. As the sample is situated so close to the beamline window of the x-ray port, radiated heat or sample blow off could have serious consequences, with breach of the experimental vacuum system a possibility.

Also under current investigation in addition to refractory oxide liquids are silicon and germanium liquids. For successful levitation, they must first be formed into spheres from the powder state. This process could be achieved with a dedicated argon filled chamber, without oxidation. Once melted, the

samples would be transferred into the SAXS/WAXS levitation chamber, also filled with pure Argon. A custom built chamber which would bolt onto the chilled water sample stage, and this system would enable x-rays to pass through the molten sample in the molten state, and monitor both wide and small angle detection simultaneously. A continuous argon environment would enable oxidising liquids like silicon and germanium to be levitated. One further restriction is space. With the close proximity of the wide angle detector to the sample, the chamber needs to be less than 600mm from the detector, yet able to accommodate all the aerodynamic levitator furnace facilities. All of this can be engineered, but the sample cannot be monitored visually for accurate positioning, using the existing video camera arrangement (Chapter 1). This difficulty can be overcome by the installation of a miniature radio camera in the chamber. A prototype sample stage including these additional features is illustrated in Figure 7.11

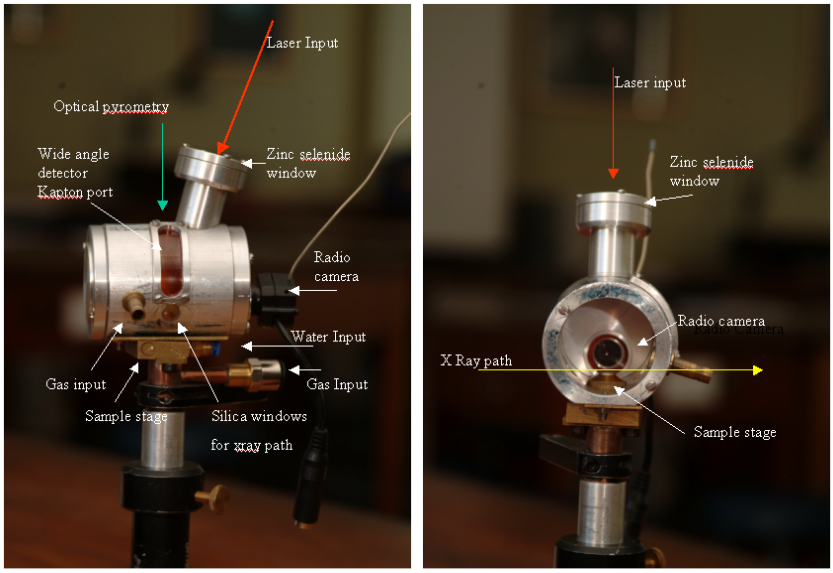


**Figure 7.11 Prototype aerodynamic levitator module designed to handle oxidising liquids and sufficiently small to be installed within the 60 cm radius space within the WAXS detector**

# Chapter 8

**X-ray Beam Alignment.**

This Chapter describes the critical alignment of a levitating high temperature liquid within the MPW 6.2 X-ray beamline at the SRS. A detailed description of the installation is also included.

In order to analyse the structural content of ceramics and liquids at different temperatures, a high intensity monochromatic x-ray beam is directed at the sample, and the resulting diffraction and scatter measured. Because the incidental x-ray beam is fixed, any movement of the sample resulting from different operating temperatures need to be compensated for insitu during the experiment.

## 8.1 X-ray beam characteristics

The specification of the 6.2 Beamline, .describes the x-ray beam characteristics of multi pole wiggler at the synchrotron radiation source at Daresbury Laboratory

- **Focusing optics:** 2 plane Si/Rh mirrors for vertical focusing. A 2-crystal, double-bounce, saggitally-bent Si (111) monochromator for energy selection and horizontal focusing. *These produce a monochromatic focused spot in the experimental hutch*
- **Collimation:** 5 pairs of horizontal and vertical slits, the final pair being just before the sample position. *These define the diameter of the x-ray beam, and minimize scatter at the sample stage.*
- **Bandpass (monochromatisation):** $\Delta E/E \sim 10^{-4}$. Photon flux $\sim e^{12}$ photons/s/0.01% band pass at 200mA stored beam current. Photon flux is energy-dependent and is peaked at 8-9 keV. *This is the intensity of the synchrotron radiation source in the x-ray region usually used for SAXS/WAXS experiments.*

- **Beamsize at focus** ~1.3 x 0.3 $mm^2$ (H x V). *This is compatible with 2mm drops.*
- **Energy range:** 5 – 18 keV. *In order to measure 2mm diameter drops, an x-ray energy of 16.9 KeV was used.*
- **X-ray detection system:** 2 1-dimensional WAXS and SAXS detectors based on RAPID2 technology (gas microgap, multi-wire). Efficiency is energy-dependent and is peaked at 8-9 keV. The WAXS detector has an acceptance angle of 60° 2θ and a resolution of ~0.06°. Minimum SAXS camera tube length is 1.3 m, maximum is 4.0 m with a maximum resolution of ~800 Å at λ = 1.40 Å. *Because of the high energy x-ray conditions RAPID2 detectors are filled with an A/Xe gas mixture. The 16.9 KeV setting was chosen to fall on the high energy side of the Xe x-ray K-edge and below the Y x-ray K-edge, as many of the liquids contained yttria.*
- **Experimental configurations:** Medium-high resolution powder diffraction based on a 2-circle diffractometer or simultaneous SAXS and WAXS. *In this experiment the SAXS/WAXS geometry was used.*

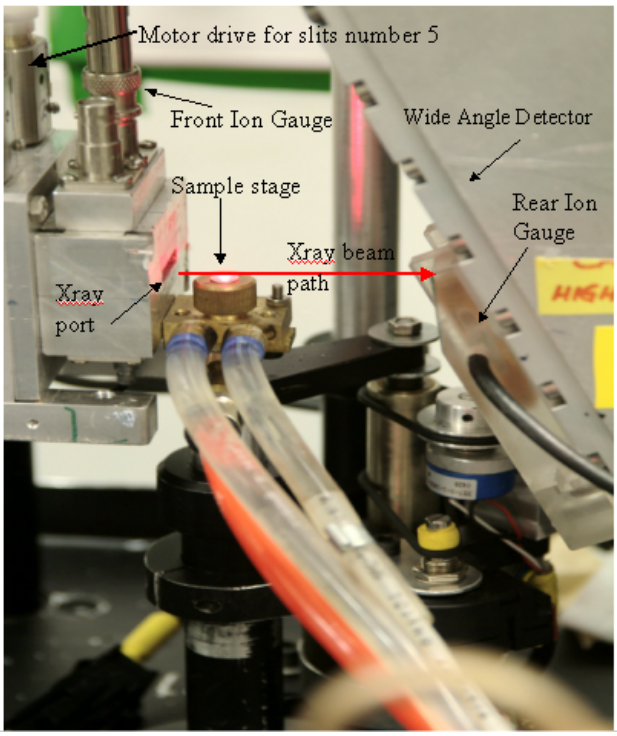


.

**Figure 8.1 Illustrating the position of the sample holder with respect to the x-beam position and the WAXS/SAXS detectors**.

### 8.2 Beam Size

The initial x-ray beam path, position and size were first established. This was achieved by a number of adjustments, culminating in a beam size of 0·37mm x 0·4mm. The initial setup is done by placing the sample holder with approximate alignment in the vertical and horizontal position in the x-ray beam path, as seen in Figure 8.5.

### 8.3 Establishing Datum Line

Measurement of the beam size and position is done without the sample in position. An x-ray sensitive green paper or Polaroid film is placed behind the sample holder and exposed to monochromatic x-rays for 1 minute. A theodolite is then used to set a datum line off this horizontal axis, and from this line, the bases of all the x-ray beam, laser optics and detectors are aligned, as can be seen in Figure 8.3.

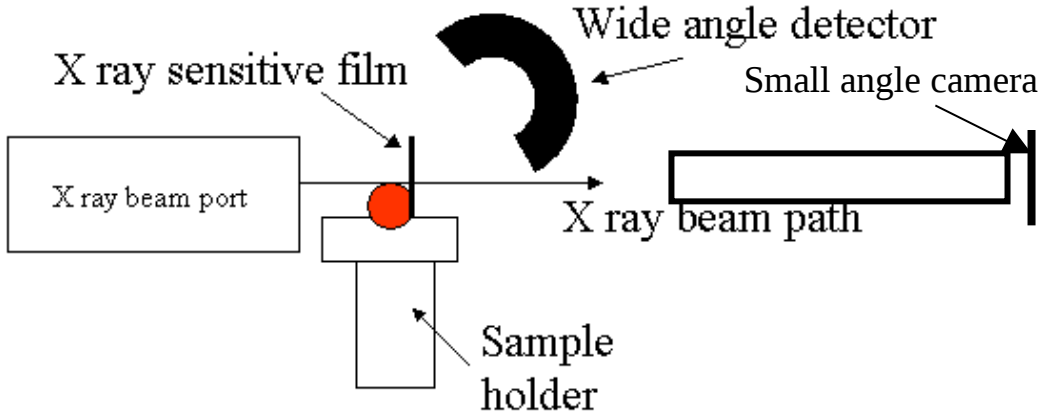


**Figure 8.2 Profile illustration position of the sample and levitation stage with respect to the x-ray beam path and the WAXS/SAXS detectors.**

For SAXS/WAXS measurements, x-ray beam energy, beam sizes and position needed to be set and calibrated before the final alignment of wide angle and small angle detectors and sample positions were optimised.

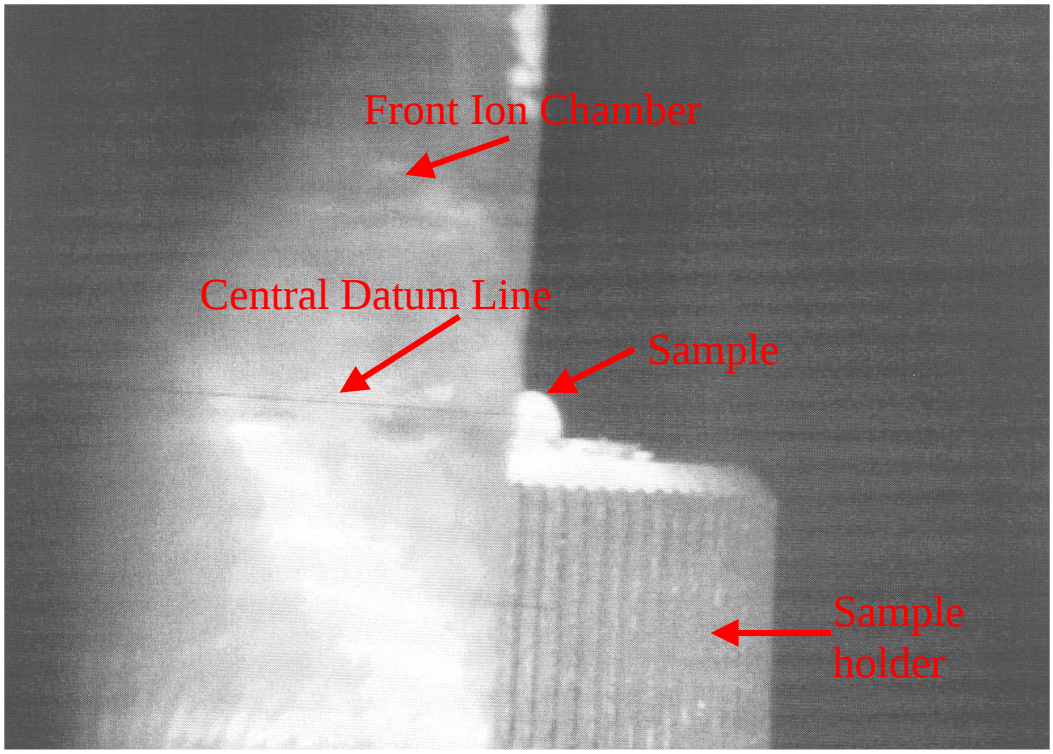


**Figure 8.3 Theodolite image illustrating central datum line taken using a mobile phone camera**.

Due to the limited size of the experimental hutch, plus the confined space within the experiment, photographic or video evidence proved difficult, but was achieved by the innovative use of a mobile phone camera attached to the theodolite eyepiece, as seen above.

**8.4 Beam alignment and size.**

With the datum line set, and the position of the x-ray beam established, the size of the beam is reduced by closing the horizontal slits. There are 5 pairs of slits situated along the beamline, which are adjustable individually, by the use of the GDA software8.5, as can be seen in Figure 8.4.

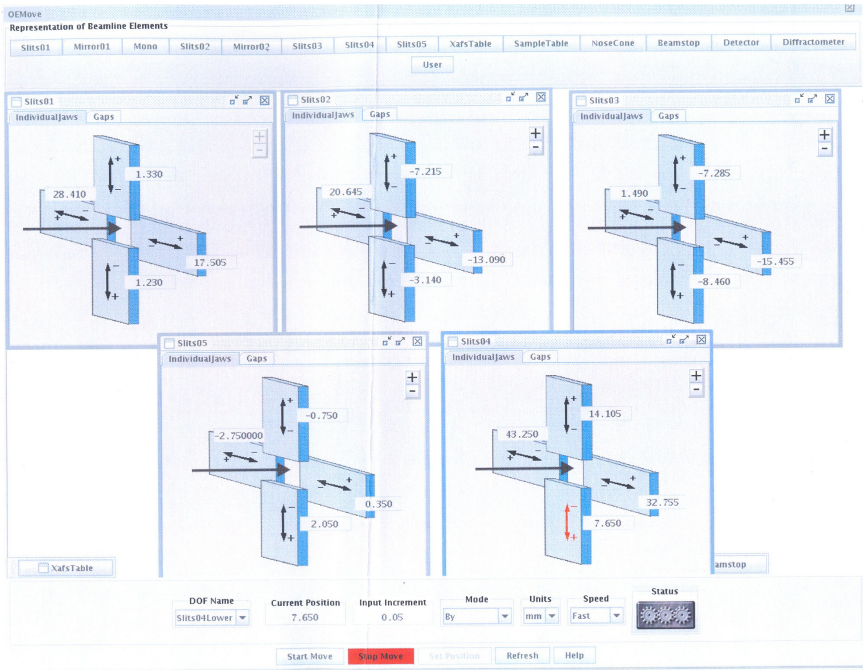


**Figure 8.4 Screen shot view of the GDA software illustrating the position and control of all 5 sets of slits.**

Each slit is reduced progressively downstream whilst monitoring the current measured on the front ion gauge, taking into consideration parasitic flare caused by the previous mirror, with final size achieved by measurement of the x-ray burn mark on the film, as can be see in Figure 8.5. The whole process may be repeated until optimum beam size of 0·37mm x 0·4mm is achieved. This is also optimised for locating the beam in the upper half of the molten drop avoiding “flare” and catching the nozzle surface.

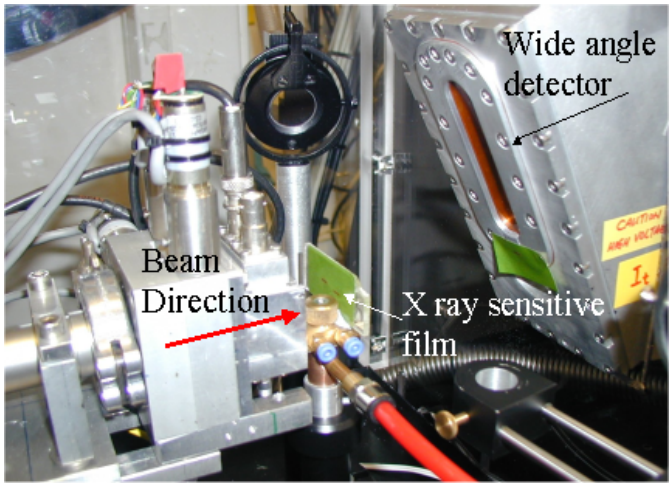


**Figure 8.5 X-ray sensitive paper positioned behind the sample, indicating beam position and size.**

### 8.5 GDA software

The GDA software is used for data acquisition and control of the individual components required for adjusting beam size, position, x-ray energy and intensity. This advanced software based on a Graphical User Interface (GUI) is designed around a single piece of software with the ability to integrate with, and control, all normal experimental functions, including equipment and station set-up.

### 8.6 XAFS table

The x-ray absorption and fine structure table (XAFS) is the main positioning system enabling sample to be positioned accurately in the x-ray beam to an accuracy of 50 microns. The four linear worm screw motors controlled by the GDA software allow for repeatable positions by the use of linear translation units in each of the motors. Once the datum line is set, any subsequent movement of the motors in the vertical or horizontal position compensate for backlash due to the gearing of the worm screws and of the motors. This may seem extreme, but has to be implemented during experiments, due to the extremely small size of steps measured.

### 8.7 Horizontal nozzle alignment.

Horizontal nozzle alignment was achieved by inserting a 0·5mm drill bit vertically into the nozzle. Horizontal movement of the EXAFS table was then controlled by the GDA software, allowing the front and rear Ion chamber readings to produce accurate positioning of the sample in the beam. This is achieved by scanning the drill bit through the x-ray beam and monitoring the rear ion chamber readings as shown in Figure 8.7.

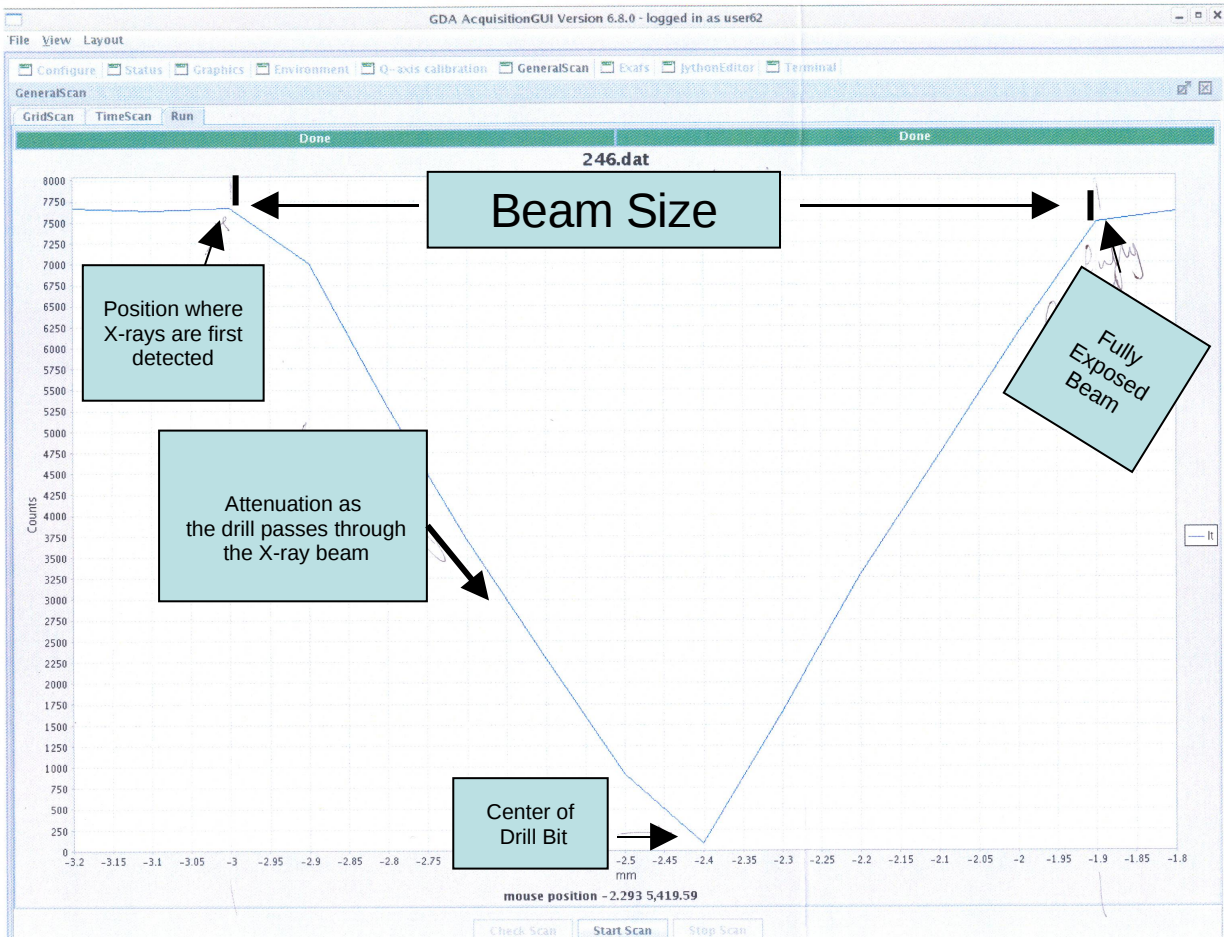
GDA AcquisitionGUI Version 6.8.0 - logged in as user62
File View Layout
Configure Status Graphics Environment Q-axis calibration GeneralScan Exafs JythonEditor Terminal
GeneralScan
GridScan TimeScan Run
Done
Done
246.dat
Beam Size
Position where X-rays are first detected
Attenuation as the drill passes through the X-ray beam
Center of Drill Bit
Fully Exposed Beam
Counts
mm
mouse position -2.293 5,419.59
Check Scan
Start Scan
Stop Scan

**Figure 8.6 X-ray beam attenuation graph for horizontal sample position.**

This can be confirmed by the use of Polaroid film to identify the beam position as can be seen in Figure 8.7. A Polaroid film is placed directly behind the drill bit, thus producing a shadow on the film. This indicates that a total beam block is accomplished, for a beam size less then 0·5mm in width.

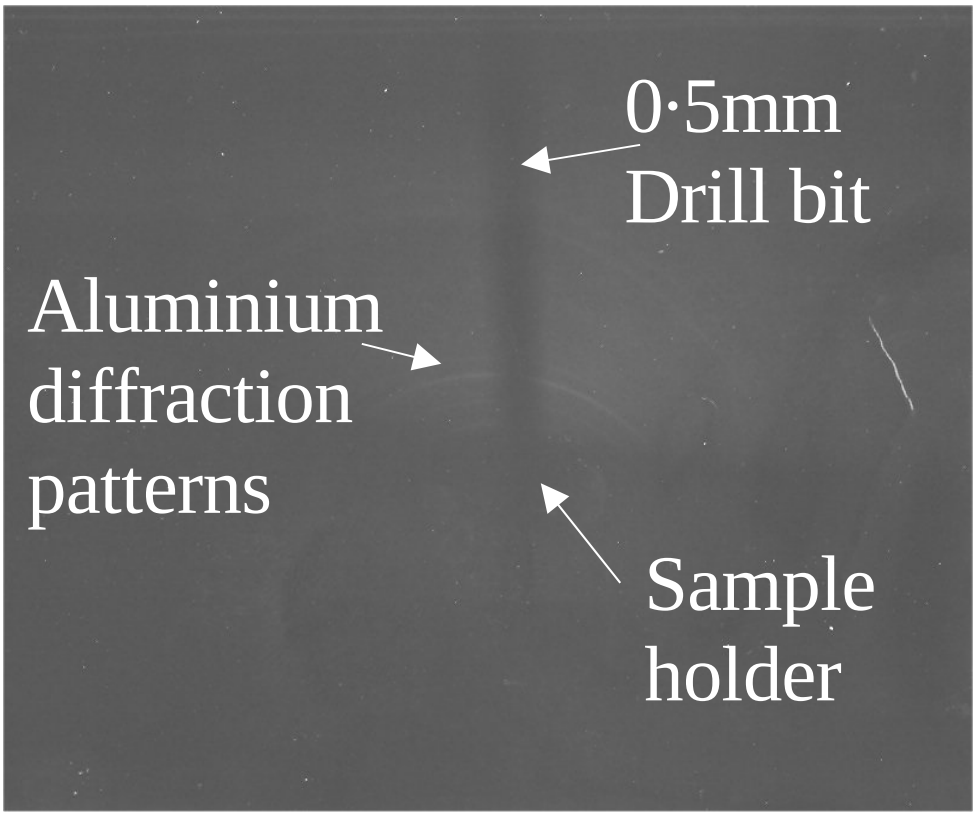


**Figure 8.7 Polaroid image illustrating the shadow of drill position and sample holder in x-ray beam.**

**8.8 Vertical nozzle position.**

The vertical position of the nozzle was achieved by a similar process, using a 0·5mm drill bit placed on the top surface of the sample stage as shown in Figure 8.8.

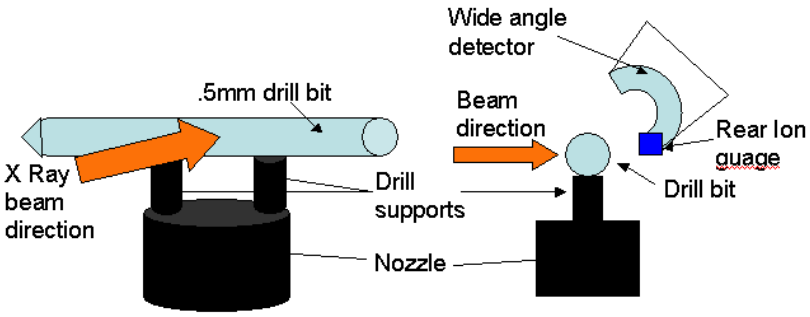


**Figure 8.8 Drill position on top of the sample stage enabling horizontal position of the x-ray beam.**

By vertical movement of the XAFS table in 100 micron steps, rear ion gauge readings measure the attenuation as the drill passes through the x-ray beam. This once again is optimized for maximum attenuation, as can be seen in Figure 8.9.

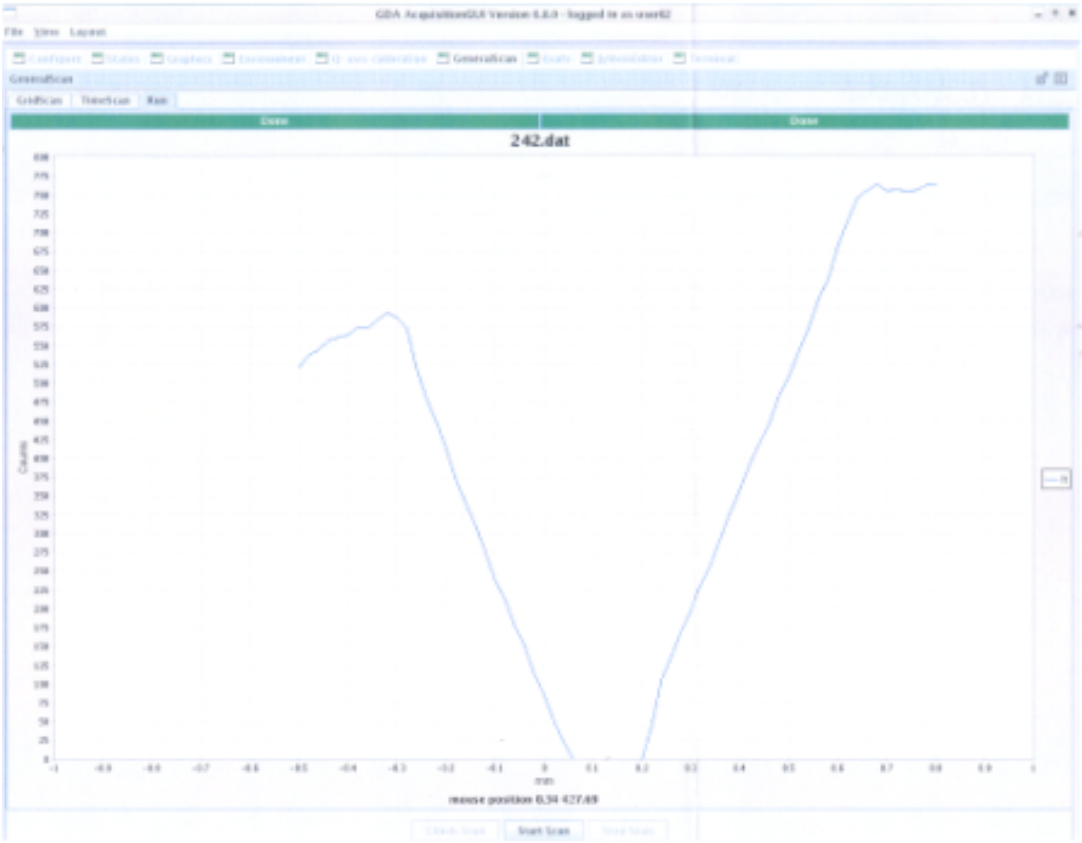


**Figure 8.9 X-ray attenuation as the drill bit passes through the beam in the vertical position.**

This innovative and calibrated method of beam positioning allows the focused x-ray beam to be positioned accurately on a 2mm sample surface.  With a beam size of 0·37mm horizontally by 0·40mm vertically.

### 8.9 Detector systems*(The Rapid2 X-ray detection system) paper ref A Berry, W Helsby et al

To enable the study of dynamic material processing, suitable detection equipment that can record high intensity diffracted and scattered synchrotron x-rays with high readout rates is needed. This requirement has led to the development of a high rate, photon counting image system called Rapid 2. [1]

The detection system is optimized to the high flux X-ray synchrotron radiation beamline multi-pole wiggler beamline 6.2. The detection system uses two one dimensional gas filled proportional chambers, which allow simultaneous acquisition of small (SAXS) and wide-angle (WAXS scattering images. These detectors achieve high rate capabilities by employing micro gap technology and parallel readout. The block diagram for the Radid2 system and the detector specification is illustrated in Figure 8.10

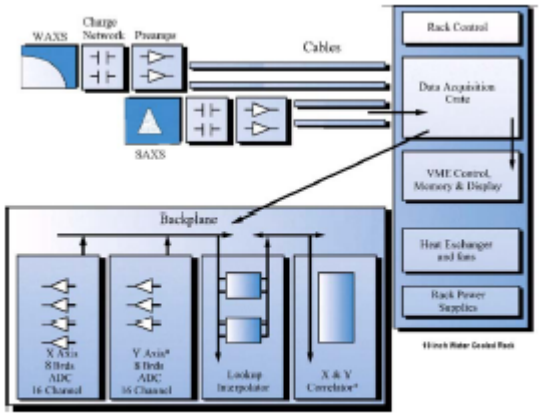

Fig. 1. Block diagram of the MPW6.2 Rapid2 system.

Specifications for MPW6.2 Rapid2 system

| Parameter | SAXS value | WAXS value |
|---|---|---|
| Detector style | 60° Quadrant | Linear |
| Energy range (keV) | 4–12 | 4–12 |
| Sample-detector spacing (mm) | 1200–4000 | 366 |
| Angular range (deg) | 3–9 | 60 |
| Angular resolution (deg) | 0.03–0.09 | 0.06 |
| Detector length (mm) | 200 | 384 |
| Spatial resolution (mm) | 0.375 | 0.375 |
| Pixel size (mm) | 0.094 | 0.094 |
| Count rate (global) (MHz) | 20 | 20 |
| Count rate (local) (MHz/mm) | 1 | 1 |
| Differential non-linearity (%) | 5 | 5 |

**Figure 8.10 Block diagram and specification of Rapid2 detector.**

With the sample position now optimized, a dedicated template on the wide angle detector enables this to be accurately positioned in the x-ray beam by the use of the theodolite, as can be seen in Figure 8.11.

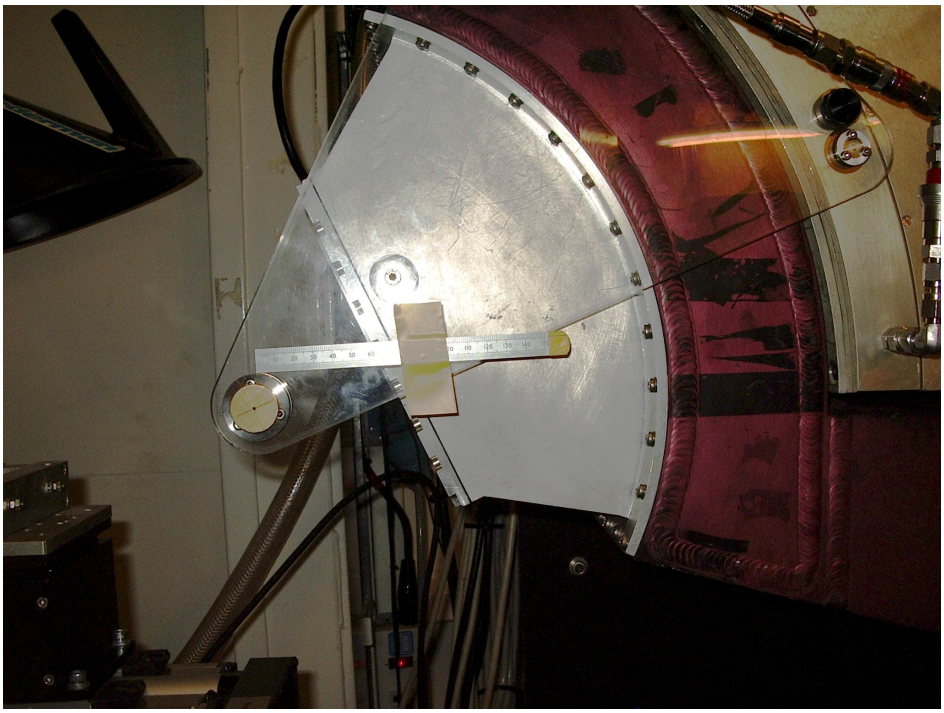

**Figure 8.11 WAXS detector template, allowing accurate repositioning of the detector in the x-ray beam.**

This position was marked with a stop block and bolted to the detector rails, the detector was then rolled back and the polycarbonate laser safety box was then installed. The detector was then repositioned, with the nose cone of the detector slotted inside the polycarbonate box, as can be seen in Figure 8.5. All of the laser optical components were installed with reference to this set datum point.

## 8.10 Conclusion

The systematic setup and alignment of the equipment and x-ray beam took approximately 4 days to achieve, but once complete, this setup was fixed, as the alignment and resolution was set for the rest of the experimental procedure. One method of improving beam position would be to use a laser beam and beam splitter aligned within the x-ray beam, thereby allowing simultaneous configuration of SAXS and WAXS detectors. This is type of development in now unlikely to happen with the closure of the Daresbury beamline.

## 8.11 References.

[1] The Rapid2 X-ray detection system

Andrew Berry, William I. Helsby, Brian T Parker, Chris J. Hall, Paul A Buksh, Andy Hill, Nick Clague, Mark Hillon, Garry Corbett, Paul Clifford, Alan Tidbury, Rob A.Lewis, Bob J. Cernik, Paul Barnes, G.E.Derbyshire.

Nuclear Instruments and Methods in Physics Research A 513 (2003) 260-263

# Chapter 9.

## LabVIEW Software Control.

National instruments LabVIEW is now recognised as the industry standard for the interfacing, simulation and control of external devices by the aid of a computer.

In this experiment it is possible to control each item of the equipment separately, but simultaneous measurement of all parameters proves too difficult for manual operation. To get high resolution manual control of each component is also impractical. In these circumstances, LabVIEW is an ideal application software, as it is capable of multitasking and controlling a wide range of different instruments. For this experiment the need to control two essential pieces of equipment is critical. Firstly the Synrad carbon dioxide laser for sample heating and melting, and secondly for control and simultaneous reading of the optical pyrometer. This is show in Figure 9.1.

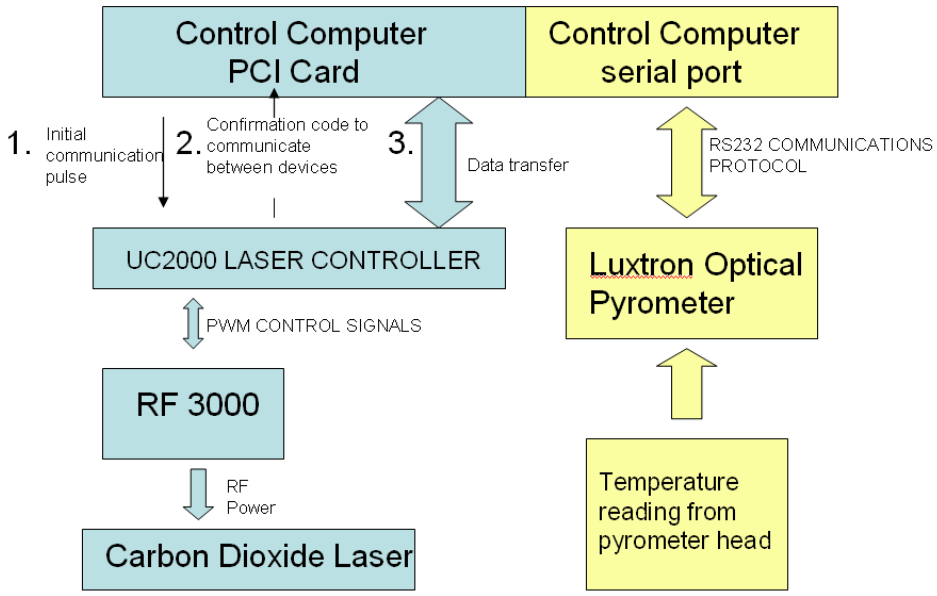


**Figure 9.1 Instrumentation for laser heating and temperature measurement controlled by LabVIEW.**

### 9.1 LabVIEW

LabVIEW software, unlike other forms of programming by control code such as visual basic or C++, is constructed by a means of building blocks known as virtual instruments or “VI’s”. Each VI is already coded by a unique programme capable of a particular job, be it mathematical, Boolean equations, graphical displays etc. Each coded building block or VI is capable of communicating with other VI’s as well as interfacing with external devices. This allows a uniquely dedicated interface and control system to be constructed for controlling and monitoring several operations.

At the development stage of the programme, LabVIEW operates on a two window system, the block diagram or construction window and the display window. The block diagram window is where all the structure of the system is developed, and the front window is the control panel for operating the system. Both windows are interlinked, so a command signal or control on the front panel will be executed by the dedicated VI’s on the block diagram.

To enable the control commands of LabVIEW to be executable and control external devices, a dedicated input/output card is used in the computer. For this application an Adlink 9112 Multi function data acquisition card was installed into the PCI slot on the computer operating the aerodynamic furnace with the following facilities suitable for this application:

1. 32 bit PCI bus
2. 12 bit analogue input resolution
3. On board A/D memory
4. 110khz A/D sampling rate
5. 16 single ended or 8 dual ended analogue input channels
6. Two analogue output channels
7. Two 16 digital input and output channels

## 9.2 LabVIEW Interfacing

As described in previous Chapters, the operation of the furnace and x-ray alignment requires precise control when controlled from one central point. Initially in this application, the control of the laser and pyrometer were facilitated by communicating via the computer serial ports. This method of control had serious limitations due to interrupt protocols. Also only two RS232 serial ports were available, so any expansion of the experiment requiring computer control was not possible.

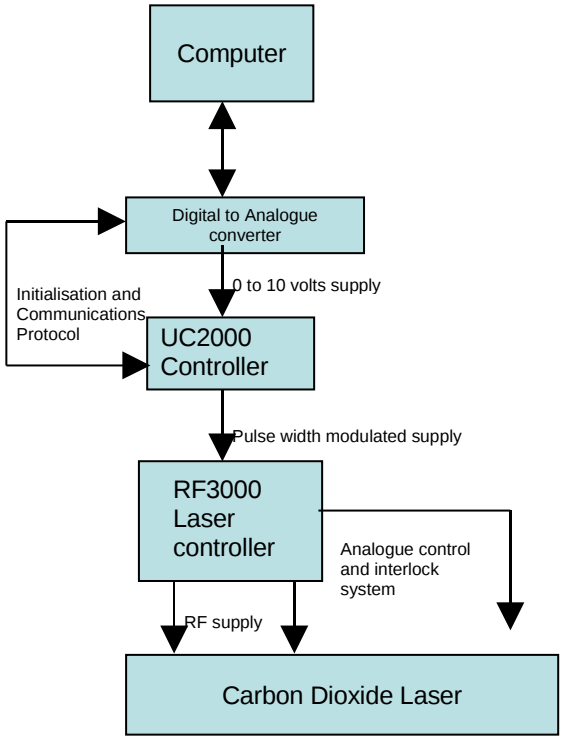


**Figure 9.2 Flow diagram of LabVIEW software initialisation for computer laser control.**

The installation of an Adlink Technologies Digital to Analogue interface card into the PCI slot of the computer, as detailed in Figure 9.2 and 9.3, allows significant control of the laser, by supplying an analogue voltage to the analogue input of the UC2000. The control voltage set on the LabVIEW programme gives a proportional pulse width modulated signal from the output of the UC2000. This is

subsequently fed to the RF3000, which in turn delivers proportional laser power required for the experiment.

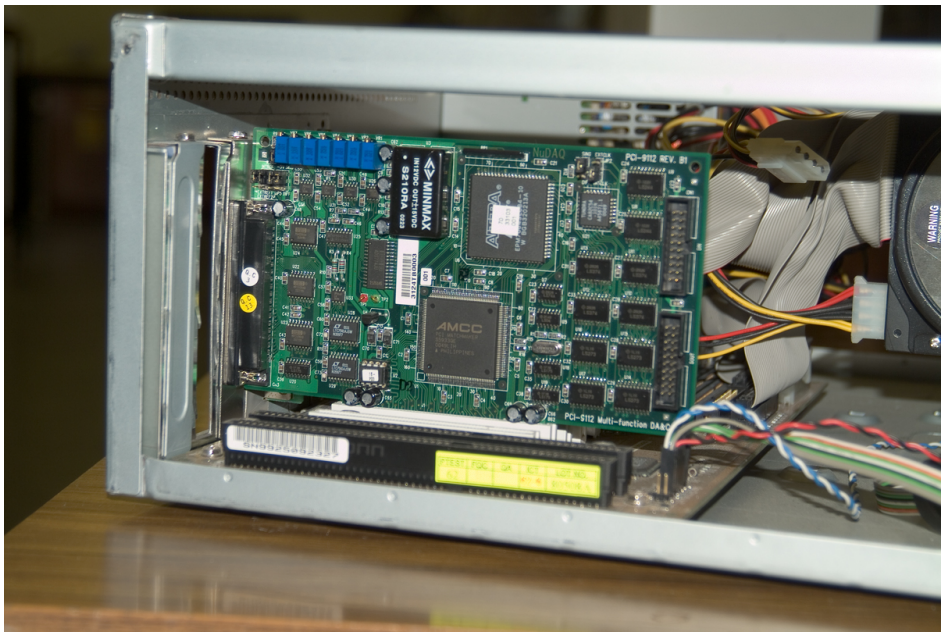


**Figure 9.3 Adlink Technology Digital to Analogue interface board which gives proportional output to the UC2000 laser controller.**

### 9.3 D/A Conversion

The operation of the D/A conversion requires the digital values to be set into the D/A data registers and the corresponding voltage will be outputted to AO1 or AO2

Connections to pins 32 Analogue output and pins 29 Ground were fed to the ANC input of the UC200. This produced the relevant voltage output to proportionally drive the UC2000,

with 12 bit resolution and an output drive capability of 5mA as show in Figure 9.4 and 9.5.

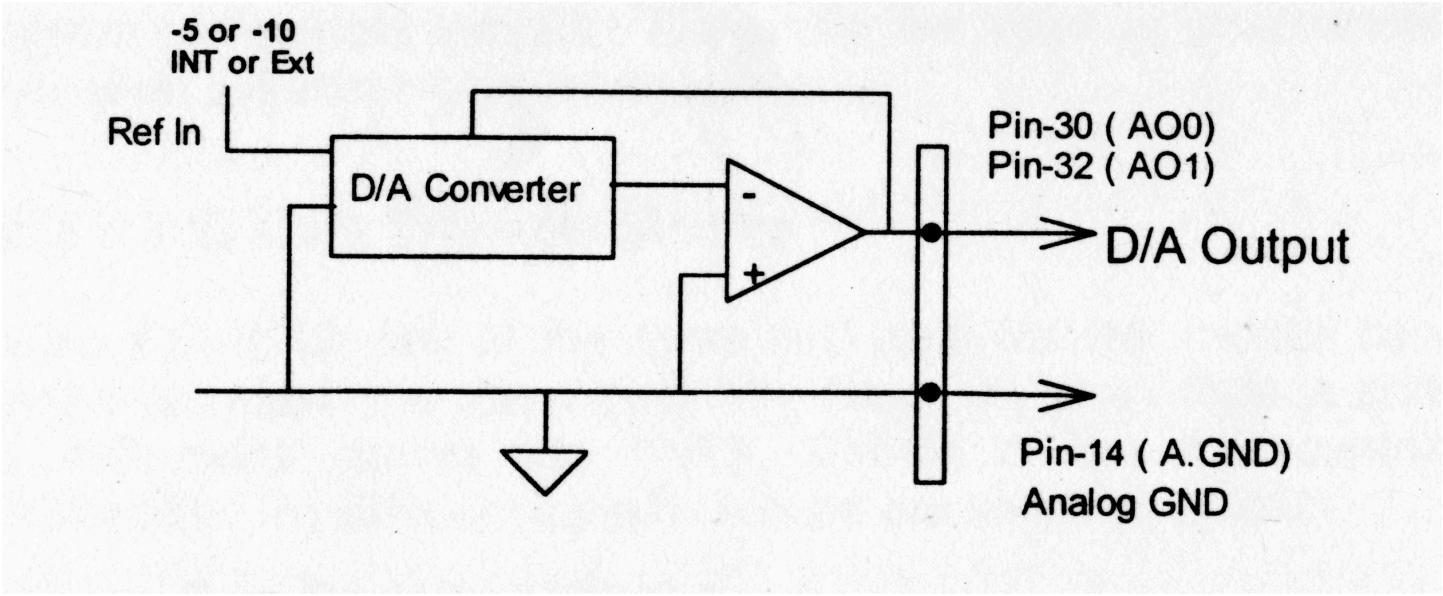


**Figure 9.4 Schematic of digital to analogue converter used to control UC2000 laser controller.**

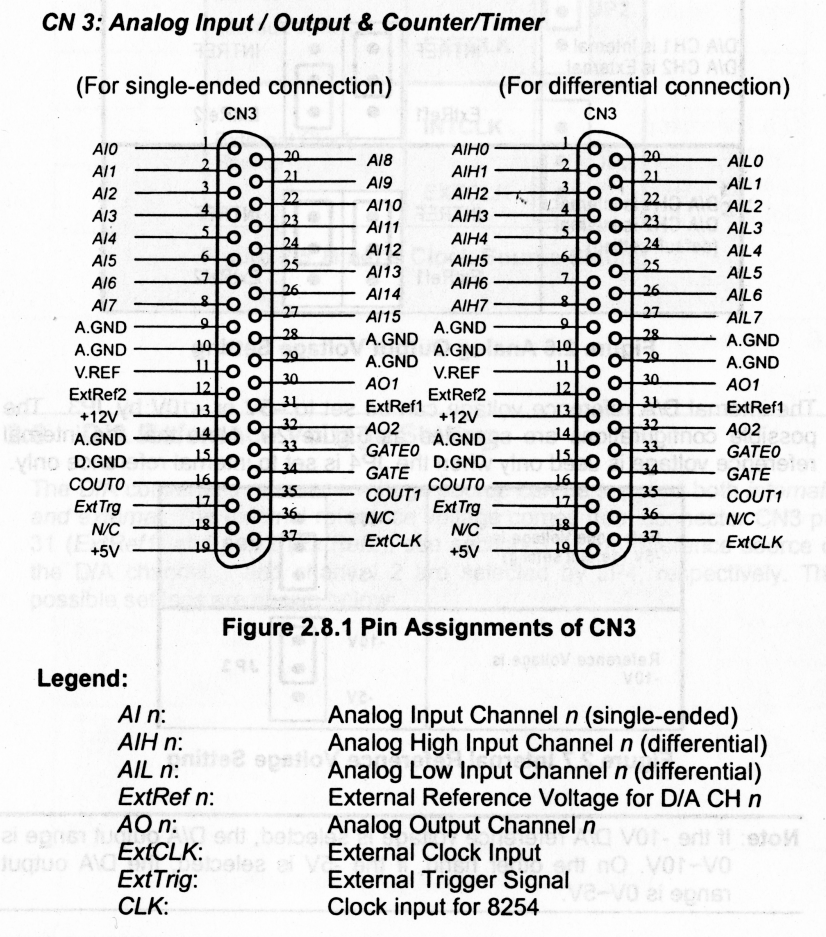


**Figure 2.8.1 Pin Assignments of CN3**

**Legend:**

| | |
|---|---|
| *AI n*: | Analog Input Channel *n* (single-ended) |
| *AIH n*: | Analog High Input Channel *n* (differential) |
| *AIL n*: | Analog Low Input Channel *n* (differential) |
| *ExtRef n*: | External Reference Voltage for D/A CH *n* |
| *AO n*: | Analog Output Channel *n* |
| *ExtCLK*: | External Clock Input |
| *ExtTrig*: | External Trigger Signal |
| *CLK*: | Clock input for 8254 |

Adlink technologies ltd/ www.adlinktech.com

**Figure 9.5 Analogue output connections of the Adlink Technologies interface board used to control the UC2000 laser controller.**

## 9.4 LabVIEW Software

When the LabVIEW application is created, the top level VI (virtual Instrument) defines the inputs and outputs for the application. Then the sub VI's are constructed to perform the smaller tasks within the top level VI. This is a subroutine working within a main programme.The modular approach is one of the main strengths of LabVIEW. Complicated applications can then be created that are hierarchical in nature, and re-use common elements within an application. The use of sub VI's make the application, debugging and maintenance easier to understand. Sub VI´s within this application area are used in the setup and communications protocol of the laser, and likewise for the setup, read temperature and corrected temperature profile of the optical pyrometer, as can be seen in Figure 9.6.

The two screens which are initialised include one for construction and development as seen in Figure 9.6, and one for experimental control via the front panel interface, as can be seen in Figure 9.7.

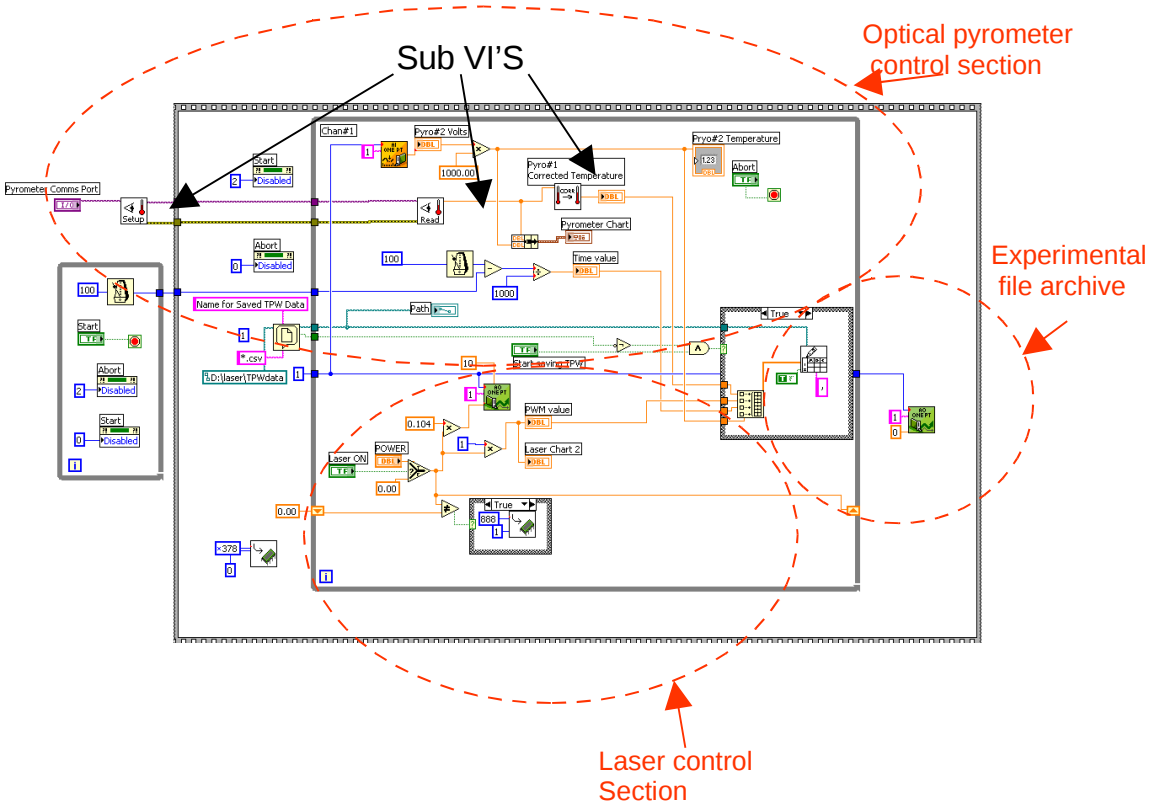


**Figure 9.6 LabVIEW construction block diagram window designed to communicate with the UC2000 laser controller and the Luxtron optical pyrometer.**

The construction block diagram in Figure 9.6 is split into two control sections. The upper section deals with optical pyrometry, and the lower section operates the control of the laser. The outer section also allows for all the operational experimental parameters to be saved to an allocated file space. All the functional controls on the block diagram are transferred to the front control panel as shown in Figure 9.7.

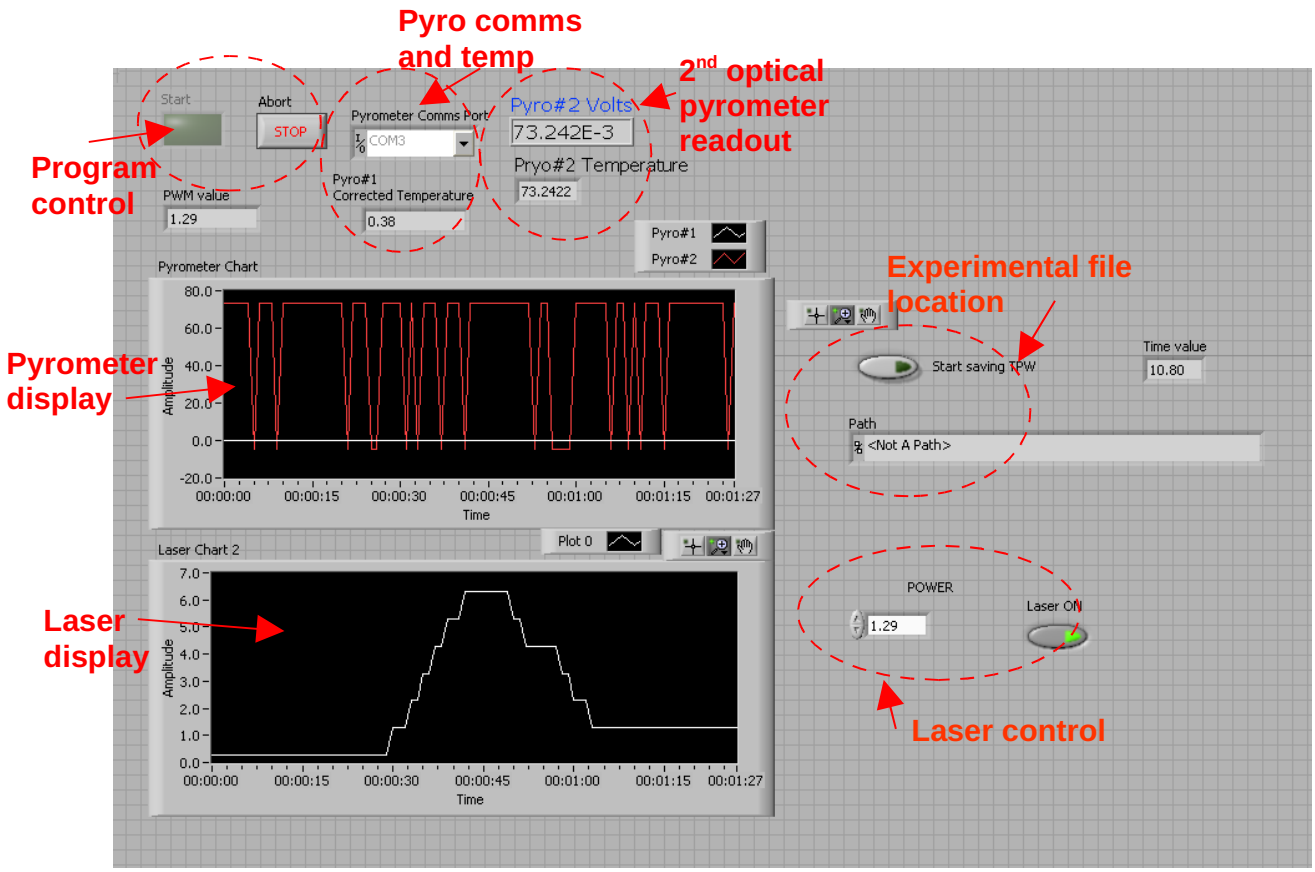


**Figure 9.7 Front panel interface for LabVIEW control of laser heating and temperature monitoring.**

## 9.5 Laser and software status

All commands within this section are associated with the communications protocol between the UC2000 and the computer. The UC2000 is set into the ANV mode (Analogue voltage mode) which allows an analogue voltage (0 – 10volts) to be produced proportional to the laser power intensity (0 –

100%). Whilst in this mode, the main ON/OFF switch on the UC2000 is not disabled by software, so that at any time that the experimental procedure, or if the laser safety is compromised, the manual Stop button can be operated. It is not possible to "Lock" this facility on in circumstances of computer failure.

A significant feature used by LabVIEW is the incorporation of error code messages. At any stage during system operation, any false coding or interrupted communication between the computer or external instruments, results in an "error message" being highlighted, at which point the system will be stopped and the problem area indicated by software.

### 9.6 Manufacturing Anomalies and Interference

Manufacturing problems were discovered in the laser system during the early development of this programme. As the power was increased over the whole range, proportional laser power was produced, until 63% power was achieved, at which point the power immediately increased to 100%. This would have caused serious instability in the sample heating and levitation, and is a critical manufacturing software safety problem. It was overcome using LabVIEW, by ensuring that when the power is incremented to 63%, software control of the laser is reduced by 0·5% to 62.5% for that duration. It is then incremented to 64% and continues up to full power. This problem was not significant, as the majority of the power used for this experiment was in the lower 50% region, but significant enough to realize potential dangers at higher powers.

This information was reported to Synrad the Laser manufacturers. Subsequent models specifications are now altered as can be seen below in Figure 9.8.

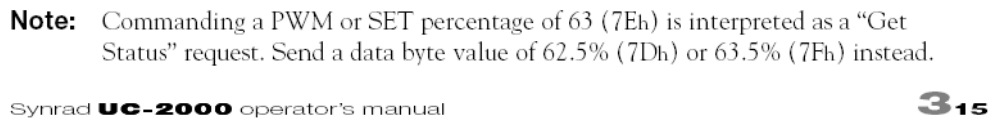
**Note:** Commanding a PWM or SET percentage of 63 (7Eh) is interpreted as a "Get Status" request. Send a data byte value of 62.5% (7Dh) or 63.5% (7Fh) instead.

Synrad **UC-2000** operator's manual 3 15

**Figure 9.8 Synrad software specification anomaly.**

**RS232 SERIAL COMMUNICATION**

This method of interfacing proved effective for pyrometer readings, but sporadic spikes or glitches occurred. These were intermittent during the experiment, particularly during the cooling stage and did not appear to correspond with instabilities in the laser or the power supply as seen in Figure 9.9. They were caused by the IRQ (interrupt request protocol) commonly used by the serial communications ports.

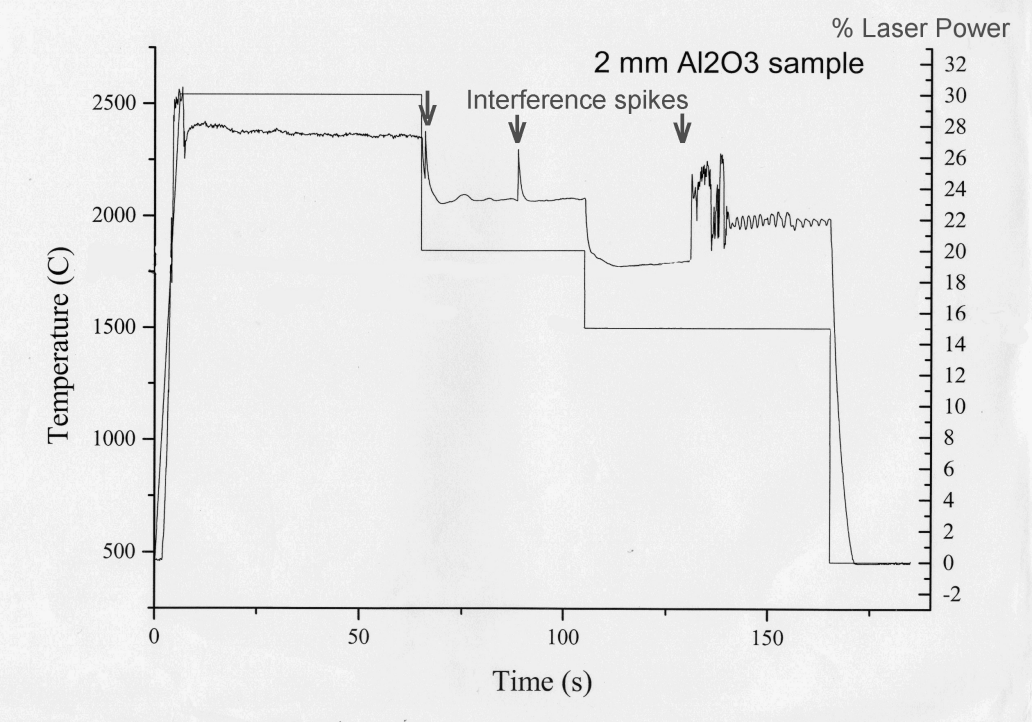


**Figure 9.9 Co plot of pyrometer output and laser power for a levitating super cooled drop, showing intermediate interference spikes.**

Interference spikes of almost 4% in laser power are enough to give the temperature swings of 250 degrees, seen in Figure 9.9. This is whilst the laser is operating in the supercooled region; it is enough to critically destabilize the sample and cause crystallisation and sample instabilities as can be see in the graph plot above. This instability was initially thought to be coming from the carbon dioxide laser, power supply, the RF3000 or the UC2000 controller, Figure 9.1 especially as the system was operating in the lower regions of power where technical specifications give power stability of 5%.

One method of identifying such interference is by the use of a digital power meter. This meter can be coupled to the communications port and operated in the same way as the optical pyrometer. By simultaneously monitoring the pyrometer and laser power meter on separate communication ports, both instruments were suffering from intermittent spikes. Laser power control was then transferred to the Adlink interface card as shown in Figure 9.2.

**9.7 Optical Pyrometry LabVIEW control software.**

Communication for this device is by the use of the RS232 Serial communications protocol, the comm1 port is located on the reverse panel of the computer.

In the design of the control software for the pyrometer, RS232 communication and calibration were first established, prior to building the main control panel. Basically, the skeleton structure must be in place before putting “meat “on the bones! For this application, sub VI´s are used for repeatable functions, where continuous communication between computer and pyrometer are required, as illustrated in Figure 9.10.

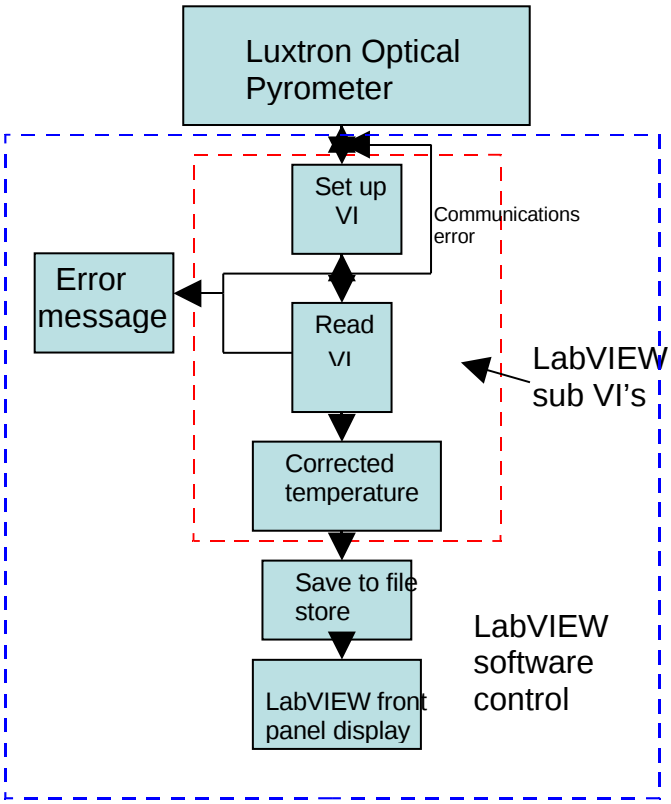


**Figure 9.10 LabVIEW software flow diagram for initialising and communicating with the Luxtron optical pyrometer.**

Another advantage of LabVIEW is that as the sub VI's are setting up and operating communications between the pyrometer and the computer, any fault or irregularities in the operation, will be highlighted within the system and an appropriate error message produced, as seen in Figure 9.10.

### 9.8 Vertical sample stage Interface

Additional to the XAFS table movement described in Chapter 8, the detailed adjustment of the sample in the x-ray beam was produced by the vertical movement of the linear shaft supporting the nozzle, coupled to a stepper motor. The controller for this motor is coupled to the LabVIEW interface board on the computer, as can be seen in Figure 9.11. This enabled the liquid drop height changes at different temperatures to be compensated for.

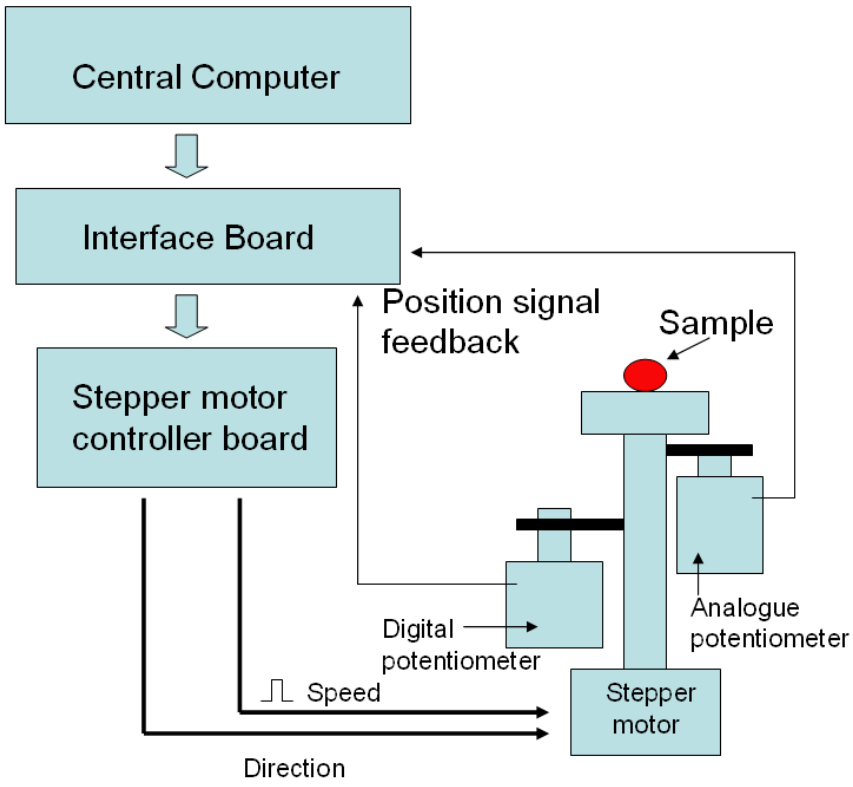


**Figure 9.11 Detailed vertical adjustment of liquid drop height at different temperatures.**

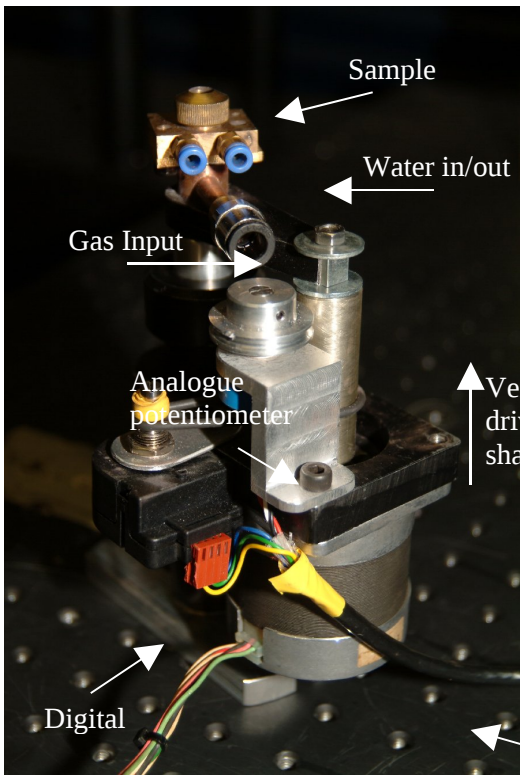


**Figure 9.12 LabVIEW stepper motor control of vertical sample stage, with analogue and digital feedback potentiometers for sample position.**

Vertical positioning of the sample stage in the beam was first enabled by the implementation of a ten turn potentiometer coupled onto the vertical shaft. This produced acceptable readings, but had limitations as only a set amount of turns could be achieved before the potentiometer hit the end stops. It was replaced for a continuous rotating potentiometer. This was more successful but resistance readings returned to zero after one complete revolution. Finally a digital coded potentiometer was built into the system. The subsequent decoded pulses were used to feedback the position of the nozzle height.

With the stepper motor drive, a certain amount of backlash was evident from the gearbox, even with fine pitched threads. With direct drive however, and coupling of the analogue and digital potentiometers, positions could be continuously monitored. An alternative method of measurement would be the use of a vertical shaft encoder, but was not possible due to space limitations.

**9.9 External triggering.**

Data capture by the wide and small angle detectors at the synchrotron facility at the moment is operated manually via the station's acquisition system. LabVIEW is capable of producing a TTL pulse that will enable the detectors to be triggered at the time that the laser is switched off, thereby eliminating human timing errors for the start of the cooling experiments, for example.

The same system was employed for triggering the high speed camera.

## 9.10 Future Developments

As the system improves, so must the developments in software control, for the increased convenience of the user and greater accuracy in data capture. One area of improvement is to incorporate the mass flow DDA controller software into the main LabVIEW programme, eliminating the requirements for a second computer and increasing the percentage control of the mass flow controller within LabVIEW.

Analysis of high speed video capture by the use of LabVIEW software is also an area currently being investigated. This will have the ability to interpret the movement of the high and low density phases of the sphere whilst in the super cooled region of the melt, by the application of false coloured imaging.

Real time video analysis could also be transferred to the main front panel of the LabVIEW controller Figure 9.7. Simultaneous coverage of the sample position and levitation, mass flow controller, laser heating and pyrometric temperature readings could then all be done on the one computer.

# Chapter 10.

## Laser Shutter.

This section deals with the design, operation and installation of a laser shutter, as part of the safety protocol required for safe operation of the carbon dioxide laser within the experimental hutch on a synchrotron radiation source such as multi pole wiggler 6.2 beamline at the Daresbury synchrotron radiation source, or I22 at Diamond light source.

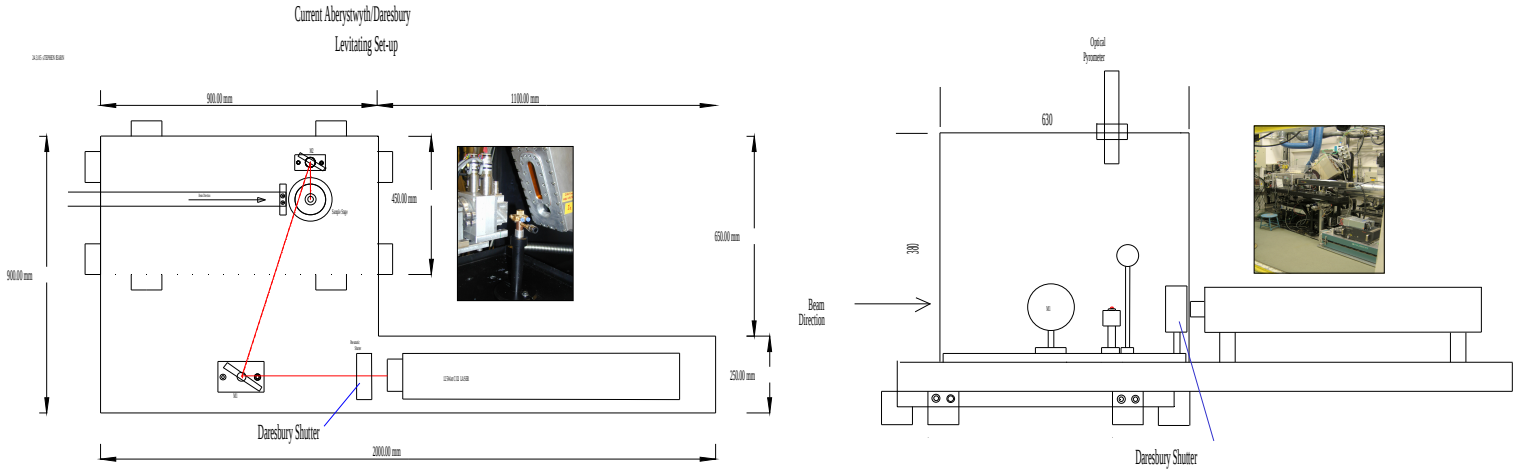


**Figure 10.1 Schematic layout of laser shutter position.**

There are two main reasons for the installation of a laser shutter:-

1. Equipment and personal safety; Laser beam block ensures that the beam is blocked in the event of laser breach, misalignment, or equipment safety malfunction.
2. Standby operations by enabling the laser to be kept in the standby state in the experimental hutch, whilst operators complete the x-ray interlock search protocol, means it can be operated continuously from the experimental control cabin.

### 10.1 Laser Beam Shutter

In conjunction with the Daresbury station staff, and Synchrotron radiation safety interlock protocol, a laser beam block was required to stop all lasing activity whatever the intensity during experiments. Therefore a shutter was placed within the polycarbonate box next to the exit of the CO2 laser. This required a customized piece of equipment to be constructed that would be capable of withstanding temperatures in excess of three thousand degrees Celsius.

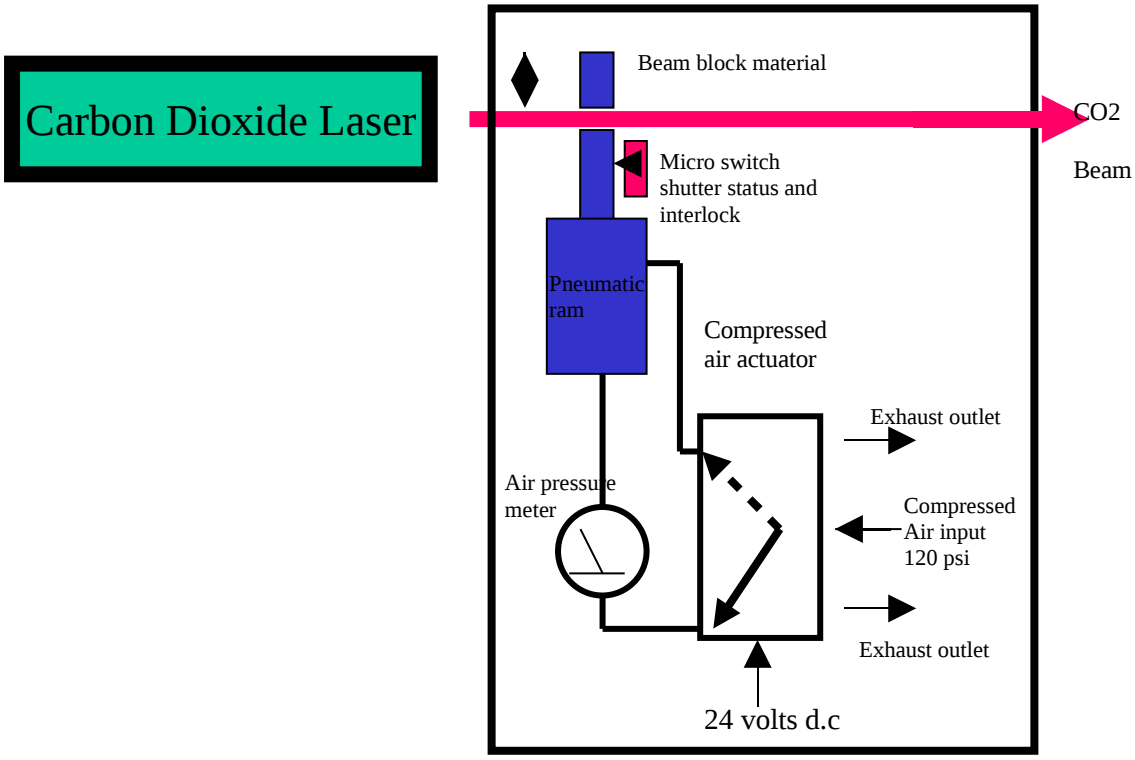


**Figure 10.2 Laser beam shutter schematics.**

## 10.2 Construction and operation

The item adapted for this use was a “fast action shutter”. It was originally used as a beam block to take the heat loading of a wiggler beamline at Daresbury Laboratory. The shutter part shown in Figure 10.3 was designed with a tungsten block mounted between two aluminum face plates, originally installed to protect experimental optics. The Tungsten block was subsequently removed and replaced by a heat absorbent material Sindanyo H91.

An engineering ceramic that can be machined, Sindanyo H91 has ingredients that include Refel silicon carbide, and Nitrasil silicon nitride. It is an alternative composite material, with similar heat absorbent properties to asbestos and is normally used for heat blocks and for electrical insulation in furnaces.

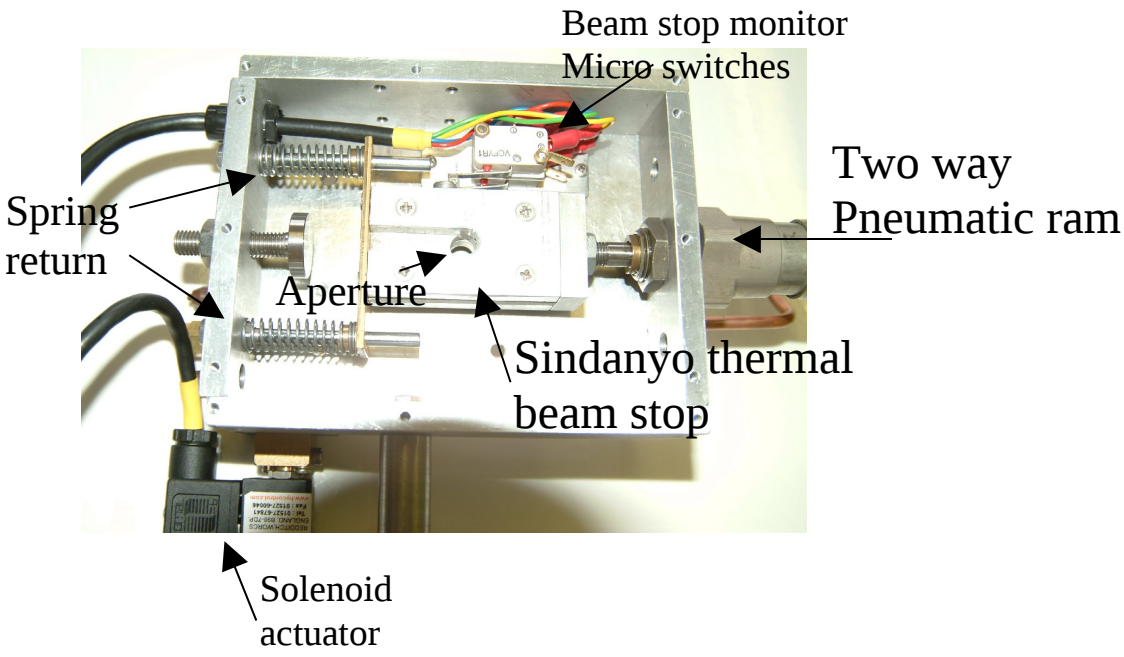


**Figure 10.3 Internal layout of the laser shutter illustrating the default position of the laser beam stop, the default return springs, interlock beam micro switches, the two way operating pneumatic ram and solenoid actuator.**

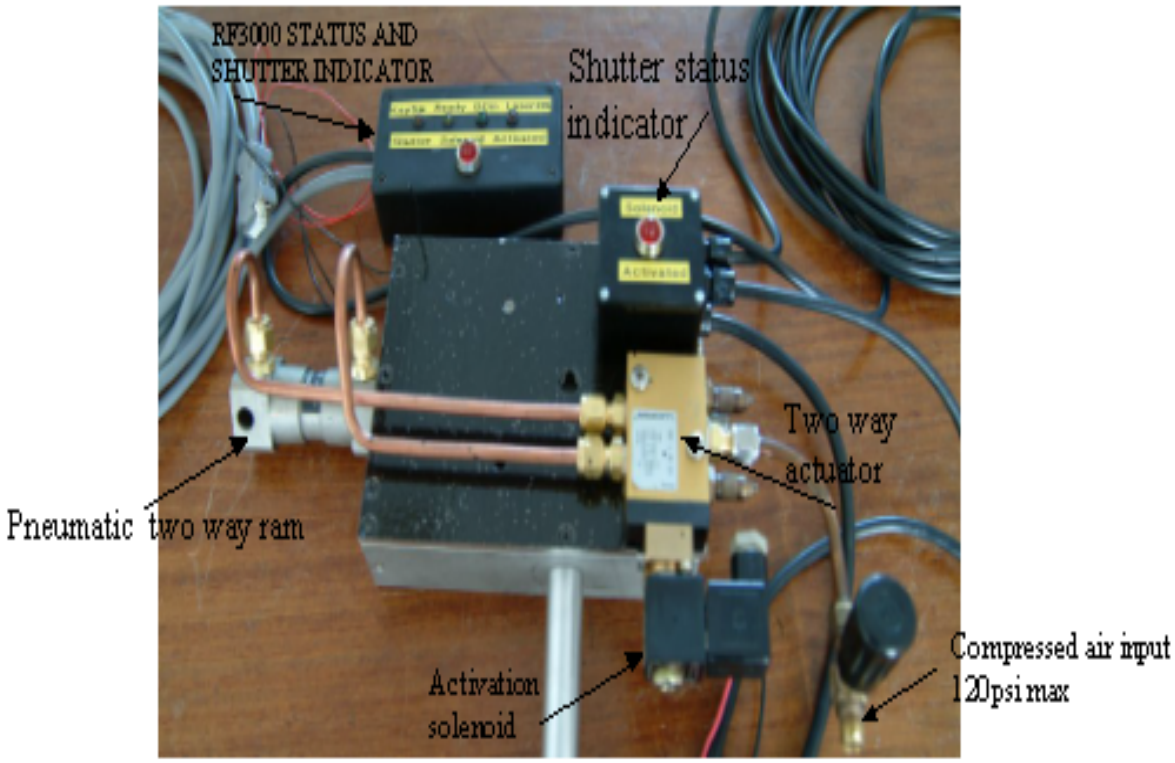


**Figure 10.4 External layout of laser shutter incorporating solenoid status indicator, pneumatic ram and two way actuator.**

A pneumatic ram requiring compressed air up to 120 psi operates the shutter.

This is operated by a two way actuator valve driven by a solenoid for opening and shutting. The closing operation is assisted by springs in the support section of the beam block. These allow the ram to open and close smoothly, with a operating time of half a second so that, in the case of air loss or electrical shutdown, the pneumatic ram will automatically default to closed beam stop. The pneumatic solenoid is operated by 24 volts, supplied by the interlock system.

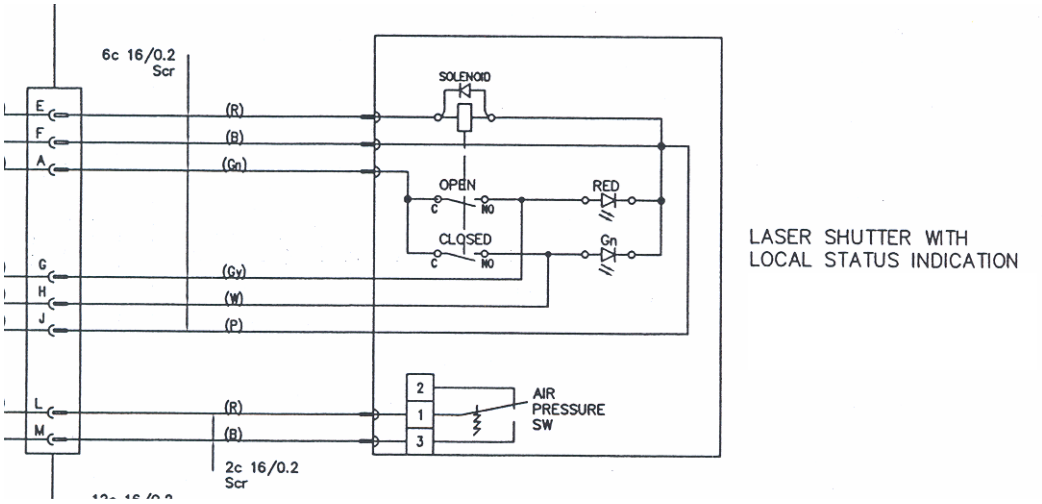


**Figure 10.5 Laser shutter circuit diagram, incorporating air pressure switch, beam block position monitoring and status indicators.**

### 10.3 Shutter status.

The monitoring system built within the shutter provides a visual indication to show that the solenoid has been activated. Additional micro switches operating on the moving shutter also identify whether the shutter is open or closed (Figure 10.5). These additions were inbuilt because of the location and manual operation of the beam stop. These indicators are located on the top of the shutter (Figure 10.4).

### 10.4 Remote indicator


**Figure 10.6 Remote laser status indicator panel and solenoid activation indicator.**

Due to the impracticality of continuous monitoring of the indicator lights on the shutter within the experimental hutch, an indicating monitoring box was coupled to the auxiliary output of the RF3000, allowing remote monitoring of all the control signals and status levels of the RF3000. Also now added to this is the solenoid activation indicator. This high intensity light emitting diode is wired to indicate that the solenoid has been activated. This monitor box is patch paneled through the cable labyrinth of the experimental hutch and is monitored in the control cabin as illustrated in Figure 10.6.

A second series of indicators are mounted on the remote key control box located in the control room; these indicator lights duplicate the condition of the laser shutter position indicators. More information on this operation can be found in Chapter 1. The whole system sits on a neoprene pad, which eliminates vibration induced into the optics table when the shutter is operated.

To be able to operate the laser remotely, the laser safety interlocks would have to be compromised whilst exiting the experimental hutch and the laser would then have to be reset. To avoid this, a 60-second timer is initiated, actuating the laser shutter into the closed position, whilst the laser is in operate mode. This allows the hutch to be swept and interlocked. Then computer laser control is restored in the control cabin by using the key switch thereby opening the shutter ready for sample heating.

## 10.5 Remote shutter key control box

If the sample is blown off the nozzle, either due to excessive levitating pressure or sample instabilities, or if the laser is likely to breach the polycarbonate safety enclosure, then the emergency stop button can be engaged. This is located on the remote key control box, as can be seen in Figure 10.7. The facility also has a “lock down” facility which must be disengaged prior to further operation. The device will engage both shutters, one electromagnetic shutter inside the laser head and the external laser shutter, immediately blocking laser beam.


**Figure 10.7 Remote shutter key control panel, with shutter status indicators, remote shutter closing and emergency laser disable panic button.**

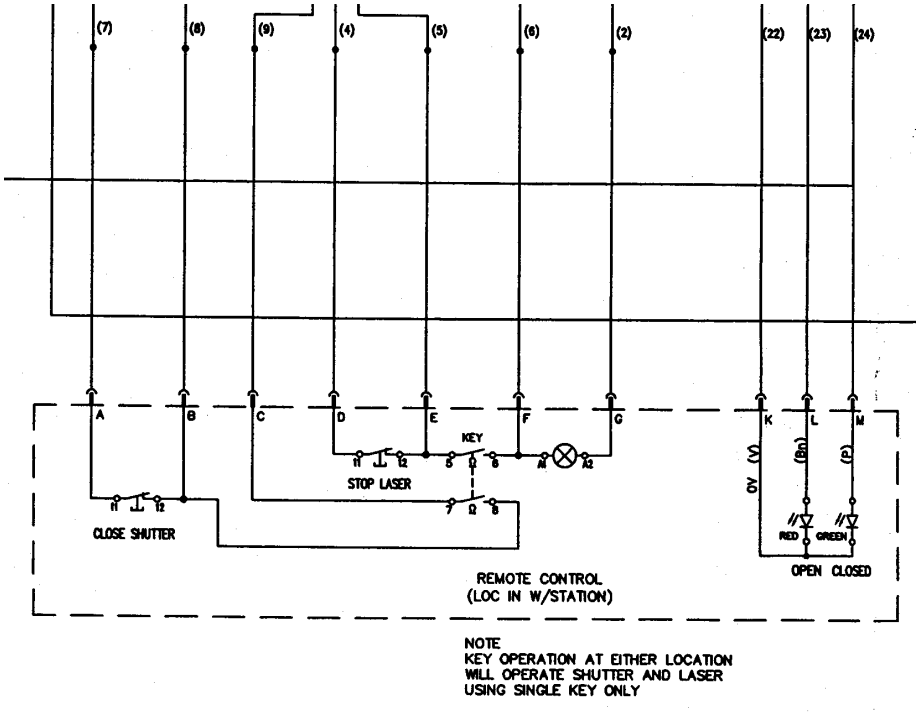


**Figure 10.8 Remote shutter control circuit diagram**

### 10.6 System upgrade

This laser shutter system has proved reliable over the duration of the research campaign at the SRS. The latest improvement is the addition of an air pressure gauge installed between the pneumatic ram and the actuator and solenoid. This acts as a visual indicator, monitoring the movement of air flow during actuation .

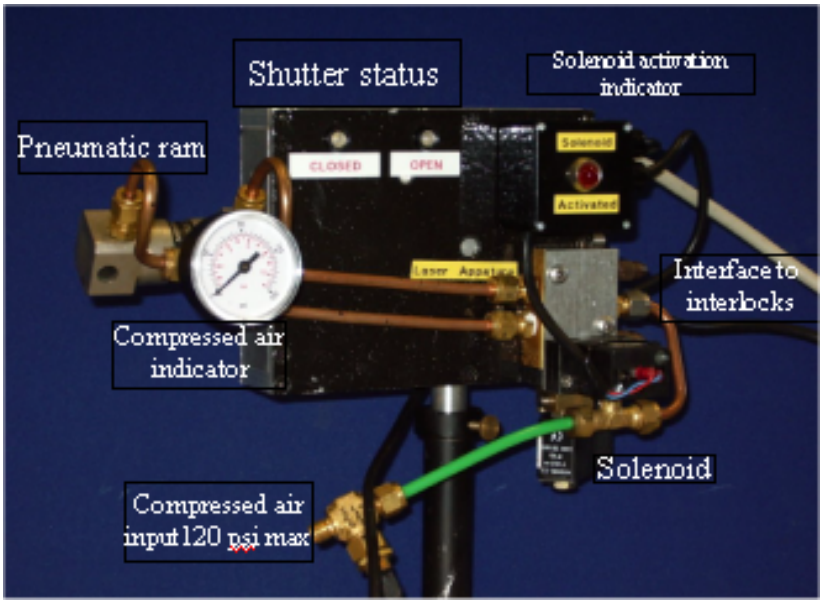


**Figure 10.9 Final operational laser shutter with compressed air indicator for monitoring air flow into two way pneumatic ram.**

### 10.7 Conclusions

An improved smaller version of this shutter has been built, and is currently under installation into the next generation of Synchrotron sources at the Diamond light source on Beamline I 22. Future developments will include a double shutter for the operation of a twin laser system that will enable the levitated sample to be heated from below as well as on top.

# Chapter 11.

**Safety protocol and video diagnostics.**

This section discusses the safety protocol associated with the safe handling of class 4 Carbon dioxide lasers. This includes interfacing the laser system with the polycarbonate experiment enclosure, installing instrumentation and interfacing this with a synchrotron beamline. In addition the various video cameras used to follow furnace operation and properties of the molten liquids.

## 11.1 Safety factors for use of class 4 lasers.

Factors to be considered for safe operation are:-

- 125 Watt Class 4 laser installation and operational protocols.
- Laser diodes for infra red laser beam alignment and Pyrometer alignment.
- Associated chilled water for laser head, power supply operation and levitator nozzle.
- Laser shutter beam stop blocks.
- Compressed air 150 psi for pneumatic shutter operation.
- Polycarbonate experimental box and interfacing to laser operation.
- Smoke detector if laser furnace malfunctions.
- Video cameras for recording sample levitation and experimental environment.
- Compressed gas for liquid drop levitation.

X-ray experimental interlock system  Laser system and safety interlocks

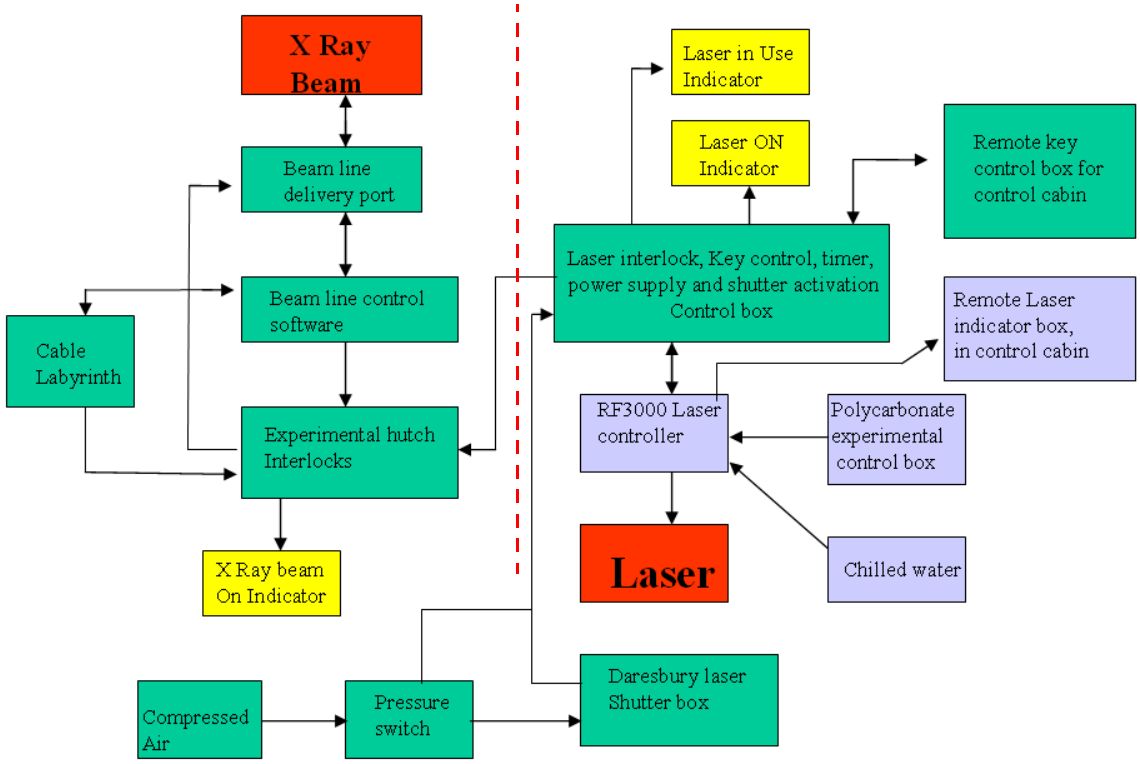


**Figure 11.1 Schematic diagram of laser levitator furnace interlock system and how it integrates with experimental beamline interlock system.**

Installations of this complexity require establishing a comprehensive safety protocol, prior to operation. Figure 11.1 shows how the Aberystwyth Levitator Furnace interfaces with the synchrotron radiation x-ray beam source.

Powerful laser beams emit non-ionising radiation. In this experiment the laser wavelength used is in the infrared region at 10.59µm, and has 125 watts output. 2mm beads are heated up and melted to 3000 degrees Kelvin.  An intense X-ray beam is passed through the levitated sample; the laser beam could pass through the experimental enclosure, and potentially through the beamline experimental hutch. James Bond science fiction from the 1970's could become science fact in this experiment.  There is a possibility this could in turn cause a breach of X-rays out of the experiment hutch, causing potential fatalities.

Similar scenarios are possible if the laser beam breached the X-ray delivery window, causing loss of vacuum in the beamline, and consequential synchrotron downtime. Similarly, laser beam breach into the wide angle and small angle detector would cause major damage and experimental downtime. Figure 8.1 shows the close proximity with which the laser beam interacts with the sample on the nozzle, intersected by the x–ray beam and close to the x-ray port and wide angle detector. The hazardous and complex nature of the set-up and experimental procedure, require the strict safety protocol outlined in Figure11.1 to be adhered to. Associated documents appended to this Chapter detail the operational set-up and use of the laser heated furnace, at the synchrotron radiation source they were produced in collaboration with Principle Beamline scientist at the Synchrotron Radiation Source, Daresbury Laboratory.

**11.2 Interlock control system**

To enable the set up and experiment to be operated, the laser must be interfaced into the X-ray beamline experimental hutch. This was the first time an experiment of this nature has been installed on a synchrotron radiation beamline at Daresbury Laboratory.

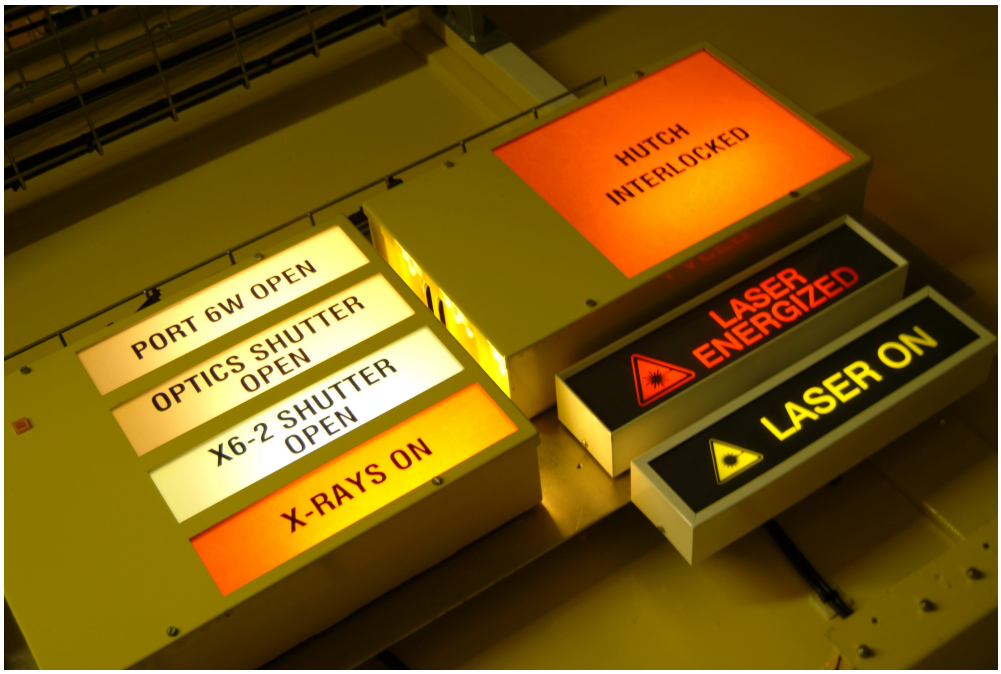


**Figure 11.2 Experimental hutch interlock hazard display panel on MPW beamline 6.2**

With all experiments associated with Synchrotron Radiation sources, a comprehensive system of safety interlocks and personal protective push buttons already exist. It is designed to be activated within the experimental hutch to ensure that any individuals present leave before the x-ray shutter is raised and high intensity x-ray beams and gamma rays enter the hutch.once the sweep of personnel from the hutch is clear and the doors closed, the safety interlock is then engaged from outside. Successful interlock and operational x-ray beam present, laser ignition and operation can commence.  The status of the x-rays and laser beam is indicated by the hazard indicator panel illuminated above the experimental hutch door.

To interface all the equipment appropriately, the circuit diagram in the appendix illustrates how individual items have been installed with the use of QM multi pin connectors, enabling the system to be set up at the start and dismantled at the end of the experimental period, without disruption to the existing x-ray and gamma ray safety interlock infrastructure.

A dedicated control box with laser power supply, key control and suitable shutter interface connecters was permanently installed into the experimental hutch at MPW beamline 6.2 at Daresbury Laboratory and is shown in Figure 11.3.

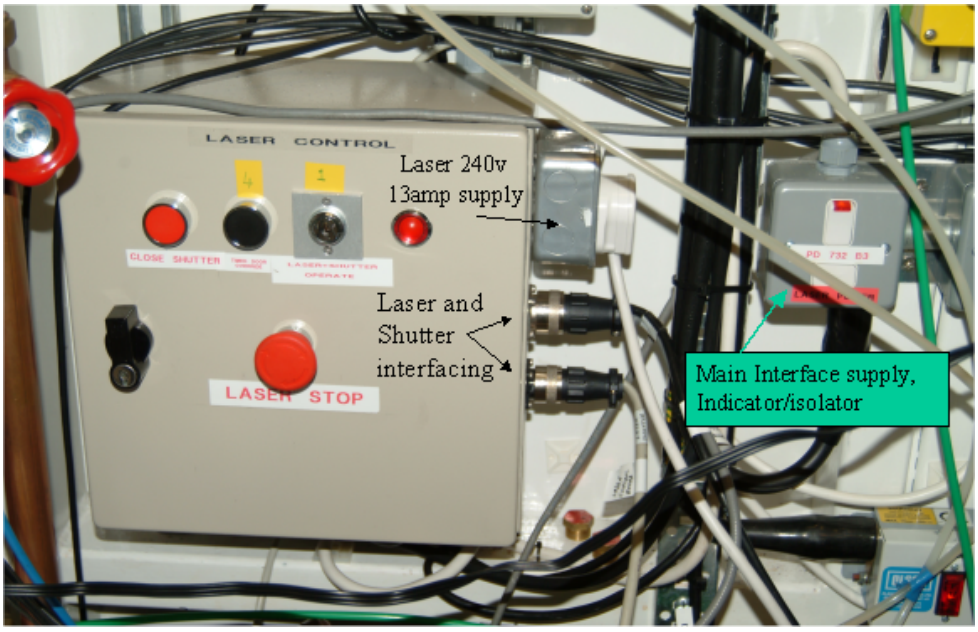


**Figure 11.3 Laser interlock control panel**

This system allows individual laser heated furnace items to be interfaced into the experimental hutch safety interlocks.

### 11.3 Experimental alignment

The following sequence describes how the laser is operated under experimental conditions within the hutch and is used for the purposes of optical alignment only.

**Note: The standing orders associated with Carbon dioxide laser experiments on MPW6.2 SRS Daresbury must be read and signed prior to any experimentation**.

A copy of the standing orders is included in the appendix.

1. Place suitable sample onto the levitation nozzle (Chapter 7).
2. Ensure preparation polycarbonate chamber lid is closed, and micro switches are engaged.
3. Turn on main isolator fused switch next to main control panel. This switch also illuminates the "laser in use" sign situated above the door of the experimental hutch (Figure 11.2).
4. Switch on 240 volt supply to the laser; this engages the laser power supply.
5. Switch on RF3000 (Chapter 9).

6. Ensure all control lights on the RF3000 are illuminated.
7. Hold experimental hutch door closed, with second person support.
8. Engage and operate key switch on main control panel, this now operates and activates the laser shutter into the open position (Chapter 10).
9. Laser diode is now operational for the alignment of the laser beam and optics onto the sample.
10. For Carbon Dioxide operation, open laser manual shutter situated on top of the laser.
11. Engage key operation in RF3000 controller. Laser “ready” light is now illuminated.

Extreme caution must be employed at this stage, as the Carbon Dioxide laser is now “live”.

12. Ensure that the UC2000 controller is at 0% , then press “RUN” and manually ramp up the laser power. Alumina samples do not get substantially hot until the laser power is at least 3% of 125watts.
13. To ensure all interlocks are now functional, open experimental hutch door, shutters will now close and the laser rendered inoperable, reset key switches and repeat steps 8 to 13 for further operation.

Once alignment is complete, the control computer, UC2000 and laser indicator box are removed to the control cabin for remote operation via the hutch interlocked labyrinth.

**For experimental purposes**.

Repeat steps 7 to 11, but this time, take out the key after it has operated the shutter, press the timed override button. This closes the laser shutter for a timed period allowing users to exit the experimental hutch and engage x-ray beam. Enter the control cabin and re engage the key on the remote control panel. Upon operation, all indicator lights will be illuminated after the shutter is operated. The aerodynamic laser furnace system is now operational and ready to use.

### 11.4 Laser emergencies

In the case of an emergency with the laser, press the laser Run button on the UC2000 (Figure 2.6). This will then switch the laser off and the indicator lights on the UC2000 and the laser controller monitor will also be extinguished.

### 11.5 Emergency Kill Switches

To instantly halt all operations operate the red Kill switch ( as can be seen in Figure 11.4). All shutters will be immediately activated and the beam isolated. Everything within the experimental hutch will then have to be reset.

The Kill switches are situated on the main interlock panel in the experimental area, labelled “laser stop” and on the portable key switch, located in the control cabin which will be situated next to the UC2000 and the control computer.

The Kill switch has a mushroom head latching close operation, to reset the switch rotate clockwise.


**Figure 11.4 Laser emergency stop and shutter control box**

### 11.6 Laser safety glasses

All glasses supplied conform to EN207 standard for laser protective eyewear and must be worn at all times during laser alignment in accordance with standing orders.

### 11.7 Polycarbonate Enclosure

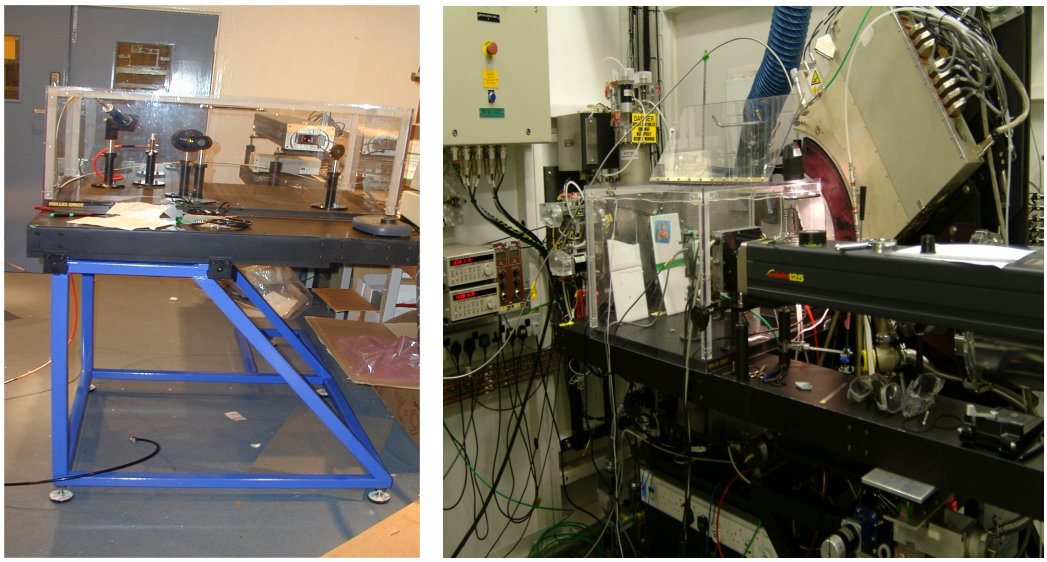

**Figure 11.5 Polycarbonate box on test bench and polycarbonate box installed onto beamline.**

Polycarbonate sheet is an incredibly strong material and is normally used in the production of riot shields and the front lenses of car headlights, and so is capable of withstanding high impacts. The optical properties are completely transparent through the visible range of the spectrum, and sharply drops to 0% transmission at 400nm thereby acting as attenuator of Infra red wavelengths, with the beam having to burn a path through the medium. This therefore is an ideal material for the experimental enclosure. A hinged door on the roof of the enclosure allows for insertion of samples and adjustment of mirrors if required. Also attached to the door are three micro switches, which prevent

opening the experimental area of the levitator with the laser powered. These micro switches are also connected into the experimental interlock system of the x-ray hutch.

### 11.8 Smoke detector

Due to aerodynamic instabilities, the sample may drop off the levitator. Beam reflections off the surface of the nozzle can also deflect quantities of heat onto the ceramic stops or onto the polycarbonate enclosure. Given sufficient infra red power these could be ignited. Smoke generated would be detected by the smoke alarm, giving us an additional audible alarm.

### 11.9 Ceramic Beam stops

White ceramic tiles used for tiling bathrooms and kitchens are suitable beam stop material to minimize stray laser beams and will stop penetration of the Polycarbonate enclosure. With average thicknesses of 3mm, full laser power will take several minutes to fully burn through the outer glaze and the ceramic tile. In areas of high vulnerability, the tiles are laminated with an air core between tiles, thereby increasing “burn through” time. They are also used to cover the viewing windows of the beamline hutch, to minimize stray infra red radiation entering the adjacent experimental control area.

### 11.10 Welding glass filters

Innovative use of welding glass filters for welding masks has been made. These devices are normally used to protect users from the harmful effects of high intensity arc welds and from infra red and ultra violet radiation to the eyes. Using various grades of filter density enables samples to be monitored across a range of temperatures and intensities by video cameras.

### 11.11 Compressed Air

Compressed air is used to operate the pneumatic shutter at the front of the carbon dioxide laser. This shutter requires 150 p.s.i. to operate, using a solenoid valve for opening and closing the shutter as described in Chapter 10. In the event of air or power loss the shutter will default to the close location. Monitoring these positions are micro switches which are integrated into the experimental safety interlock system.

### 11.12 Compressed Gases

Compressed gases in this experiment, Argon and Nitrogen, although inert in their composition, are stored in pressurized gas vessels at 3000 psi. With regulated pressure fed to the mass flow controller (Chapter 4). Installation, movement, replacement, and operation must only be done by trained personnel, wearing appropriate personal protective equipment; failure to comply could result in serious injury.

### 11.13 Chilled Water

The carbon dioxide laser requires cooling water of a minimum of 2 gallons per minute at less than 70psi. for stable operations. Achieving stable conditions is important as the system needs to provide power over long periods required by the super cooled liquid experiment. Cooling of the laser was achieved with the use of a chilled water supply. Water pressure and temperature are monitored by the RF3000 power supply controller. In the event of loss of water within the system, the interlocks associated with the laser and experimental hutch is de-activated rendering the experiment inoperable until the fault is rectified.

**11.14 Video Camera Surveillance.**

Extreme conditions associated with this experiment require additional safety measures. These are achieved by the use of a number of dedicated video cameras capable of monitoring the sample environment and experimental operations. The cameras are also vital for following the operation of the laser furnace and operational behaviour of the heated liquid drop.

The cameras include a variety of CCD devices, and are placed in various locations as shown in Figure 11.6. The two main monitoring cameras are situated outside the polycarbonate box. For reasons of safety they are operated using long focal length lenses. The radio cameras are more adaptable, because of their size, and the unnecessary use of umbilical video cables. Receivers located outside the polycarbonate box pick up the dedicated video signal which is then relayed to the video monitors in the

experimental control area.

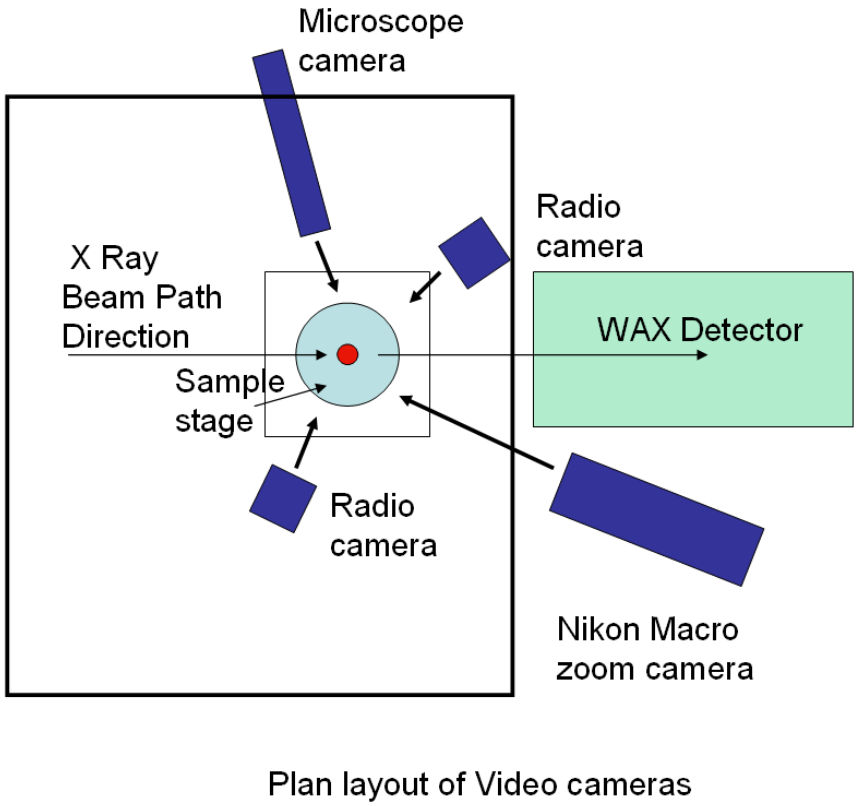


**Figure 11.6 Plan layouts of video cameras**

**11.15 Radio Cameras.**

**Figure 11.7 Radio camera on optical mount.**

The nature and size of these types of cameras allow them to be situated in close proximity to the levitated samples, without the need for additional cables. The 2.4.GHZ cameras do have a limited automatic exposure level. This saturates at high intensities, but does not cause any damage to the camera; it does produce a secondary ghost image, which can be used as a visual indication of levitation sample.

**Figure 11.8 Video footage of liquid sample.**

### 11.16 Microscope camera.

A standard JVC 1/2 inch CCD camera with Automatic exposure (Figure 11.9), is coupled to a Bausch and Lomb Mono zoom 7 microscope lens with a magnification of 1.5 to 10.5. Due to the focal length of this particular lens, it is situated only 10cms away from the sample. With lenses of this magnification, depth of field is minimal, but it is located in a position where the angle of the sample can be monitored, as can be see in Figure 11.6.

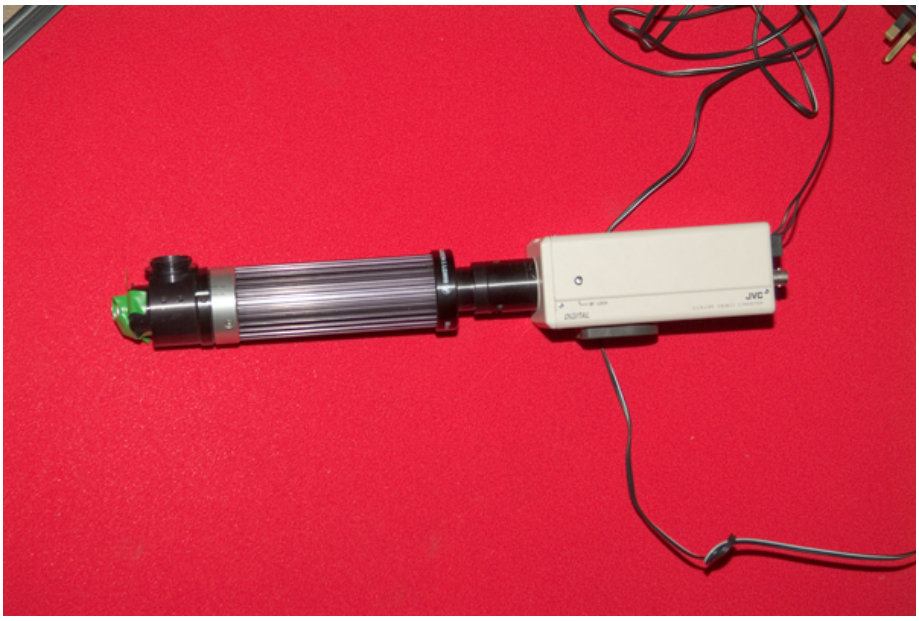

**Figure 11.9 Microscope camera.**

A welding filter capable of attenuating high intensities is placed in front of the camera lens, so that the sample can be monitored without the camera going into saturation.

### 11.17 Sample plane video camera.

Another CCD camera is situated at 45 degrees to the beamline and is fitted with a Nikon 200mm macro zoom lens.  This camera is mounted so that the vertical height of the sample
can be measured and monitored as it levitates; it is used as a magnified visual reference of sample position with respect to the x-ray beam position, as can be seen in Figure 11.10.

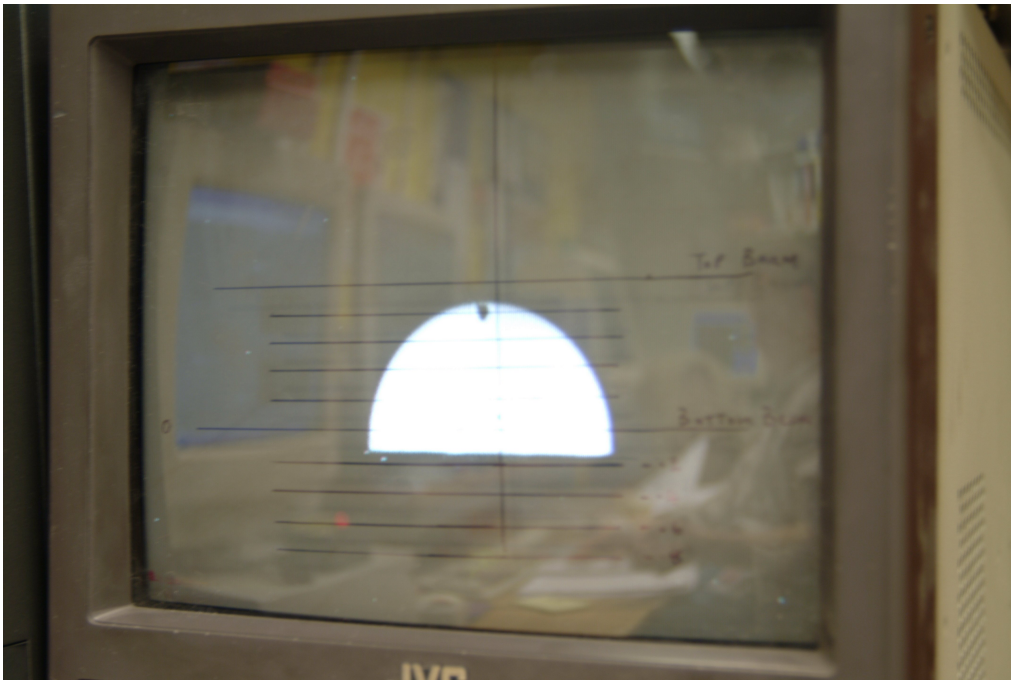

**Figure 11.10 Video monitor illustrating the calibrated position of the liquid sample in the x-ray beam.**

Again another welding filter of different grading is placed at the front of the lens. This allows visual monitoring of the sample at elevated temperatures

### 11.18 External Safety Camera.

This camera is a standard CCD camera with pan and tilt facilities, including zoom and focus, and is wired as part of the infrastructure of the experimental beamline hutch, allowing the external environment of the experiment to be monitored remotely from the control room.

### 11.19 High speed camera

The use of a Photo-Sonics high speed camera has allowed the process of recalescence or supercooling to be studied frame by frame. These facilities are capable of recording macro images of molten sample at 2500 frames per second, this image is then downloaded to a dedicated pc for analysis. Like to rest of the control equipment used on the beamline, remote capture of video and monitoring is achieved with the Ethernet output fed into the control hutch during experiments. This allows complete camera control of shutter speed and exposure with a typical frame rate of 1000 frames per second.

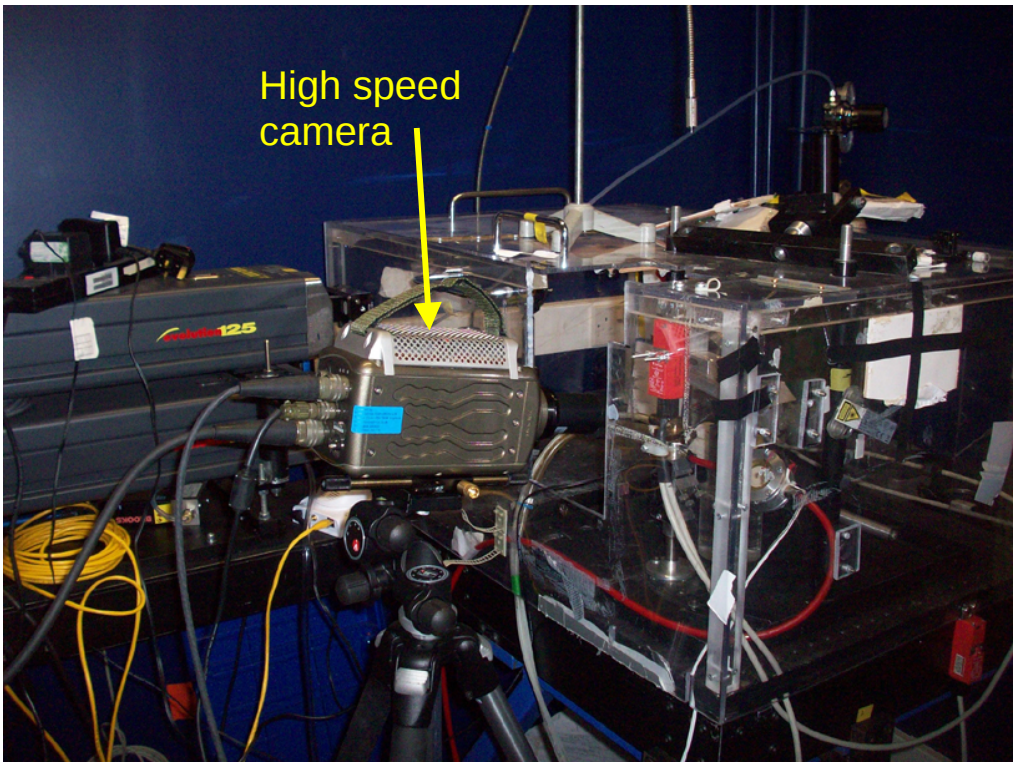


**Figure 11.11 Photo-Sonic high speed camera remotely controlled to study molten samples.**

### 11.20 Recording video imaging of liquid drops.

This is achieved by the use of a dedicated video recorder coupled to the external reference camera. These facilities enable recording times of 6 hours onto tape. A recent innovation is the use of a multi camera close circuit surveillance system capable of monitoring 4 cameras simultaneously. This facility also has the ability to time stamp and zoom into the digital displays.

The use of this type of insitu monitoring has enabled the discovery of the polymorphic “rotor effect”, which is a high to low density phase transition observed whilst samples of alumina –yttria are in the supercooled region of the melt.

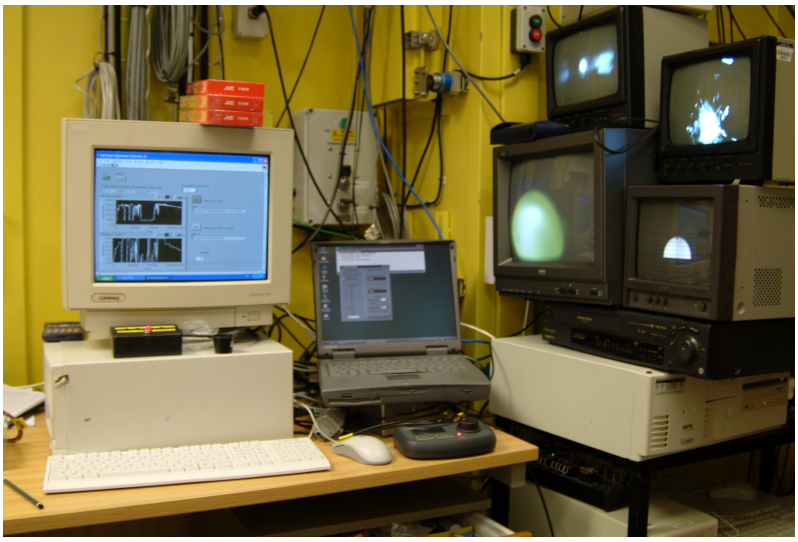

**Figure 11.12 Experimental control desk incorporating LabVIEW laser and pyrometer control computer, mass flow control computer, and video camera monitoring station and recording facilities.**

Future developments will utilize a dedicated DVD recorder and high capacity hard drives to record video information. Use of high speed cameras, thermal imaging cameras and three-dimensional visualization is also contemplated.

**INSERT HIGH SPEED CAMERA SPEC HERE**

# Chapter 12.

## Results

This Chapter describes how the constructed experiment was capable of investigating the phenomena of

1. Melting of materials
2. Recalescence
3. Super cooling
4. High and low density transitions

All the experiments at the 6.2 beamline used monochromatic x-rays, with an energy of 16.9 KeV, with a focused beam of 0·37mm x 0·40mm at the sample. The diffraction measurements were carried out using the 60 degree aperture Rapid2 detector [1] using an argon xenon gas mixture on the gas filled detectors, with an exposure time of 2min. The scattering measurements used a quadrant Rapid2 detector at the end of a 3.5 meter SAXS camera. The exposure was also 2 minutes.

### 12.1.Melting

The crystalline sample spins in the sample holder whilst it levitates at room temperature. The speed is dependant on how uniformly spherical the sample is. As the laser heats up the sample, surface melting generates more spin, which can cause instabilities in the levitation as the sample goes into the melt, causing serious oscillations. At this point, mass flow of gas into the levitator can be increased to minimise this, as faster flow will increase sample spin but reduce instabilities. However this can also have the negative effect that, if the flow is increased too much, there is the danger of blowing the sample out of the levitated gas stream.

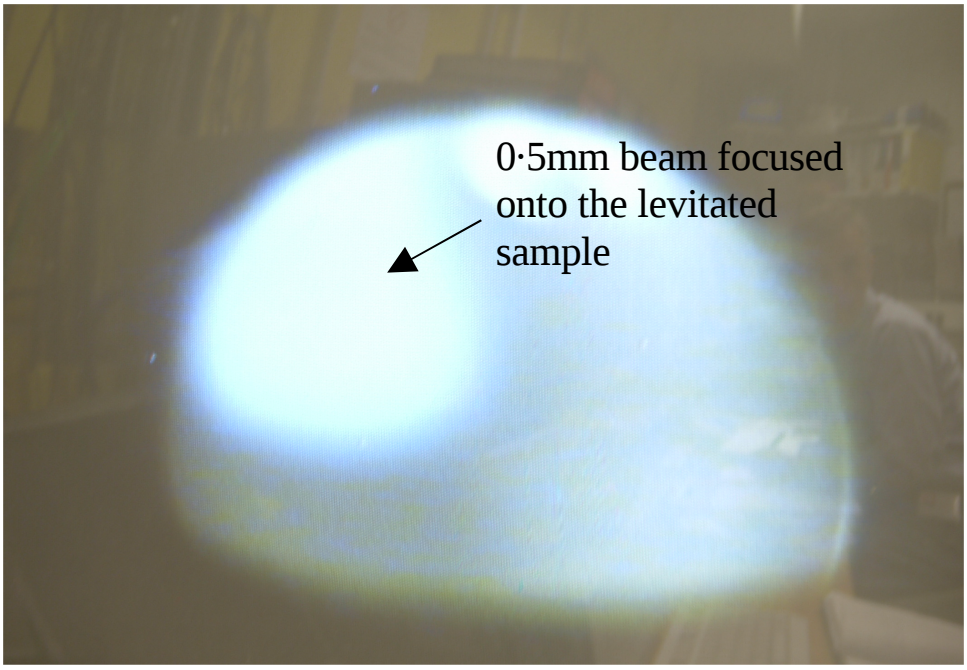


**Figure 12.1 Real time video capture of levitating molten sample, illustrating laser beam hot spot.**

When the sample is almost completely melted and levitating stably, the physical properties of the sample changes. The subtle changes producing the melt are monitored by the optical pyrometer, as seen in Figure 12.2. The decrease in density is also measured by the increase in sample diameter, as discussed in a subsequent paper on ***In Situ*** **structural studies of Alumina during melting and freezing** [2].

### 12.2 Recalescence

This phenomenon is achieved by heating the levitated sample by the carbon dioxide laser, to in excess of 2100º C, until the alumina sample is completely melted, but still maintaining its spherical shape and stable in the levitating air stream. Power to the laser is then shut off, and the sample allowed to cool down rapidly to room temperature.

The resulting phenomena is evident when the temperature of the cooling sphere suddenly increases, as can be see in Figure 12.2, then loosing energy and decreasing down to room temperature.

Simultaneous measurements of WAXS and SAXS are recorded during this period, enabling an understanding of alumina at the atomic and nano structure scale to be achieved. This technique also allows the thermodynamics of alumina to be studied in the crystalline and liquid states [2].

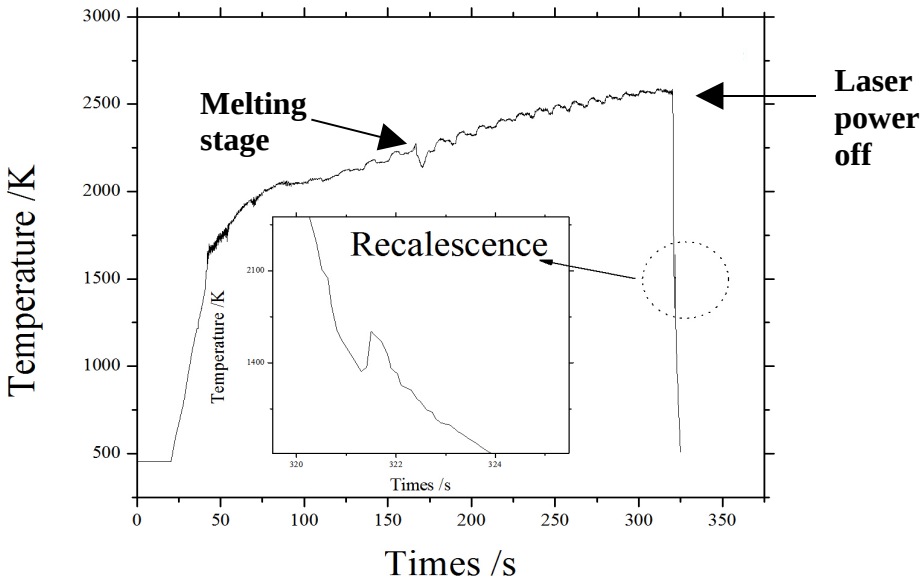


**Figure 12.2 Co plot illustrating heating and cooling cycle of alumina, highlighting the melting stage and recalescence regions as special regions of interest.**

### 12.3 Supercooling

This experiment investigates the formation of glass from a viscous liquid. This is achieved by the cooling of the sample whilst still in the liquid state (melted), as described in the subsequent paper, **Development of structural order during supercooling of a fragile oxide melt** [3]**.**

Supercooling is maintained by a manual or automated control (via LabVIEW) of the laser power. With manual control the laser power can be reduced in steps from the molten state. At each level, 2 minute readings are taken by the wide angle detector and the small angle detector. These steps are determined by the melt temperature of the sample, and how far into the super cooled region the sample can be taken before crystallisation occurs.

An automated version of the laser controller is also available. This can reduce power for a specific rate, over a finite period. The main disadvantage of this type of control is that when the temperature of the sample reaches the critical stage before crystallisation, dramatic temperature readings occur, with fluctuations of over 100º C. Stable sample temperatures in this region can therefore only be controlled by manual laser control. The lowest temperature achieved for a 2mm magnesium aluminate sample whilst still in the liquid state, using this apparatus was 1296ºC, using 6.28% laser power.

The development of fast detectors such as Rapid2 with acquisition times of less than 100ms have enabled time resolved measurements of structural changes to be measured as the liquid transforms to the crystal, or the glass transition is approached , as can be see in the subsequent SRMS-5 Conference paper, **Investigation of high temperature liquid oxides with synchrotron radiation [4].**

### 12.4. High and low density transitions

Experimental techniques using the levitating furnace have developed as more samples have been investigated. One such material Yttria(20%) and Alumina (80%) or YAG20 revealed significantly new phenomena, and an unexpected discovery. The levitated sample was heated until it melted, and subsequent SAXS and WAXS readings taken in the super cooled region as the laser power was decreased almost to the point of re crystallisation, as shown in Figure 12.3. At temperatures around

1800K the SAXS signal exhibited a peak in intensity which is attributed to a liquid-liquid transition, as described in the subsequent science paper, **Detection of first order liquid-liquid phase transitions in Yittria oxide-aluminium oxide melts.[5]**

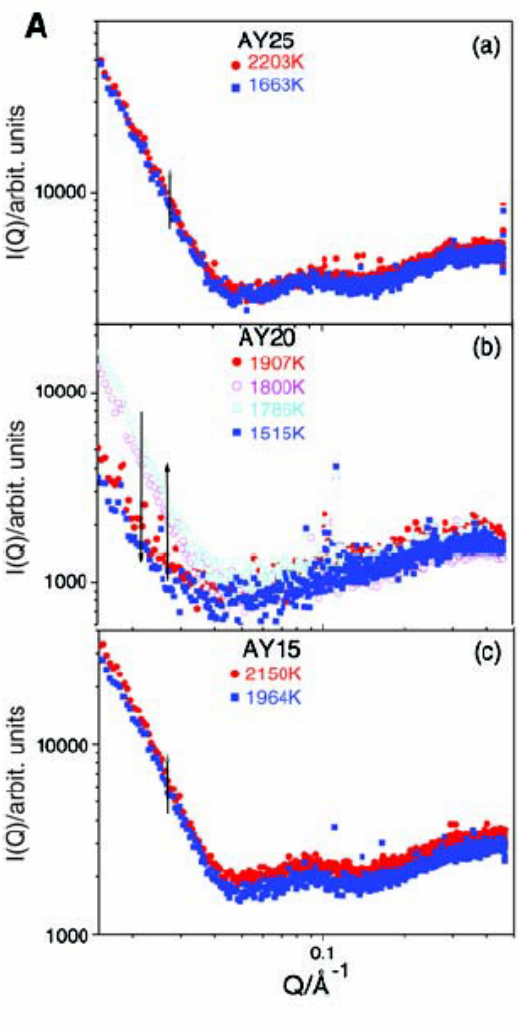


**Figure 12.3 SAXS data for supercooled AY15, AY20 and AY25 liquids revealing the intensity of random fluctuations measured at the Synchrotron Radiation Source beamline 6.2.**

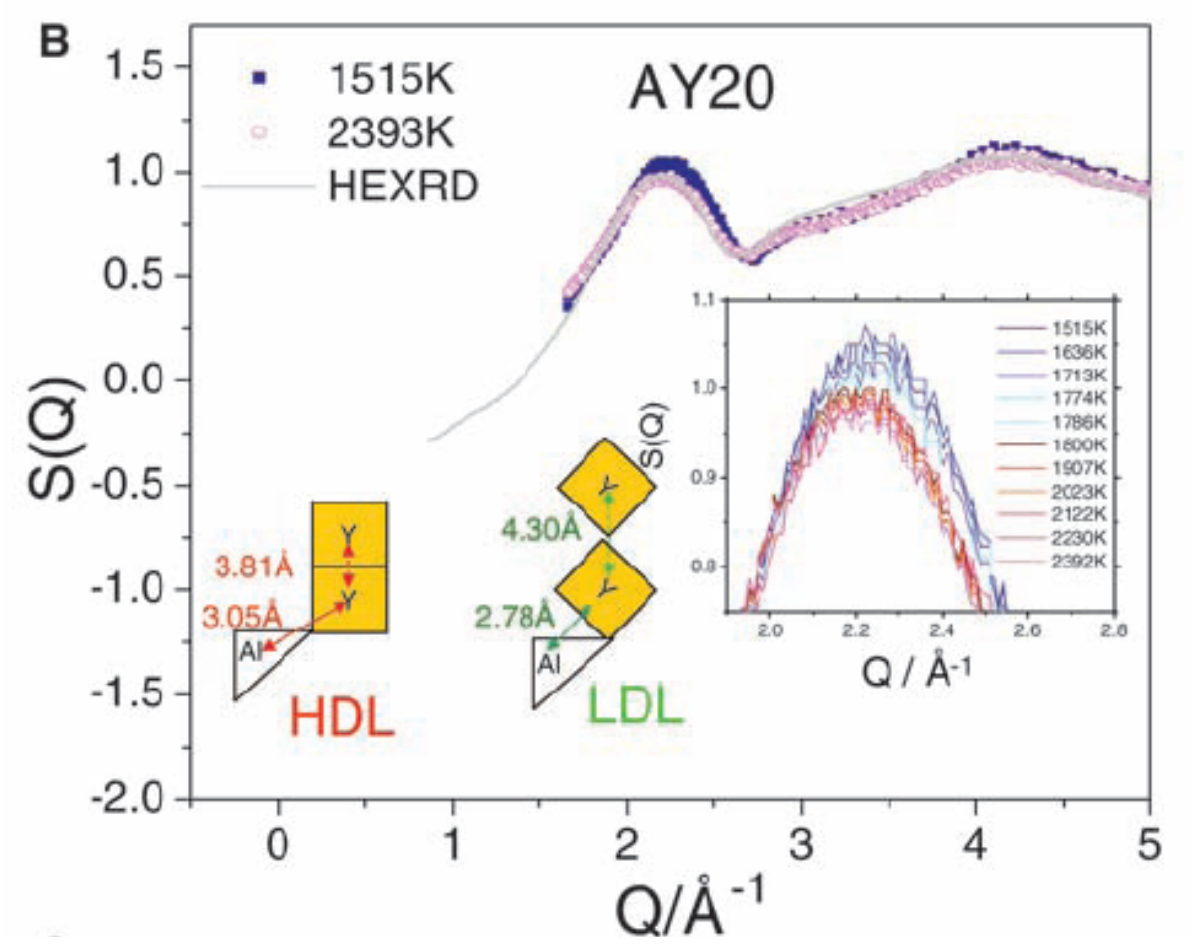


**Figure 12.4 Illustrated are changes to the principle peak for AY20 between 2392K and 1515K, measured at the Synchrotron Radiation Source beamline 6.2.**

One particular and noticeable characteristic was the tumbling effect of high and low density areas on the surface of the sphere as shown in Figure 12.5. These coincide with the peak in SAXS (Figure 12.3) and the shift in the first peak of the WAXS pattern (Figure 12.4). They take the form of an "oscillating rotor" oscillating repeating at ~ 4HZ, which is sustainable for periods of an hour. The whole experiment was repeated using different AY20 samples with reproducible results.

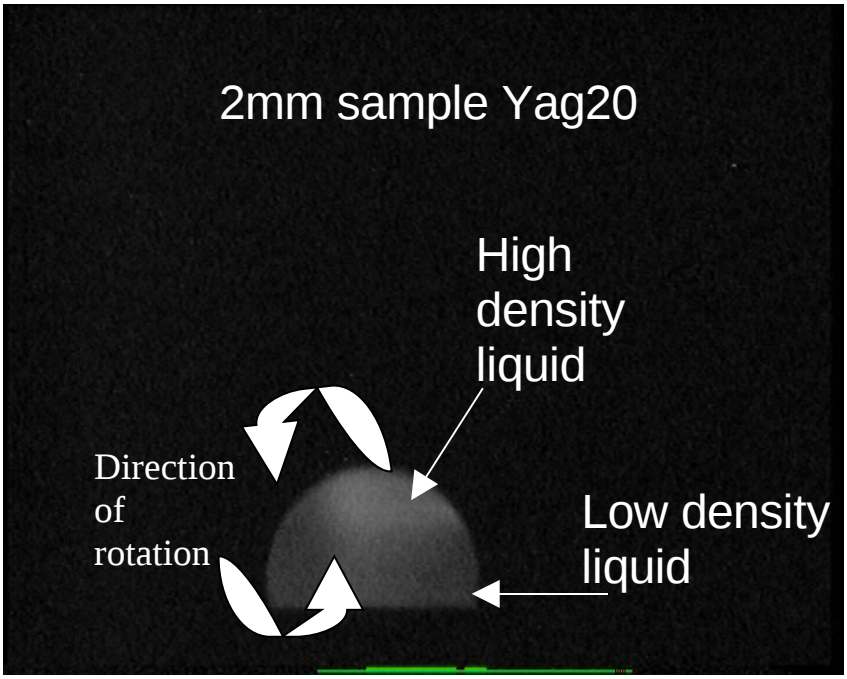


**Figure12.5 Oscillating rotor.**

This oscillating rotor effect (Figure 12.5) was investigated in detail using the video images, in order to be able to understand the phenomena. A series of still images taken from the video footage of the sample as it rotated can be seen in Figure 12.6.

**Figure 12.6 Sequential rotating images of the liquid sample in the supercooled region.**

By applying false colour imaging to the frames via a LabVIEW application, the following sequence can be observed to follow the brightness at the top of the drop, as shown in Figure 12.7

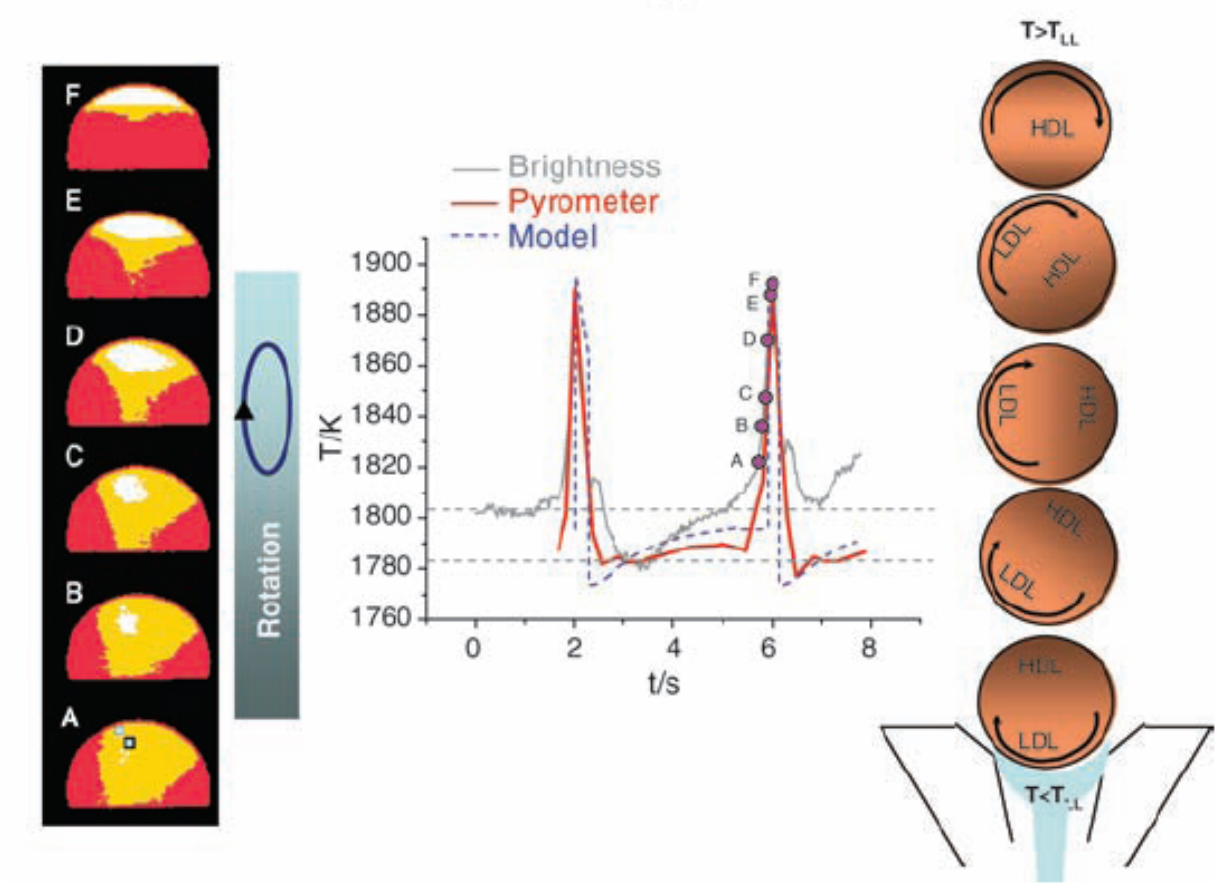


**Figure 12.7 Video images A to F illustrating horizontal rotation. Fluctuating image brightness for one pixel area compared with pyrometer output for one 4-s cycle. 180° rotation takes 600ms, after which the bead is virtually stationary.**

This sequence also corresponds to the real time data recorded by the optical pyrometer, measuring the temperature profile as the sample rotates in the levitated air stream as can be seen in Figure 12.8.

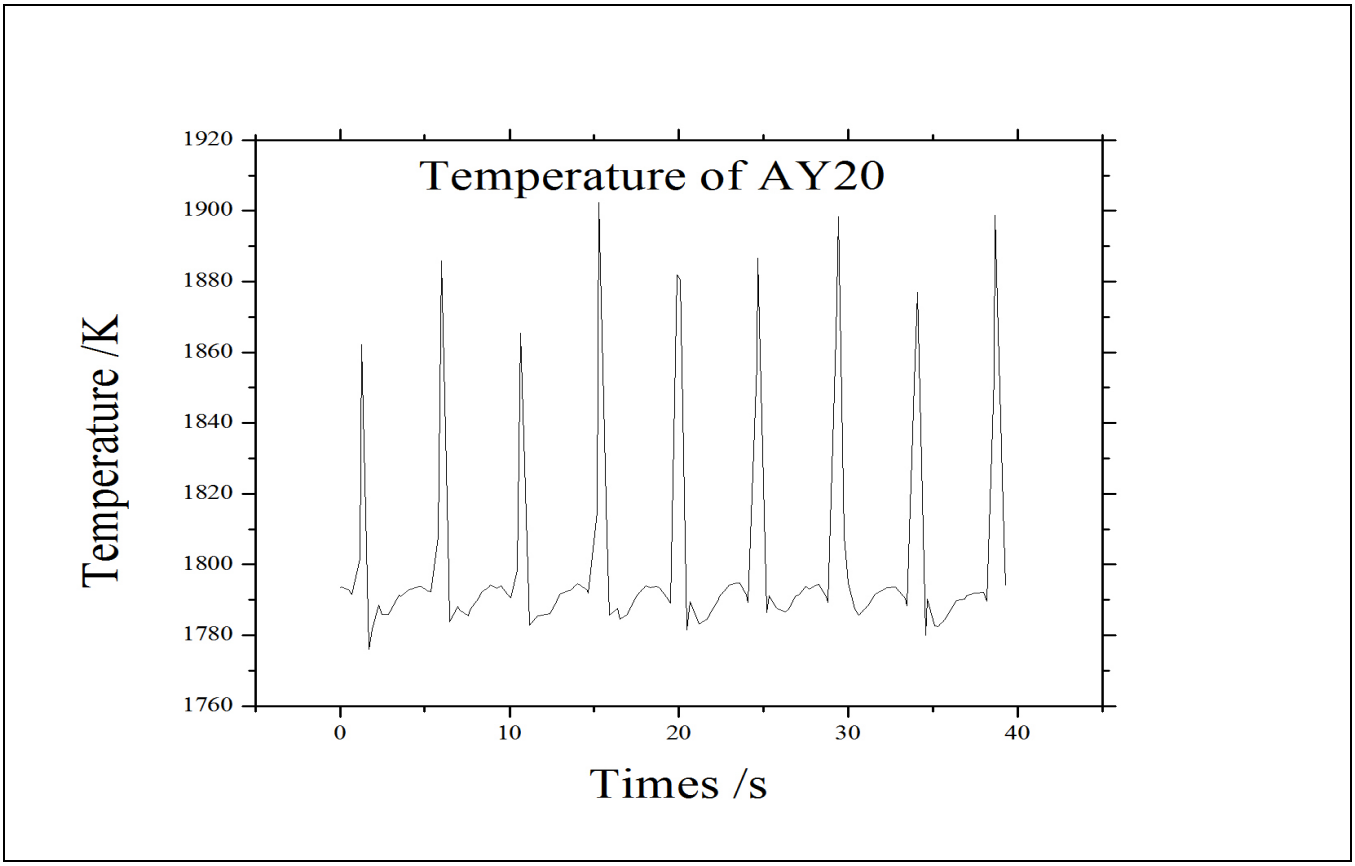


**Figure 12.8 Pyrometer readings of oscillating polyamorphic rotor.**

Further details and an in-depth analysis can be found in ref {5}

### 12.5. Future experiments

Further investigations into this discovery will be made. The use of microscopic high speed cameras, set up in a stereo configuration, will allow reproduction in 3-dimensional visualisation and modelling. The use of thermal imaging cameras will enable the temperature gradient of the liquid-liquid state, as the sample rotates from the high to low density states, to be analysed.

## 12.6. Conclusions

The success of this experiment would not have been possible without the facilities, help and support of the SRS staff at Daresbury laboratories. Unfortunately the end of an era has arrived with the closure of this Synchrotron. The next generation of experimental research is now available at the Diamond Light Source. These exciting new facilities have already seen the installation of the first ”Red” experimental operation of the Carbon Dioxide laser and levitator at D.L.S. The Materials Group is looking forward to new areas of experimental discovery in the future at this new synchrotron radiation source.

At the experimental level, development of a new sample stage is currently under construction to facilitate a twin laser system to be controlled by LabVIEW. This will allow more homogeneous heating of the sample by heating from both the top and bottom.

LabVIEW upgrades continue to be developed with alterations in experimental facilities. There are also three other areas of development.

### 12.6.1. Twin laser system.

Software development will require a twin laser system to operate via LabVIEW control. This will have the facilities to operate in tandem or individually, with power applied proportionally to the second laser. Included in the software control, will also be a certain level of automation.

### 12.6.2. Twin laser shutter.

A double laser shutter system will also be designed to be incorporated into the experimental setup. This will have identical design features to the current one, but will be capable of simultaneous beam block of both lasers. This shutter will be designed and installed to specifically run on the Diamond Light source.

### 12.6.3. Video monitoring

Diamond Light Source facilities use internet protocol cameras to monitor the experimental facilities. The intention is to incorporate these cameras into the software control system of the levitator, to give greater flexibility for monitoring the experimental environment, and to reduce significantly the use of additional monitoring equipment.

### 12.6.4. Temperature monitoring

Another area highlighted since experimental commissioning has begun at Diamond Light Source, is the requirement to monitor more closely the remote temperatures of the laser cooling system, and the sample stage head. Although there are two separate areas, the remote temperature monitoring of the laser head is vital, as any overheating of the laser could result in irreparable damage to the equipment. The sample stage nozzle temperature will be monitored via a thermocouple. As the sample intermittently sticks to the stage, any significant rise in temperature will confirm this. Both these items will now be included in the main LabVIEW programme.

Two other areas for future investigation are levitation of silicon samples and high viscosity liquids. Currently completed is the development of the silicon chamber, with dedicated windows and remote radio cameras which allow monitoring of samples in a pressurised argon atmosphere (Chapter 7.7.) The second area of investigation is the novel design of a cryogenic levitator. This sample stage will be capable of levitating high viscosity samples at room temperature and below.

### References

[1] A.Berry, W.I.Helsby, B.T.Parker *et al.,* Nucl Instrum. Methods Phys. Res. A **513**, 260 (2003)

**Published papers**

[2] In press 2009 G.N.Greaves, M.C.Wilding, **S.Fearn,** D. Langstaff, F. Kagl, Q. Vu Van, L.Hennet, I. Poznyakova, O.Majerus, R.J.Cernik, C.Martin. **In situ structural studies of alumina during melting and freezing.** Advances in Synchrotron Radiation.

[3] L.Hennet, I.Pozdnyakova, A.Bytchkov, D.L.Price, G.N.Greaves, M.Wilding, **S.Fearn,** C.M.Martin, D.Thiaudiere, J.F. Berar, N.Boudet, M.L.Saboungi.**Development of structural order during super cooling of a fragile oxide melt.** Journal of Chemical Physics **126**, 074906 (2007).

[4] L.Hennet, I.Pozdnyakova, G.N.Greaves, S.Krishnan, M.Wilding, **S.Fearn**, C.Martin. **Investigations of high temperature liquid oxides with synchrotron radiation.** SRMS-5 Conference Chicago, **115**, (2006)

[5] G.N. Greaves, M.C. Wilding, **S. Fearn**, D. Langstaff, F. Kargl, S. Cox, O. Majérus, Q. Vu Van, C.J. Benmore, R. Weber, C.M. Martin, L. Hennet. **Detection of First Order Liquid-Liquid Phase Transitions in Yttrium Oxide – Aluminium Oxide Melts.** *Science* 2008, **322**, 566-570 (2008).